IV. $\mu^+\mu^-$ COLLIDER STUDIES

A. Sessler/A. Tollestrup, Chairs

IV. $\mu^+\mu^-$ COLLIDER STUDIES, *A. Sessler* (LBNL)/*A. Tollestrup* (FNAL), Chairs

Muon Colliders - *R. Palmer* (BNL)
Higgs Factory Collider Ring Lattice Studies - *A. Garren* (UCLA/LBNL)
Muon Collider Rings - *C. Johnstone* (FNAL)
Lattice for 50-50 GeV Muon Collider - *K.Y. Ng* (FNAL)
JHF: Japan Hadron Facility - *Y. Mori* (KEK/Tanashi)
Ultimate Luminosity Muon Collider (Problems and Prospects) - *A. Skrinsky* (Russia)
New $\mu^{\pm}$ Cooling for $\mu^{\pm}$ Colliders and Possible Realizaton at JHF/KEK - *K. Nagamine* (KEK/Riken)
Muon Dynamics in a Toroidal Sector Magnet - *J.C. Gallardo* (BNL)
A First Look at Emittance Exchange in a Bent Solenoid System - *R.C. Fernow* (BNL)
Ionization Cooling for $\mu^+\mu^-$ Colliders - II (~Fermilab) - *D. Neuffer* (FNAL)
3-D Cooling Scheme - *F. Mills* (FNAL)
Three Bypasses of Bottle Neck of Data Flow in Neutrino-Higgs Factory and Device R&D of QMC-QMD Based on EEEE Laws for PPPP - *J. Shen* (IHEP, China)
Bunching Near Transition in the AGS - *J. Norem* (FNAL/ANL)

MUON COLLIDERS

The 4th International Conference on Physics Potential and Development of $\mu^+\mu^-$ Colliders
Fairmont Hotel,
San Francisco, CA
December 10, 1997

R. B. Palmer

Brookhaven Nat. Lab.
SUNY, Stony Brook
LBNL

COLLIDER PARAMETERS

c of m energy	GeV	3000	400	100		
p Energy	GeV	16	16	16		
p's/bunch	10^{13}	2.5	2.5	5		
bunches/fill		4	4	2		
rep rate	Hz	15	15	15		
p power	MW	4	4	4		
μ/bunch	10^{12}	2	2	4		
μ power	MW	28	4	1		
wall power	MW	204	120	81		
collider circ	m	6000	1000	300		
min depth (ν)	m	300	0.7	0.01		
rms dp/p	%	0.16	0.14	0.12	0.01	0.003
rms ϵ_n	π mm mrad	50	50	85	195	280
β^*	cm	0.3	2.3	4	9	13
σ_z	cm	0.3	2.3	4	9	13
σ_r spot	μm	3.2	24	82	187	270
tune shift		0.043	0.043	0.05	0.02	0.015
luminosity	$cm^{-2}sec^{-1}$	$5\ 10^{34}$	10^{33}	$1.2\ 10^{32}$	$2\ 10^{31}$	10^{31}
c of m dE/E	10^{-5}	80	80	80	7	2
Higgs/year	$10^3\ year^{-1}$			1.6	4	4

All Cases 6D emittance = $170\ 10^{-12}\ (\pi m)^3$

King

NEUTRINO RADIATION

- Radiation $\propto E^3/length^2 \propto E^3/depth$
- Use: 1/10 Federal Limit = 10 mR/year

THEN

- Negligible Problem at 1.5 TeV
  - $\approx$ 1 mR/year
- E = 3 TeV ok at 300 m Depth
  - $\approx$ 10 mR/year
- E > 3 TeV Requires:
  - Beam Wobbles, and/or
  - Special Locations, and/or
  - Better Cooling

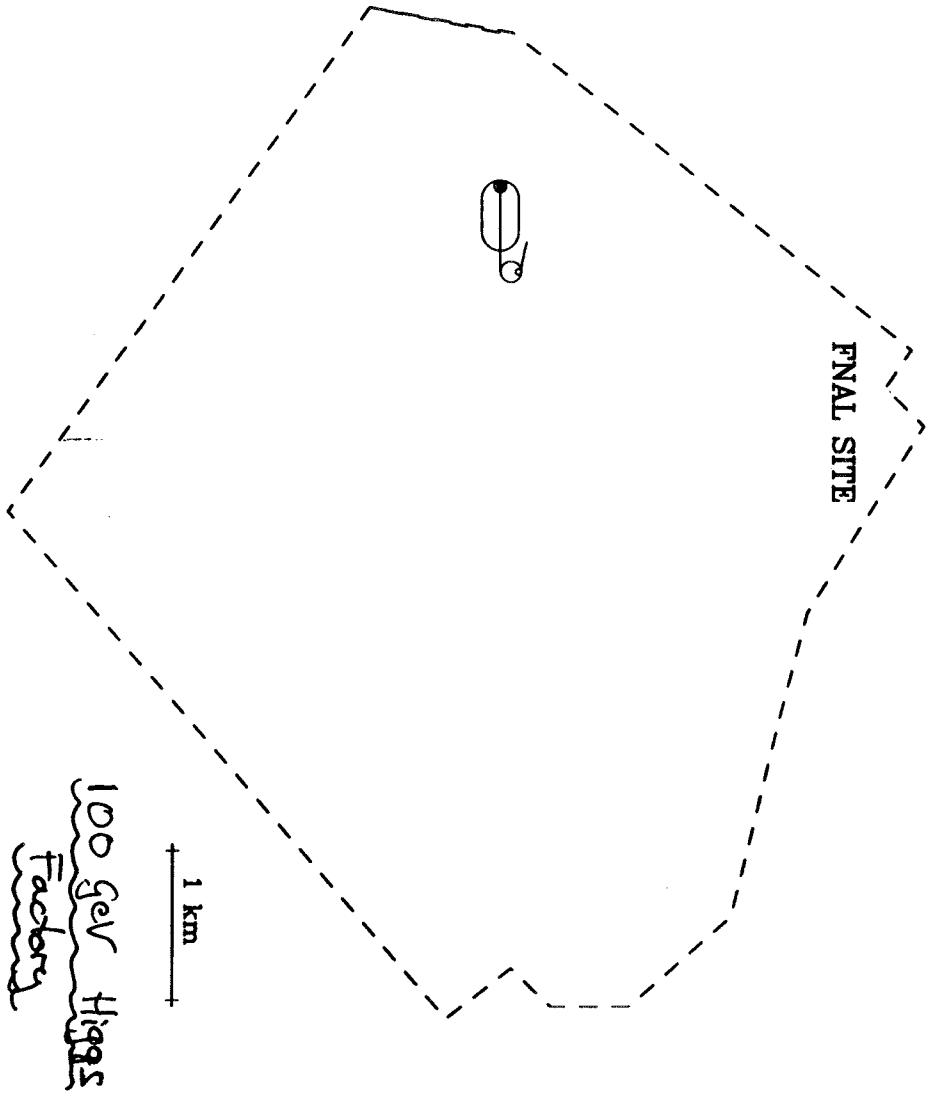

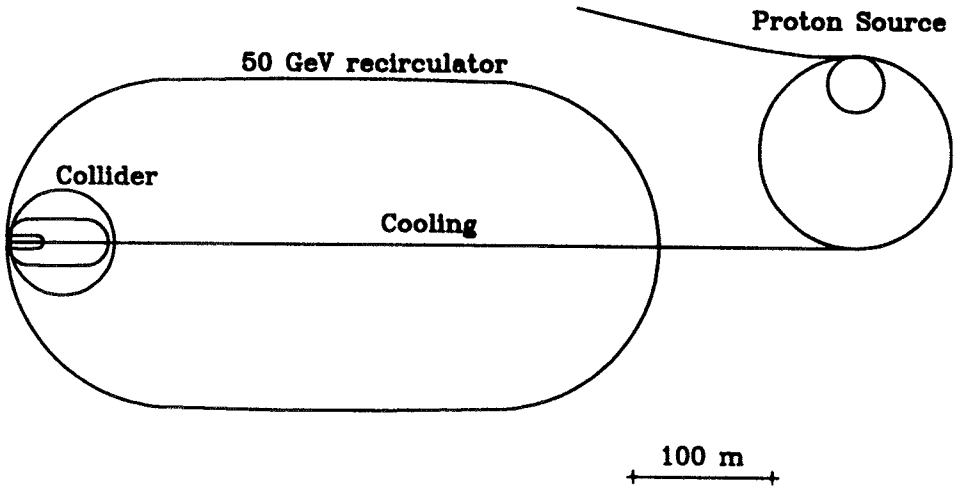

100 GeV HIGGS FACTORY

Nov 1996

PROTON SOURCE

NEED:

- Proton Beam Power 2-4 MW
- Very short bunch: rms 1-2 nsec

- FNAL PROPOSAL: 4 MW
  - Upgraded linac (.4 → 1 GeV) 16 GeV
  - Higher field operation in Booster
  - New Pre-Booster

		Linac	Pre-Booster	Booster
Final Energy	GeV	1.0	4.5	16
Protons/bunch			$5\ 10^{13}$	$5\ 10^{13}$
No of bunches			2	2
Rep. freq	Hz	15	15	15
Circumference	m		180.6	474.2
Norm. 95% emit.	π *mm mrad*		200	240
sp ch tune shift			.39	.39
Final Field	T		1.3	1.3

- BNL PROPOSAL: 2 MW
  - Upgraded linac (.2 → .6 GeV) 24 GeV
  - Increased AGS rep rate: 2.5 Hz

Mokhov

TARGET, CAPTURE & DECAY

- **TARGET**
  - **High Z material preferred**
  - **Small diameter preferred**
  - **: Serious heating problem**
  - **: Liquid jet ? Mercury ?**
  - **EM forces entering capture magnet**
  - **: Insulating material: PtO_2 ?** ← $\rho = 10.2$, $T_m = 450°$
- **CAPTURE**
  - **20 T, 15 cm Diam Solenoid**
  - **Resistive insert (8 T)**
  - **Superconducting Outsert (12T)**
- **DECAY & PHASE ROTATION**
  - **5 T Solenoid Channel**
  - **rf to compact energy spread (30-90 MHz)**
  - **Momentum selection gives polarization**

start of jet

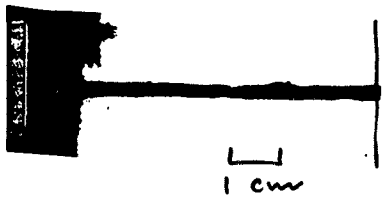

continuous flow

CERN Demonstration of Liquid Hg Target
C. Johnston (CERN)

Jet speed 20 m/sec
Reynolds No. >100,000

But problems in High B fields. ?

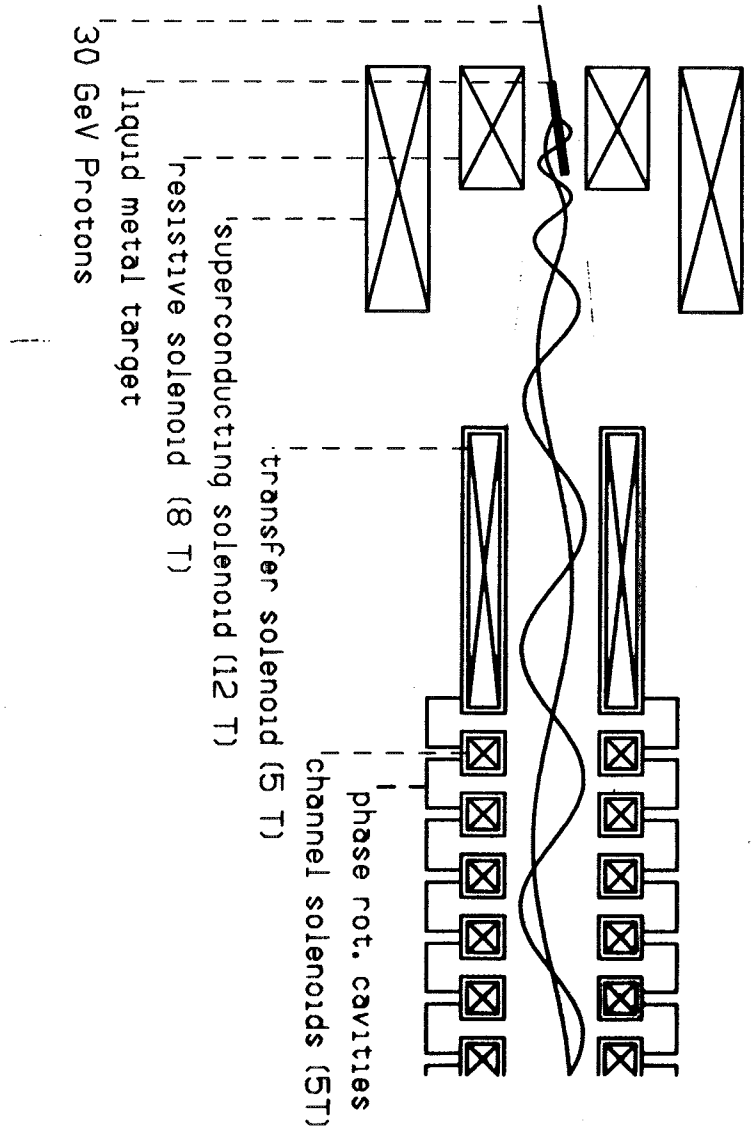

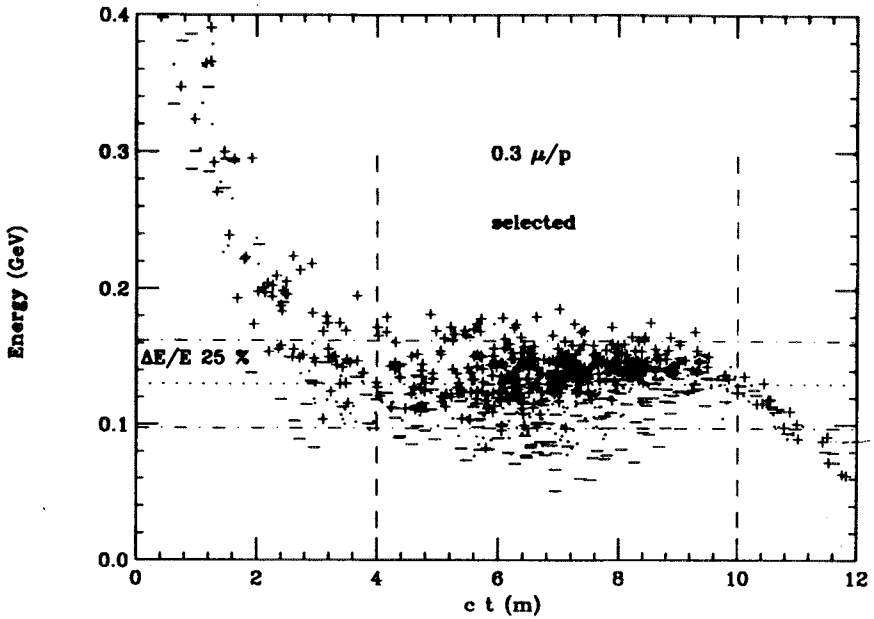

No obvious Problems

Rossmanith

- Polarization vs $\mathcal{L}$ loss

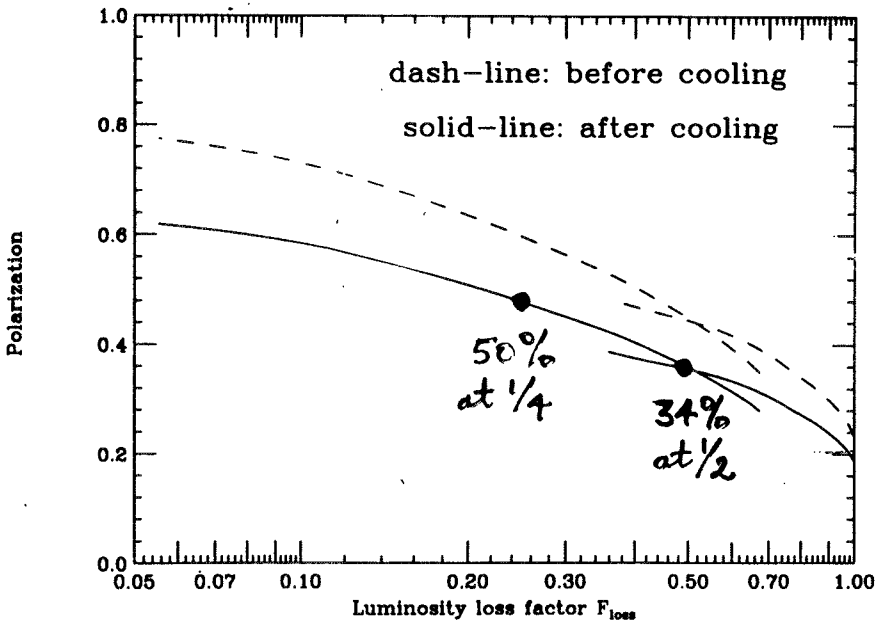

IONIZATION COOLING

- **TRANSVERSE**

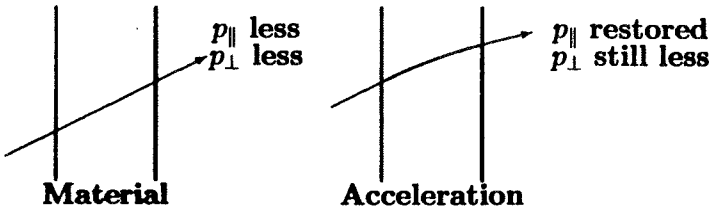

- **LONGITUDINAL COOLING (exchange)**

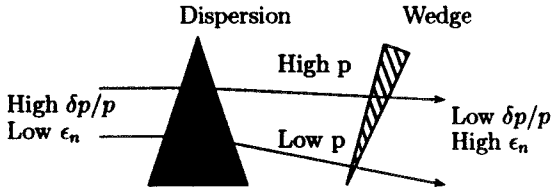

TRANSVERSE COOLING

- **Energy Loss lowers $\epsilon_\perp$**
- **Coulomb Scattering Increases $\epsilon_\perp$**
- **Equilibrium:**

$$\epsilon_\perp \propto \beta_\perp \frac{1}{\beta_v L_R \, dE/dx}$$

NEED

- **High $L_R \, dE/dx$**

  Low Z material
  Hydrogen > Lithium > Beryllium

- **Low $\beta_\perp$**

1 cool { Gallardo / Farnow

HOW TO GET LOW $\beta_\perp$

– Alternating solenoids (Early Stages)

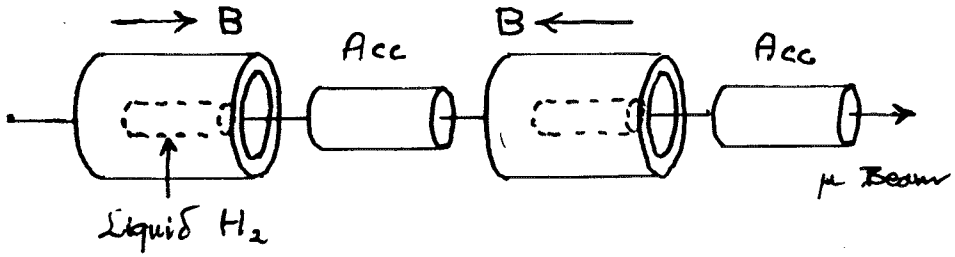

Neuffer

– Lithium Lens (Late Stages)?

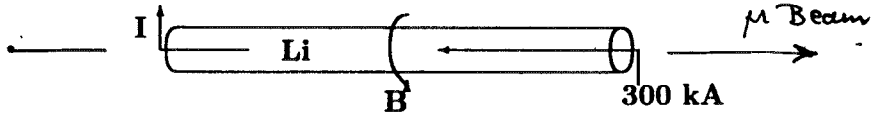

pulsed Current

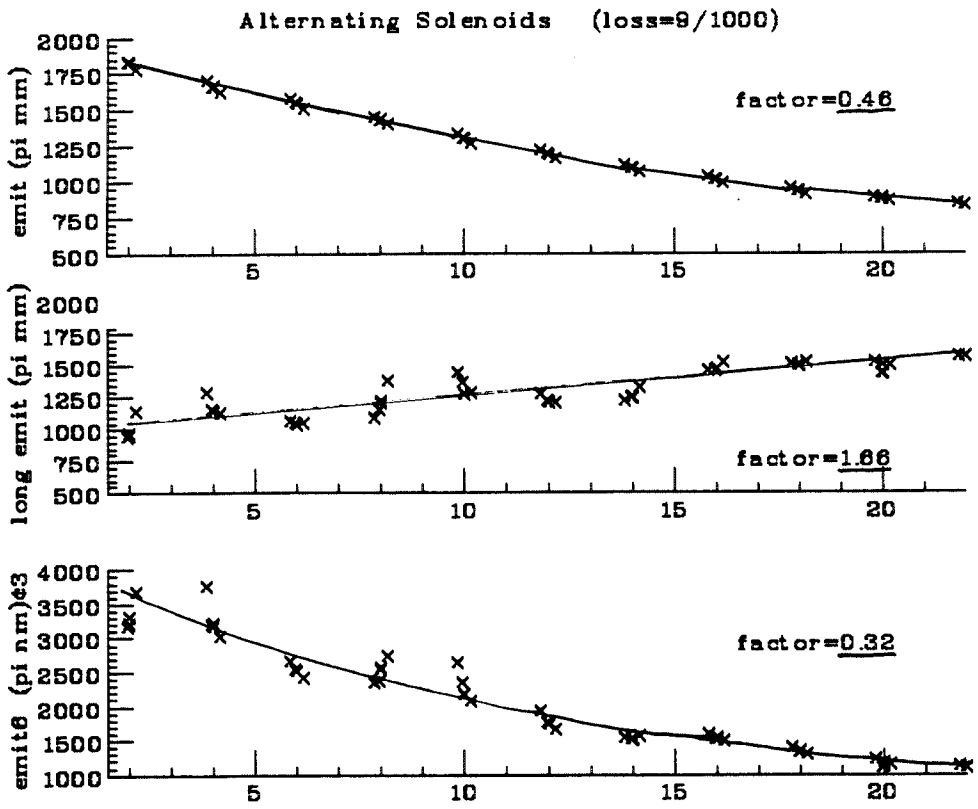
Alternating Solenoids (loss=9/1000)
emit (pi mm)
factor=0.46
long emit (pi mm)
factor=1.66
emit6 (pi nm)^3
factor=0.32

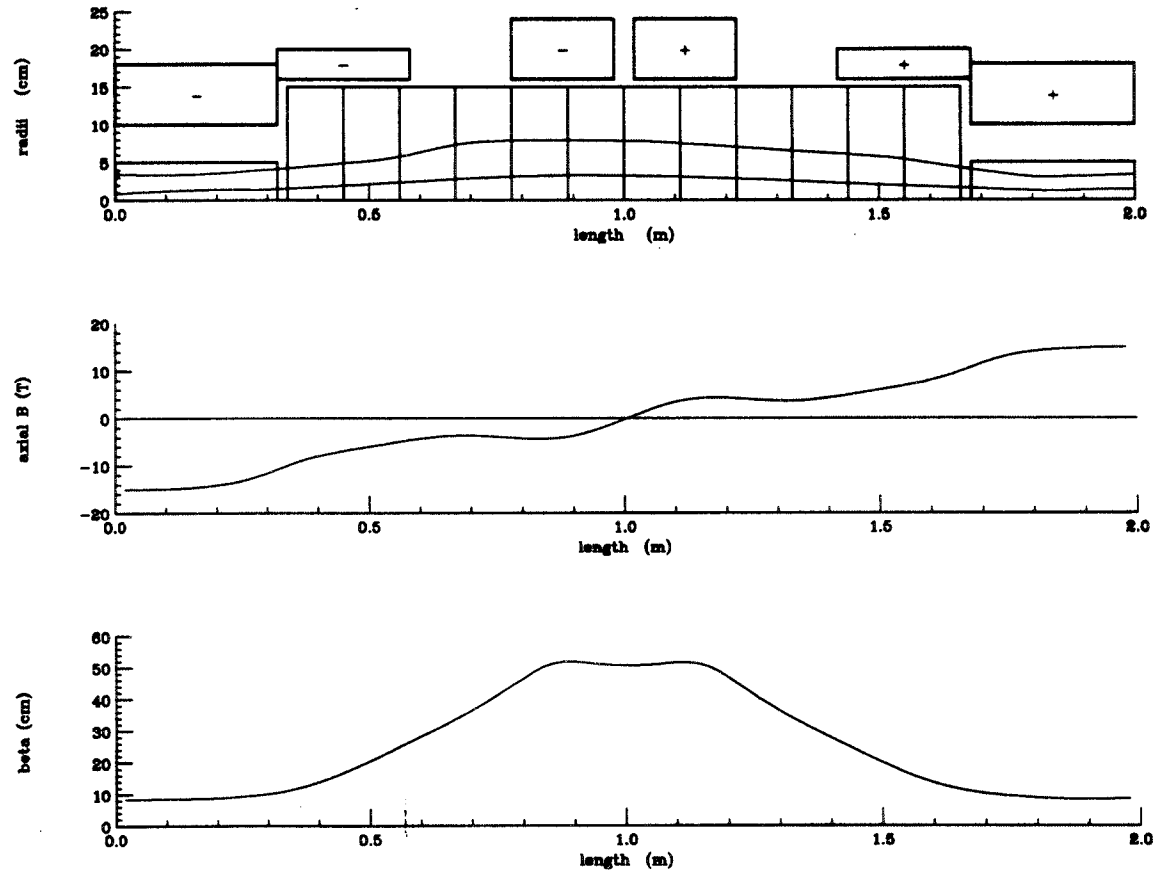
radii (cm)
length (m)
axial B (T)
length (m)
beta (cm)
length (m)

Alternating 30 T solenoids + LH + Be foils (30T) 146 MeV/c

Final Stage for Higgs

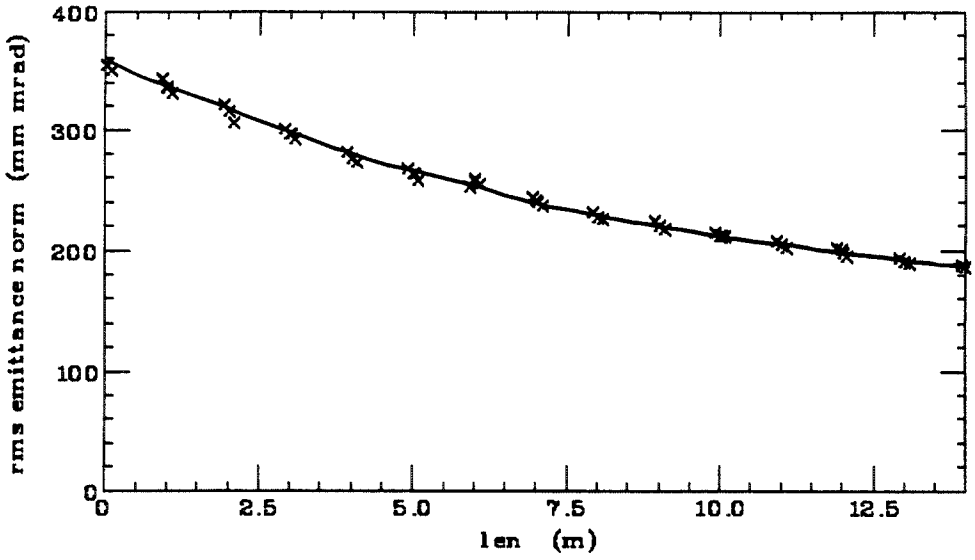

Warning: No Space Charge

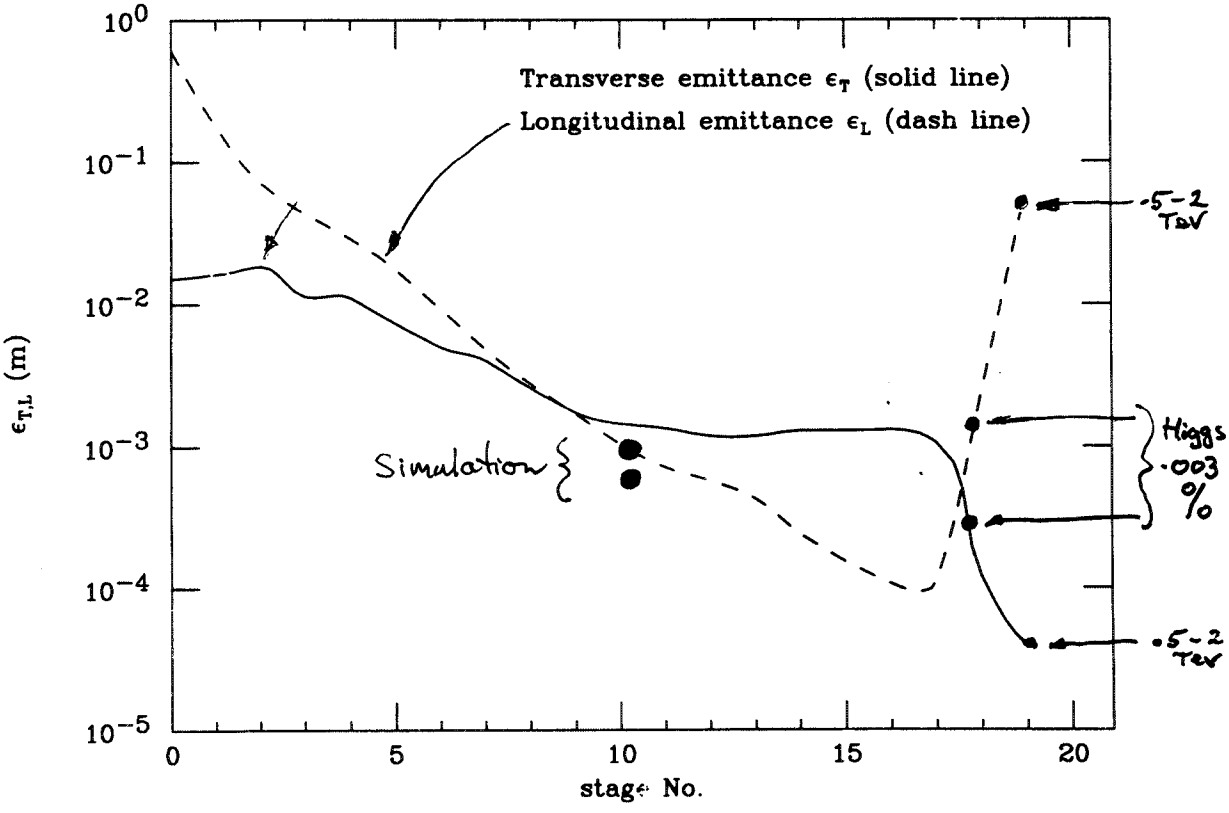

Farnow

FOR LONG COOLING

HOW TO GET DISPERSION

- Spectrometer

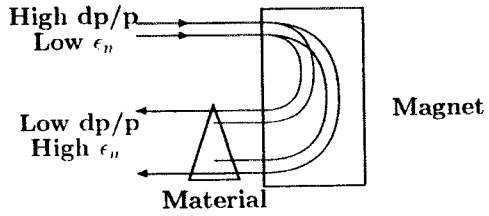

- Bent solenoids

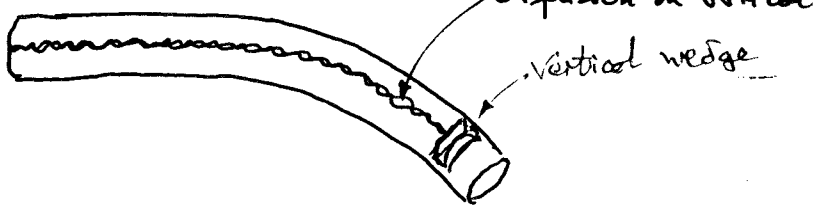

- FOFO with Alternating Bends

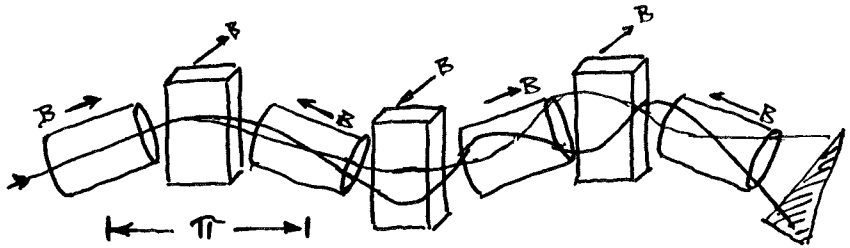

Alternating 30 T solenoids + LH + Be foils (30T) 146 MeV/c

Final Stage for Higgs

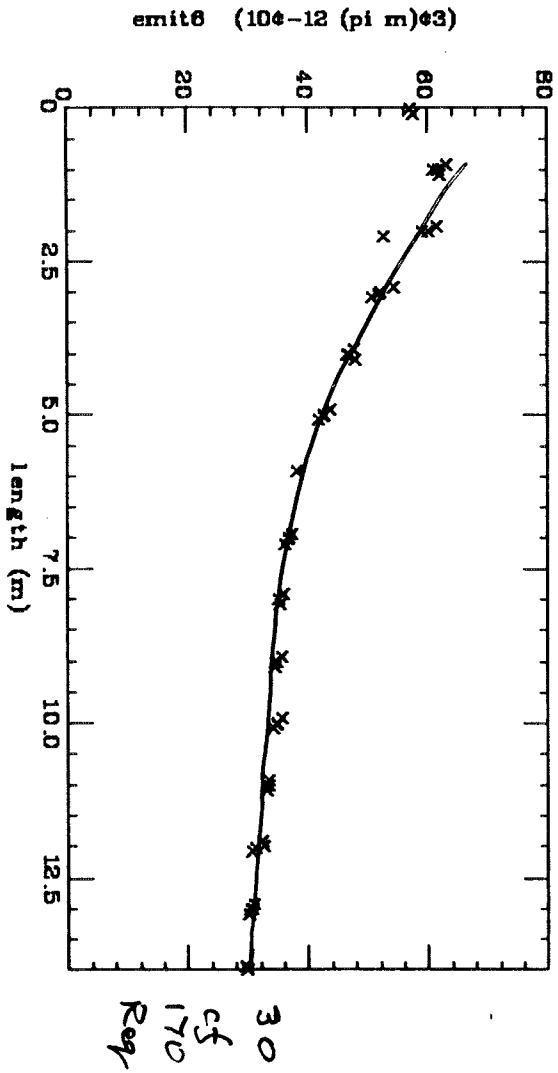

Warning: No Space Charge

ACCELERATION

- Acceleration must be rapid:
  - Linac
  - Recirculating Linac ($\approx$ 10 turns)
  - Pulsed Synchrotron (10-40 turns)
- Longitudinal emittances initially large:
  - long bunches: initial low frequencies
  - large dp/p: initial large apertures
- Instantaneous acc power high (worse at low E)
  - low E: SLED and/or low temp, allow sag
  - Med E: sc cavities, pre-fill, allow grad sag
  - High E: sc cavities + cw rf power
- Cost Optimization
  - Low E: Linac
  - Med E: Recirculating
  - High E: Hybrid pulsed/sc Magnet Synchrotron

HIGGS ACCEL. SEQUENCE

acc type rf type		linac sledCu	linac sledCu	recirc sledCu	recirc sledCu	recirc SC Nb	sums
E_{init}	(GeV)	0.10	0.20	0.70	2	7	
E_{final}	(GeV)	0.20	0.70	2	7	50	
circ	(km)	0.04	0.07	0.06	0.18	1.21	1.57
turns		1	1	8	10	11	
decay loss	(%)	2.31	3.98	6.74	7.77	9.88	27.29
decay heat	W/m	0.85	1.88	10.50	12.39	12.14	
B_{fixed}	(T)			2	2	2	
pipe width	cm			30.66	21.22	10.44	
pipe ht	cm			10	8	4.30	
RF Freq	(MHz)	90	90	120	170	400	
Acc/turn	(GeV)	0.20	0.40	0.17	0.50	4	
acc time	(μs)			1	6	43	
Acc Grad	(MV/m)	8	8	8	10	15	
grad sag	%			13.08	16.82	27.15	
rf time	msec	0.55	0.56	0.37	0.24	2.04	
peak rf /m	(MW/m)	2.72	2.56	2.21	4.40	0.20	
ave rf power	MW	0.61	1.10	0.28	0.88	1.99	4.88
total wall p	MW	4.71	8.50	1.67	5.20	5.87	25.94
beam power	MW	0.00	0.01	0.03	0.12	0.92	1.08
wall-beam eff	%	0.06	0.15	1.93	2.22	15.62	4.16

No obvious Problems

COLLIDER RING

- Low beta
  - 3mm at 3 TeV, 4 cm at 100 GeV
  - Needs local chromatic corr.
  - Large Quadrupole Magnets
- Short Bunches
  - equal to above beta's
  - Needs nearly isochronous ring
  - Use Flexible Momentum Compaction
- Tungsten Beam Shield
  - 6 cm at 3 TeV, 2cm at 100 GeV
  - large dipole coil diams
    16 cm at 3 TeV, 8 cm at 100 GeV
- Status
  - feasibility demonstrated at 4 TeV
  - NEW: Lattice ok with good aperture

Garren Johnstone Ng

worst: { 6% for 300 × 300 μ
-5% for 150 × 50

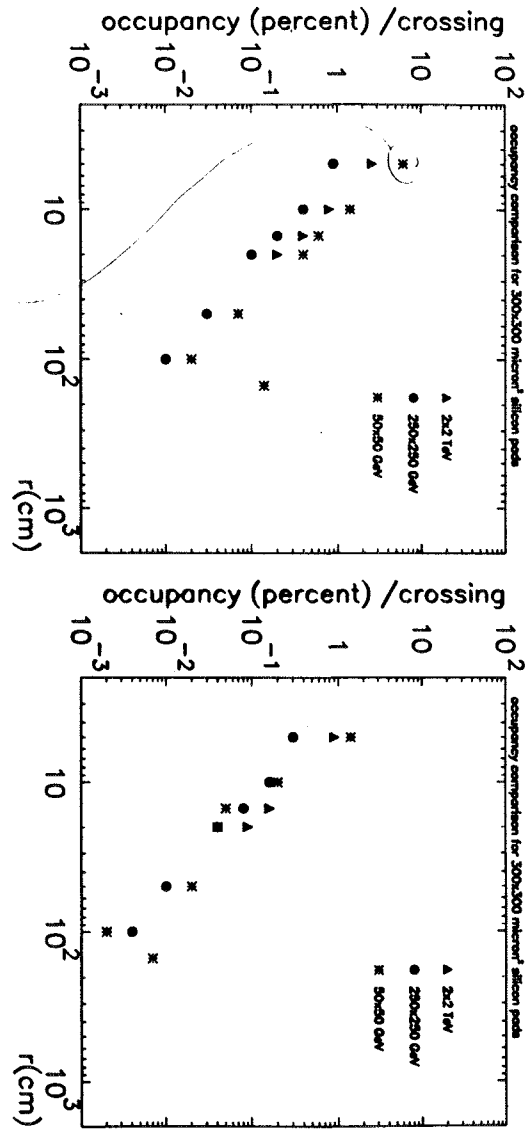

Stumer et

O. Benary, I. Stumer

- 7 -

Muon Collider Backgrounds ; July 26 1997

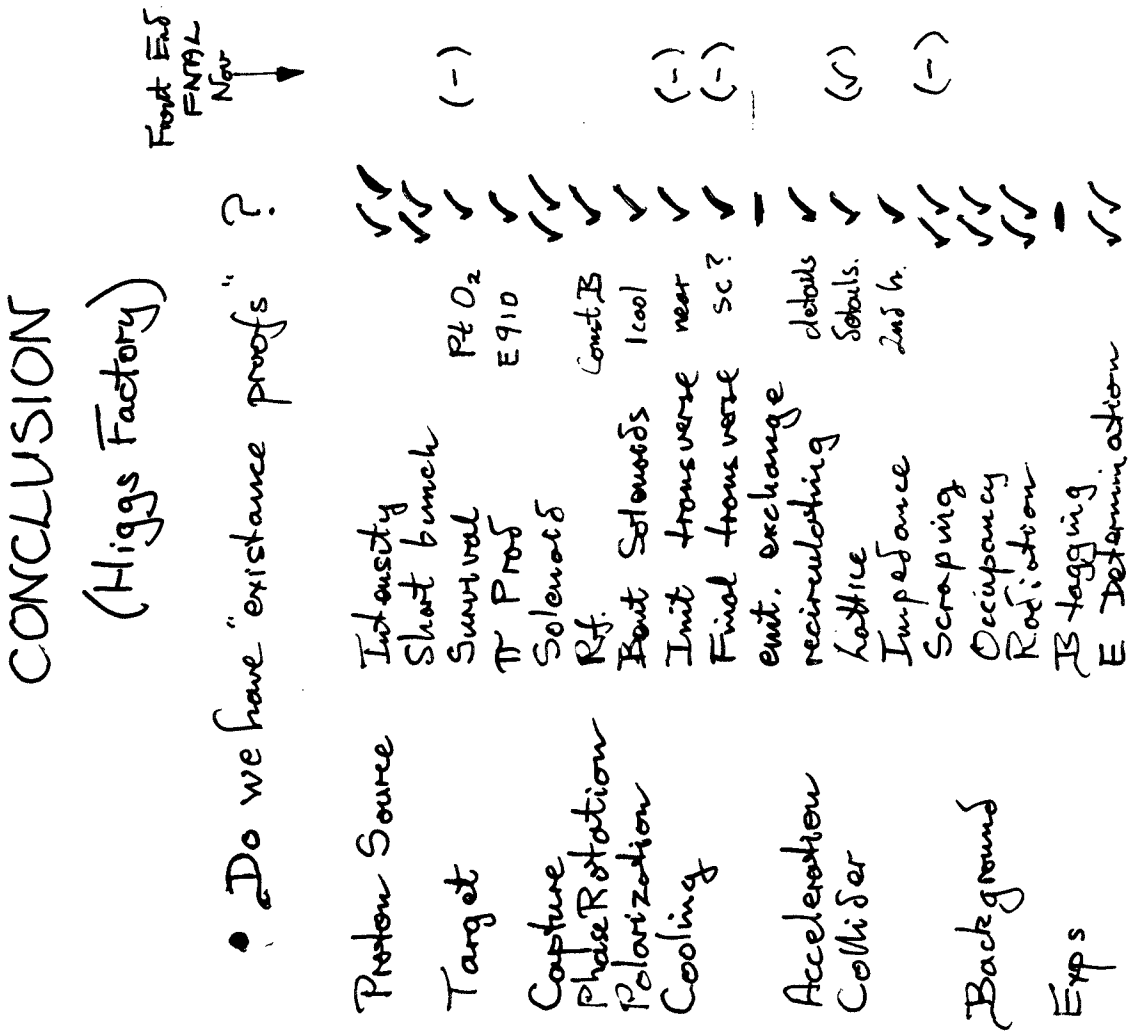

Radiation damage by neutrons on silicon detectors

assume 1000 loops , 15 Hz , 1 year = 10^7 seconds

acceptable hits per year = 1.5 10^{14}

c.m.	μ's/bunch	neutrons/cm^2/crossing	Hits/year	*Lifetime*
Tev	10^{12}	above 100 Kev	10^{13}	years
4	2	100	3.	5
.5	4	50	3.	5
.1	4	30	1.8	8

Seems OR

CONCLUSION

It is said that the Muon Collider will Require Several Miracles

But Remember

- **Antiproton-Proton**
  - **Lithium lens**
  - **Stochastic cooling**
  - **Accumulation**
  - **Superconducting Magnets**
  - **10^7 turns**
- **Electron Linear Collider**
  - **Few nanometer spot**
  - **10 times smaller emittances**
  - **Damped Accelerating Structure**
  - **Sled II Pulse Compression**
  - **New Klystrons**
  - **New Generation of Feedbacks**

Miracles require R and D

HIGGS FACTORY COLLIDER RING LATTICE STUDIES

Al Garren

MUMU97

December 11, 1997

Designs for a 50 GeV collider ring lattice are progressing well, but have not yet converged.

This talk, and the next ones by Carol Johnstone and Bill Ng, are about the current status of this work - which has been done mainly by Carol, Dejan Trbojevic and myself. My talk is mainly a description of a lattice by Carol and myself. Carol's talk will discuss design considerations, alternatives and stability range. The talk by Bill Ng has a discussion of the Trbojevic lattice, to which he contributed.

We have had essential help and input from:

Weishi Wan - tracking runs with COSY

A. Drozdin - designs for halo scraping and injection

I. Stumer and N. Mokhov - shielding studies and designs

Bill Ng and Ernest Courant for lattice contributions

Juan Gallardo and Martin Berz for helpful advice

Two lattices

Currently there are two lattice designs, one by Trbojevic and one by Johnstone and myself. For this talk, I will designate them by authors initials : T for Trbojevic's and JG for the Johnstone-Garren lattice.

These rings have both similarities and differences:

The designs of the Interaction Region are similar but not identical.

Both use the same principle for sextupole correction, however the structures of the Chromatic Correction Sections differ.

The arc modules are different in design and number.

The matching sections between the regions differ.

The JG lattice contains a long straight section for scraping and injection, the ring is closed geometrically and has zero momentum compaction.

The T lattice has not yet been completed; there is no scraping-injection straight section, the ring does not close and the momentum compaction is not quite zero.

After the T lattice has been completed, comparisons of ring size, dynamic aperture, and suitability for injection, scraping and rf will be made. If possible, the best features of each will be combined in a future design.

The balance of this talk is a description of the JG lattice.

The JG lattice

The first figure shows the lattice and beta functions of the full ring. The interaction region is in the center. One can see that the ring is symmetric about the IP. Three beta function curves are shown, for β_X, β_Y, and D.

The second figure shows the lattice and beta functions of the half ring with the IP at the left end. Each half ring is composed of six lattice components, which are labeled under the lattice schematic at the top.

The third figure shows an expanded view of the lattice schematic of the half ring, without the beta functions, with the six lattice components labeled. These components are:

IR - Interaction Region - this region begins with the IP; and contains the low beta quadrupoles, as well as dipoles and quadrupoles for matching into the the Chromatic Correction Section.

CC - Chromatic Correction Section - this region contains two pairs of sextupoles that control the horizontal and vertical chromaticity of the ring. The members of each pair have a betatron phase separation of 180^0

CCMAT - this region matches betas from CC into ARC.

ARC - this section, which contains dipoles and quadrupoles, is used to adjust the tunes and momentum compaction. Its bend angle is chosen to bring the total bend angle of the ring to 360^0.

SSMAT - this section matches the beta functions from the ARC into the SCRAPE, a straight section.

SCRAPE - this region is used for scraping, injection and rf.

Following these three figures, six others are shown, one for each component of the lattice.

In all of the lattice schematics, the boxes centered on the line represent dipoles, those above or below the line represent focusing or defocusing quadrupoles, respectively, and the small boxes centered on the line represent sextupoles.

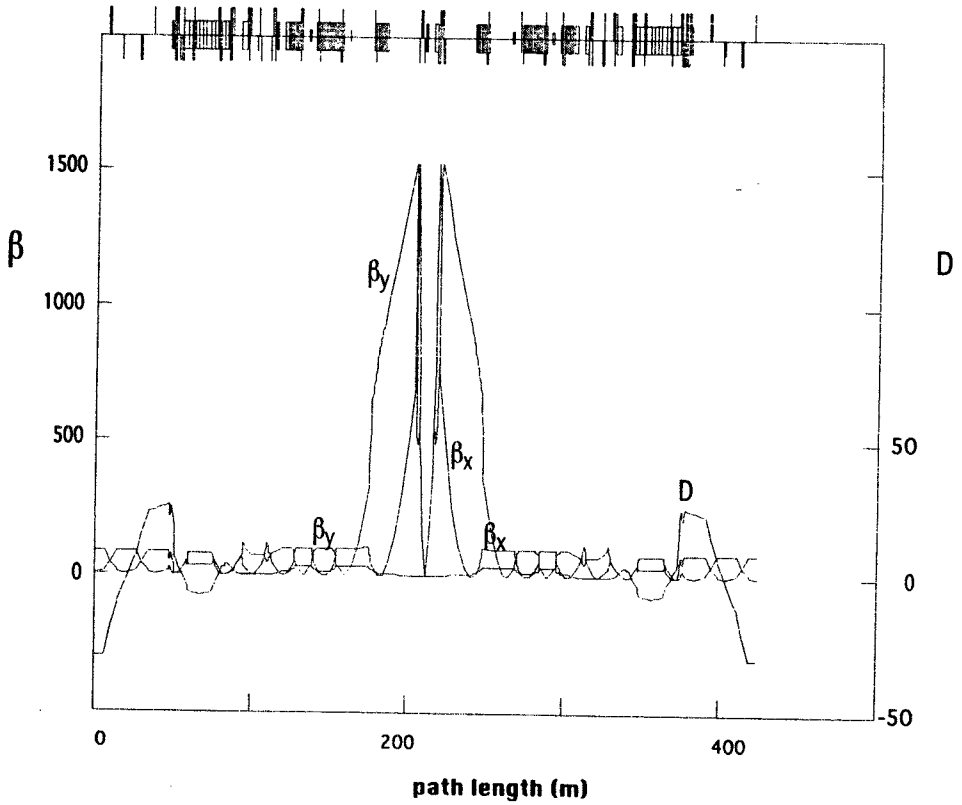

RING

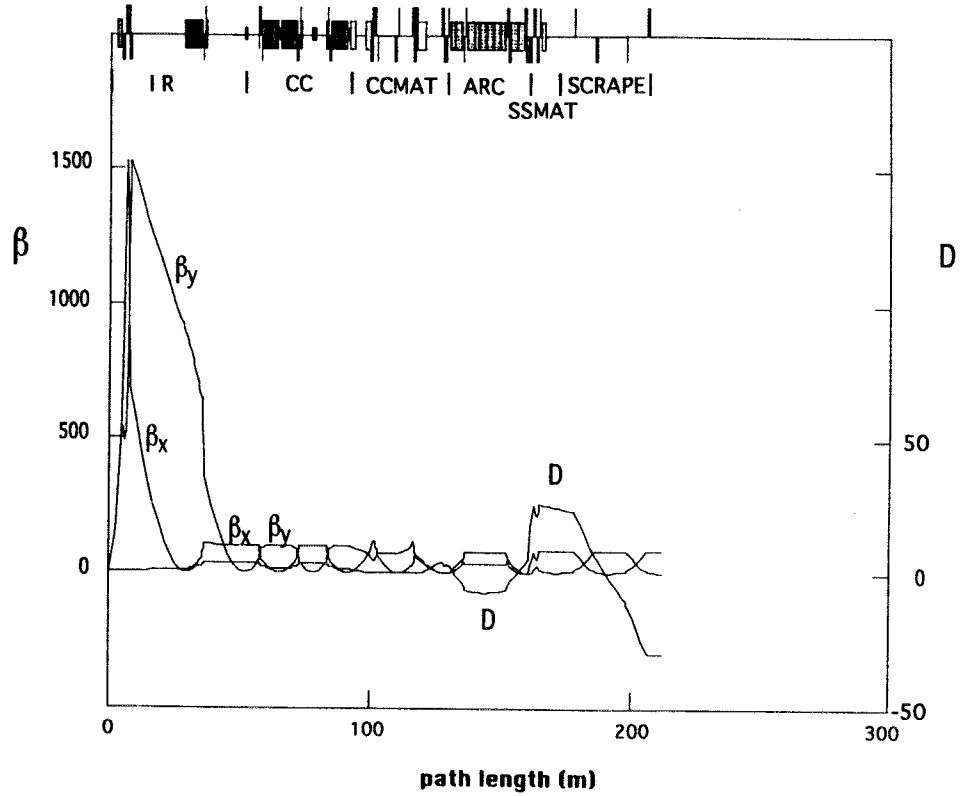

HALF RING

BEAMLINE OF HALF RING

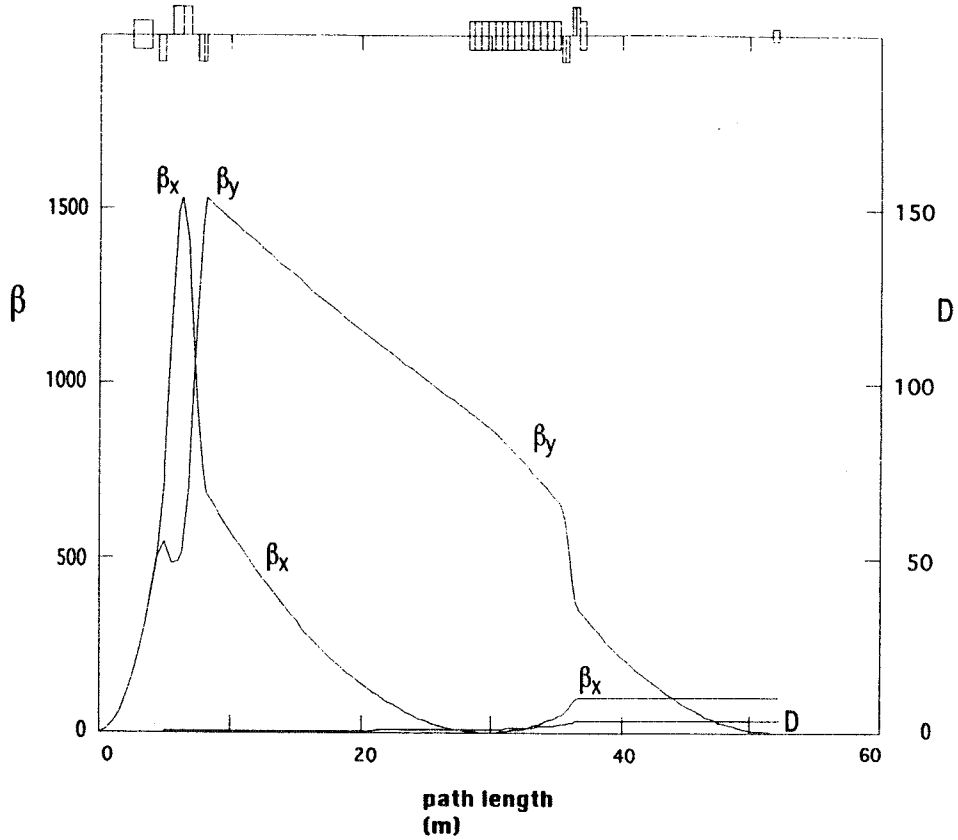

INTERACTION REGION

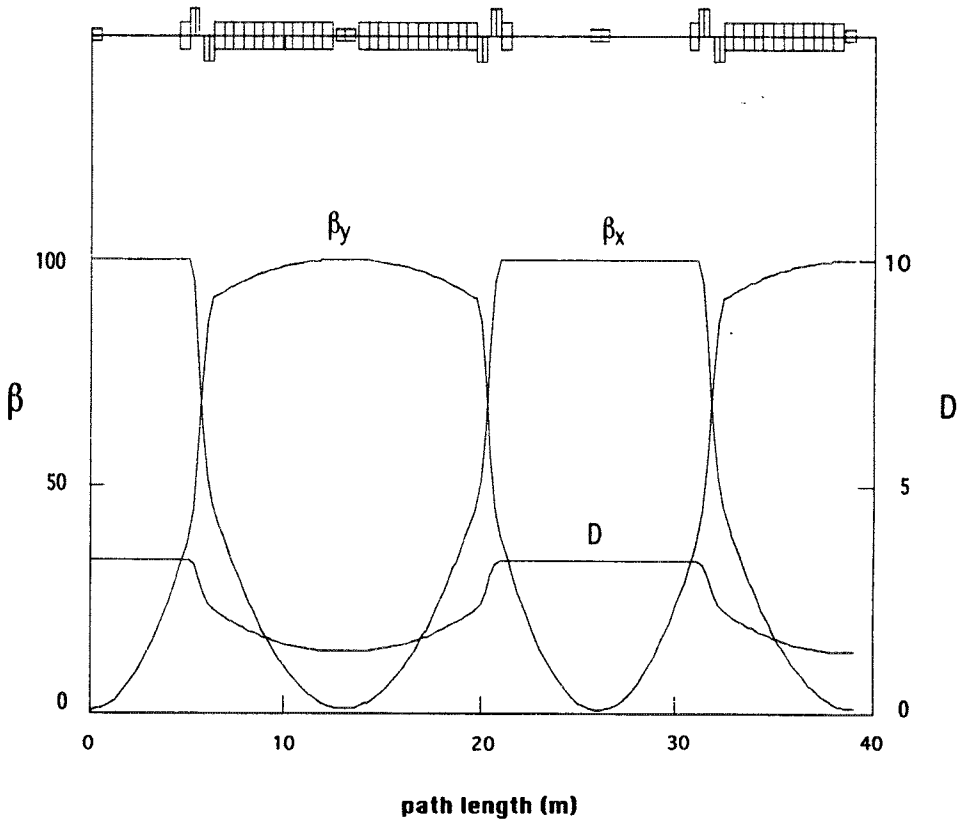

CHROMATIC CORRECTION SECTION

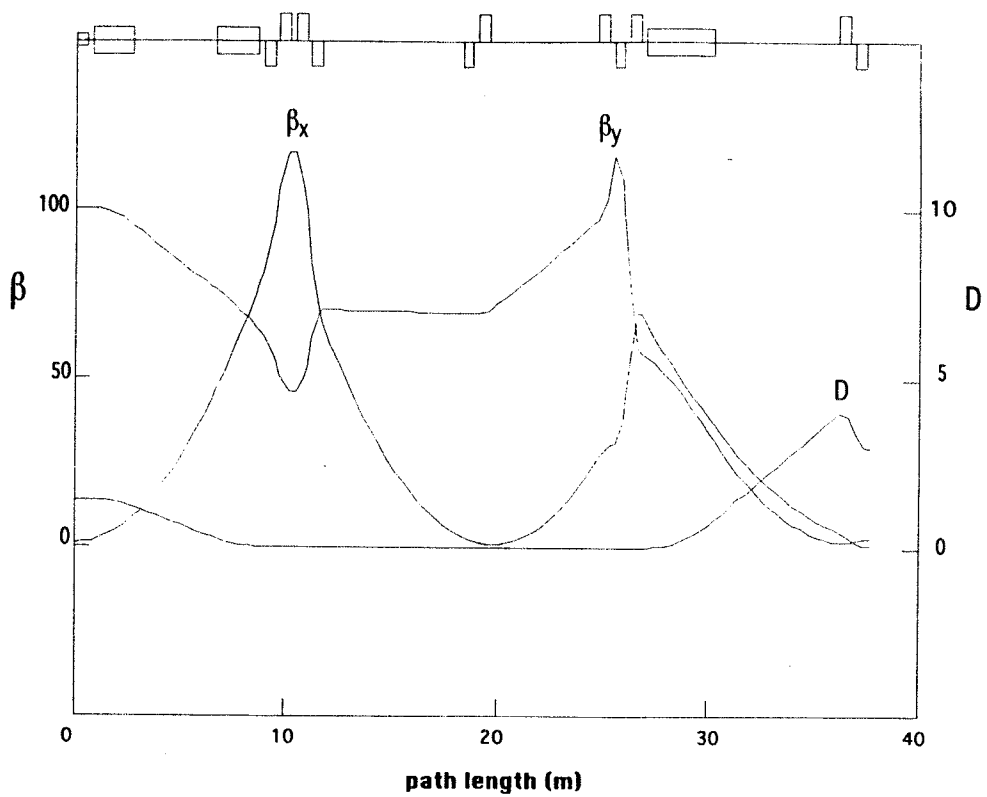

MATCHING REGION BETWEEN CHROMATIC CORRECTION SECTION AND ARC

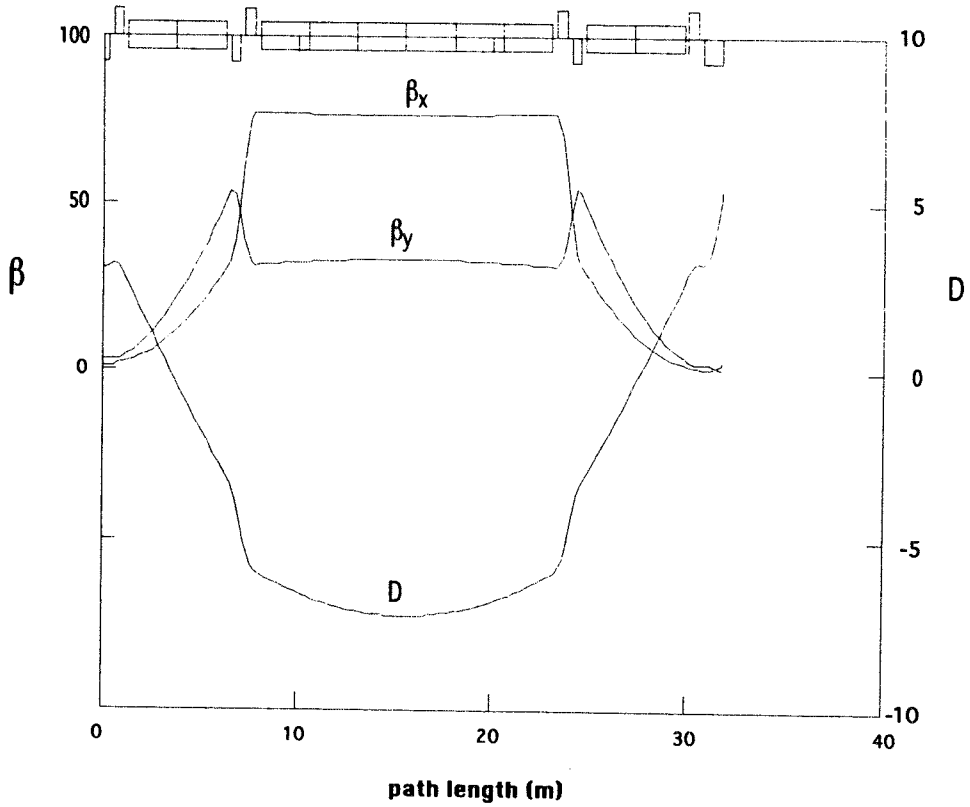

LOW MOMENTUM COMPACTION ARC

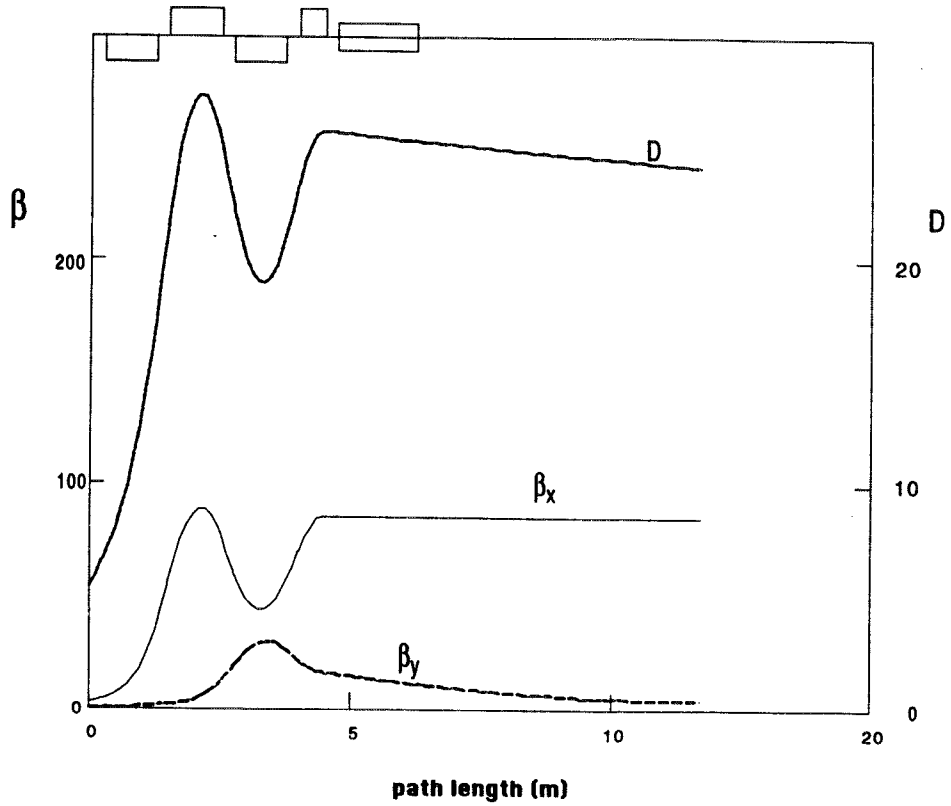

MATCHING SECTION TO SCRAPING STAIGHT SECTION

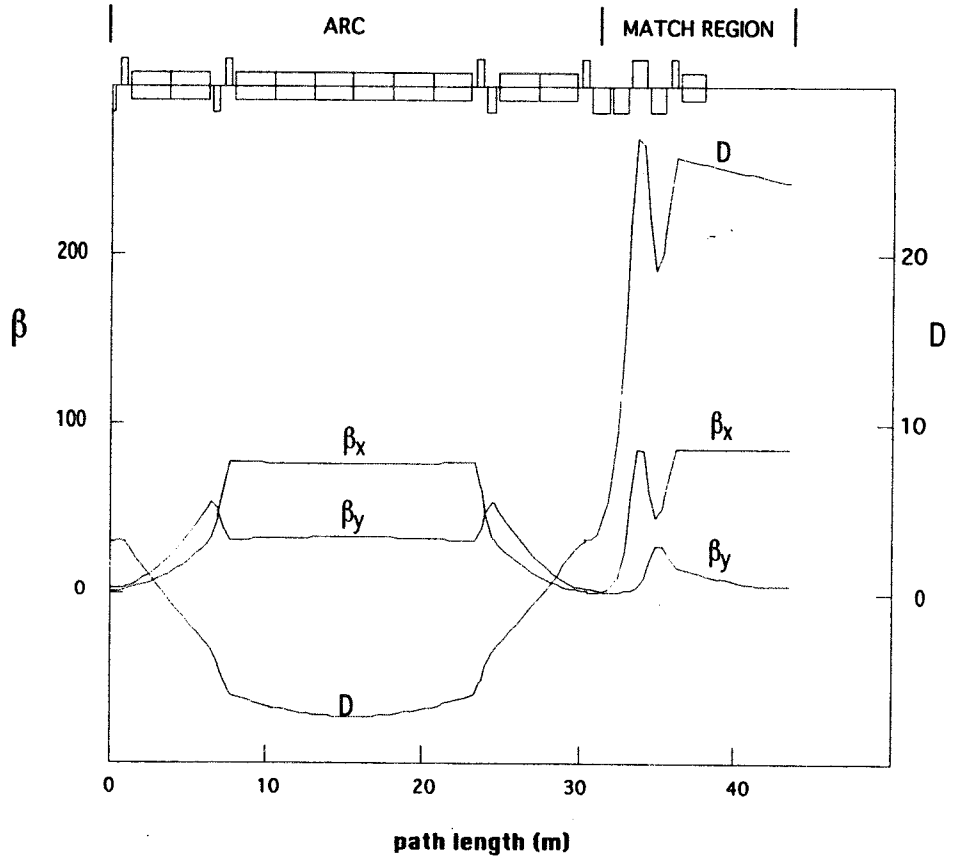

ARC AND MATCHING REGION TO SCRAPING STAIGHT SECTION

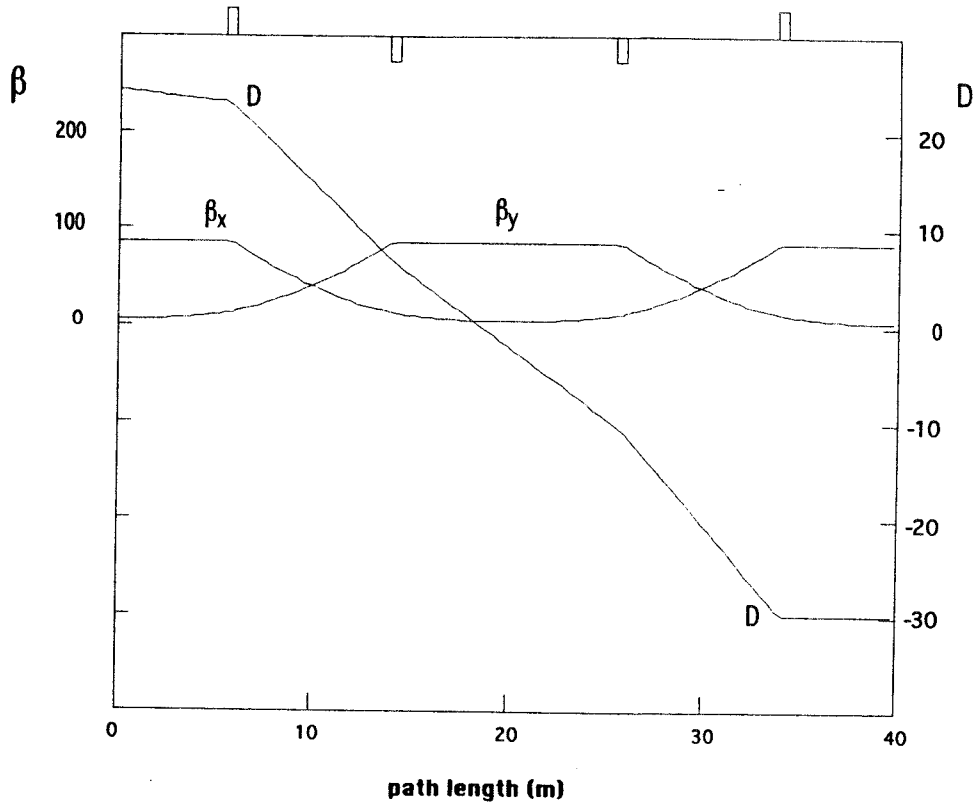

LEFT SIDE OF SCRAPING STAIGHT SECTION

Muon Collider Rings

LATTICE: ME, Fermilab
Martin Berz, Michigan State
Al Garren, UCLA/LBL
Bill Ng, Fermilab
Dejan Trbojevic, BNL
Weishi Wan, Fermilab

Scraping & Beam Losses: Sasha Drozhdin

Bkgrounds & Detectors: Nikolai Mokhov
Iuliu Stumer

SPECIAL ACKNOWLEDGEMENT SECTION

Juan Gallardo, Bob Palmer, Ernest Courant, BNL

David Cline, Kevin Lee, UCLA

CAROL JOHNSTONE (FNAL)

CERN COLLABORATORS

Bruno Autin

Walter Scandale

Andre Verdier

IR DESIGN

Yes, Virginia, there is no Santa Claus

The IRs do NOT scale with energy

50 on 50 GeV

- Backgrounds are soft; Dipole (sweep) immediate to IP
- IR triplet (low-β quads) are short (.6 - 1.4m)
- 8T poletip fields (higher fields will not help IR design)

250 on 250 GeV

- Backgrounds are high & large angle
- This may be the hardest machine design
- Interim Solution: relax β^*, move IR quads back from IP

1.5 on 1.5 TeV

- Backgrounds high energy, but small beam divergence, little makes it into detector from IR region
- Background - sweep dipoles for arcs are essential (8T & 8m long bucked pair)
- IR quadrupoles are long (up to 10m) IR design assumes 12T poletip fields
- Shielding superconducting magnets is tricky & conflict with strict impedance requirements

- LOCAL CHROMATIC CORRECTION IS REQUIRED
  NONE OF THE RINGS WORK WITH GLOBALLY-DISTRIBUTED SEXTUPOLES

	Chromaticity	β_{max}	Circumference	Scraping
50 on 50 GeV	-60 - -90	1.5 km ($\beta^* = 4$ cm)	300-500 m	SOLID COLLIMATOR
1.5 TeV on 1.5 TeV	-2000	150 km ($\beta^* \approx 3$ mm)	7.5-8.5 km	electrostatic septum ⊕ extraction lambertson

↑ 2 x LHC IR (β^* of .5 m)

50 on 50 GeV IR

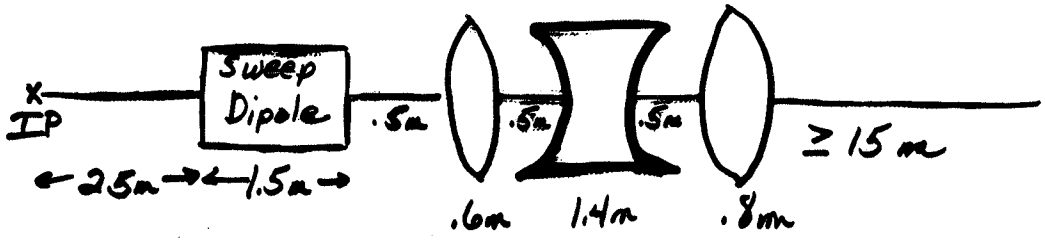

50 on 50 GeV

←— 4.5 m —→ ←— 3.8 m —→

250 GeV on 250 GeV

←— 7 m —→ ← 10 m? —→

2.5 on 1.5 TeV

←— 4-6 m —→ ←— 28 m —→

IP ← triplet →

LATTICE as of 9/97

Circumference ~380 m no scraping/injection

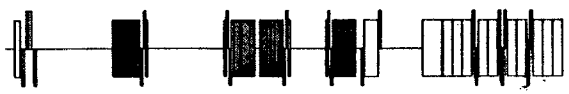

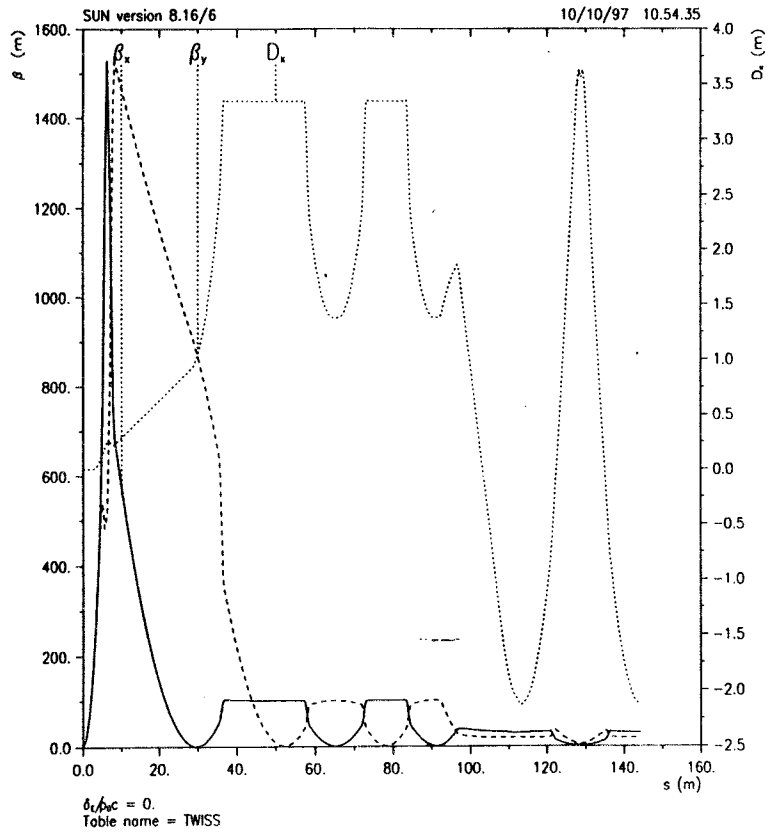

THE RACE TO SHRINK THE 50 on 50 MACHINE BEFORE THE FAIRMONT

LINDER WENTZLER [illegible]

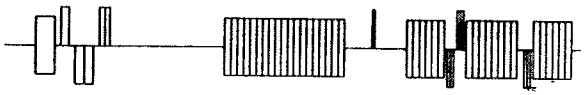

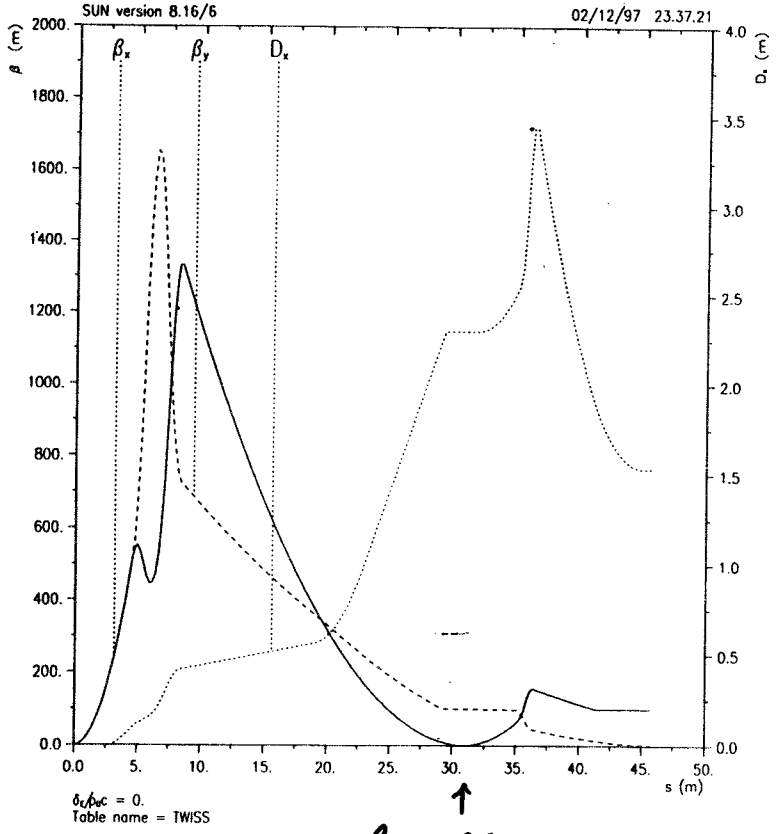

$\beta_x \approx .25$ m

Johnstone [illegible]

Circumference 300 m (to close need 40-50 m straight which will be used for scraping/injecti

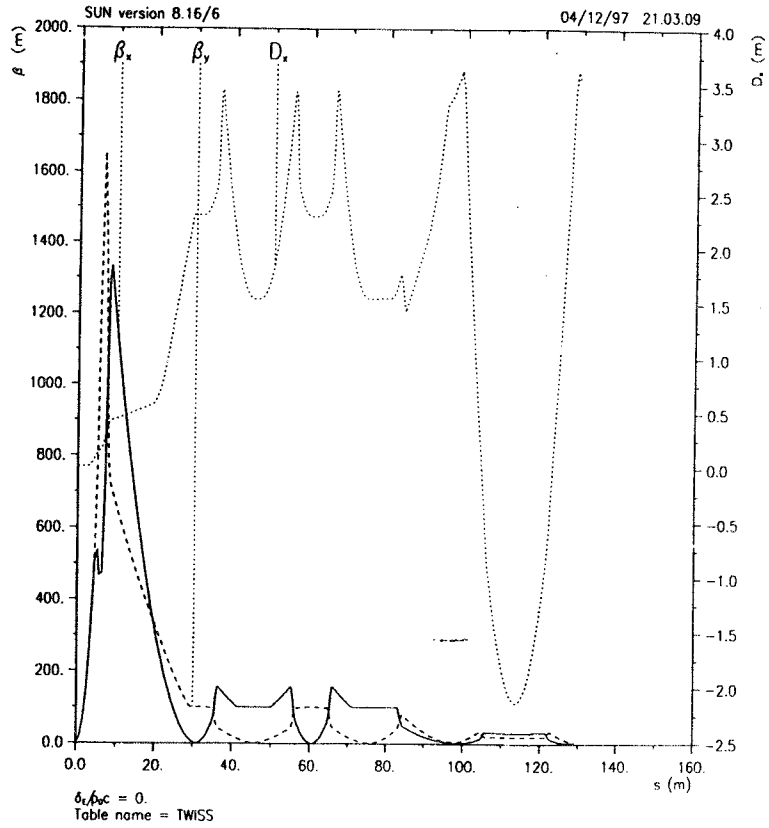

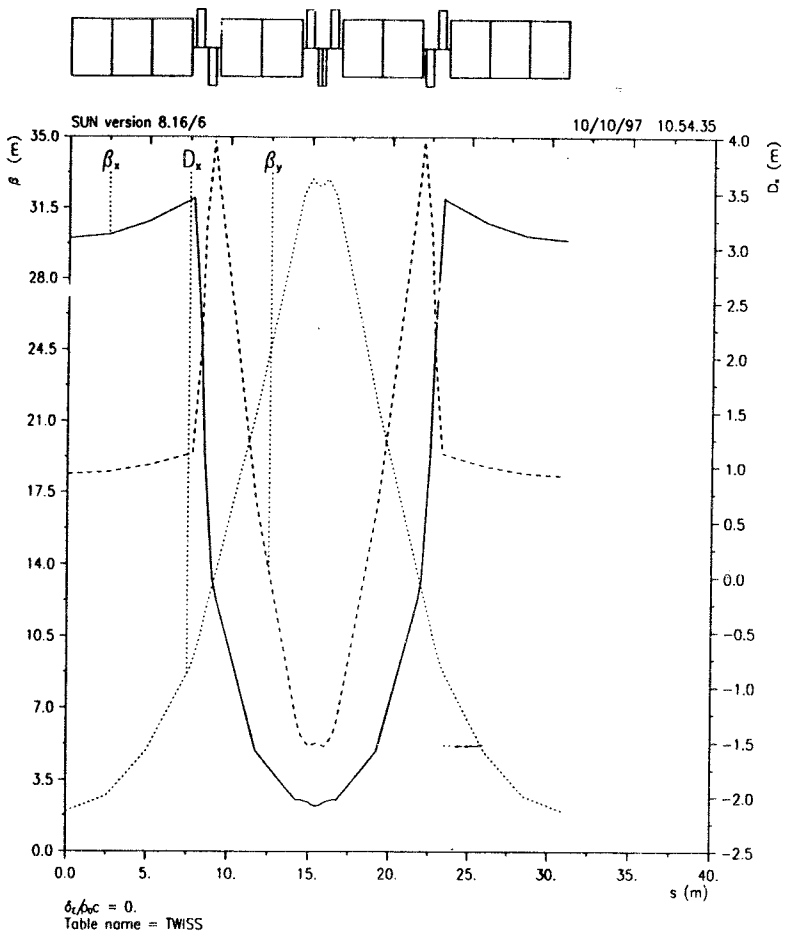

→ New FMC arc module based on a double low-β. Center F quad adjusts momentum compaction w/o disturbing β functions. β functions comparable to FODO

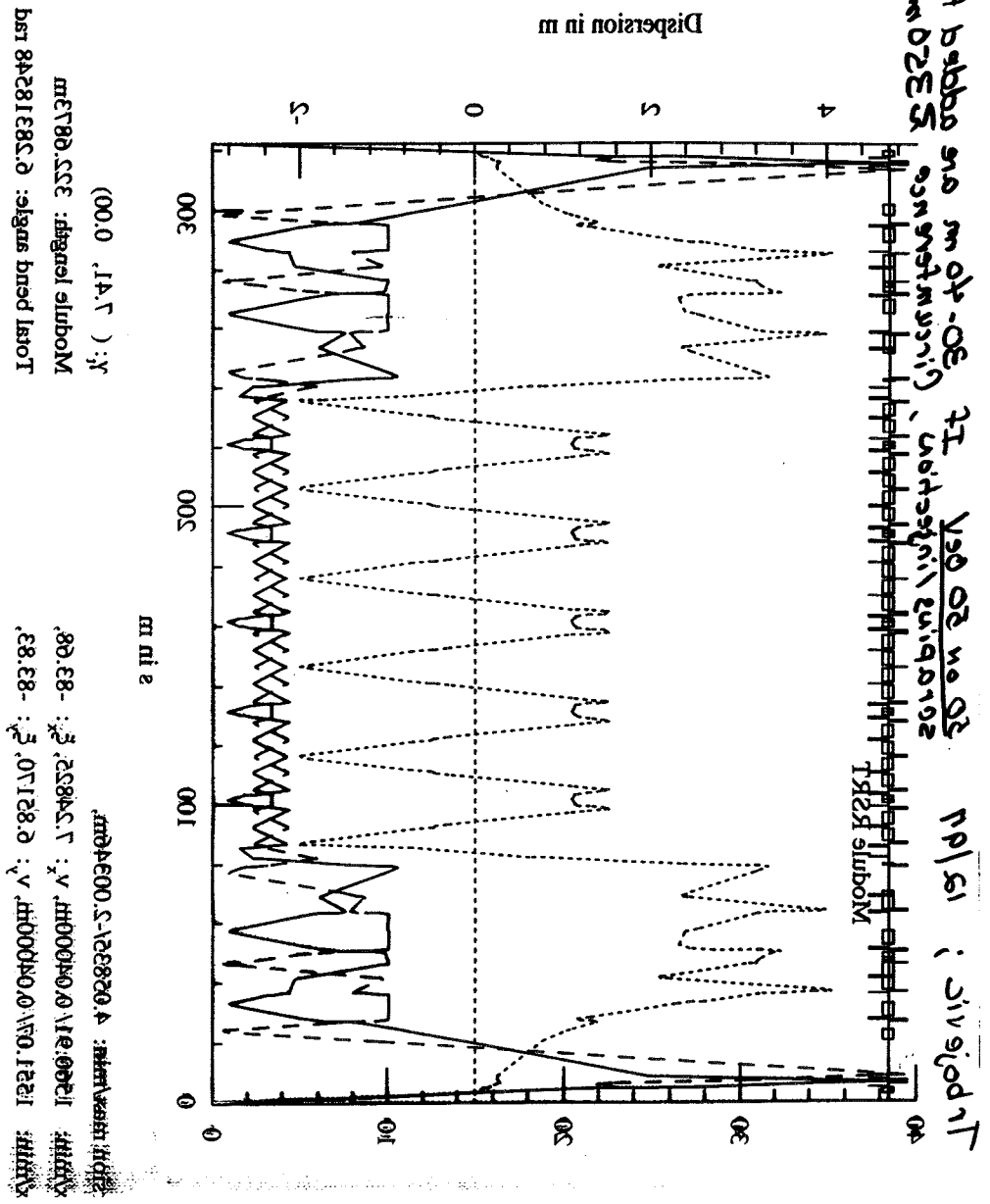

CHROMATIC CORRECTION SEXTUPOLE STRENGTH REDUCED BY A FACTOR of 10

[for the high resolution, low-momentum spread lattice]

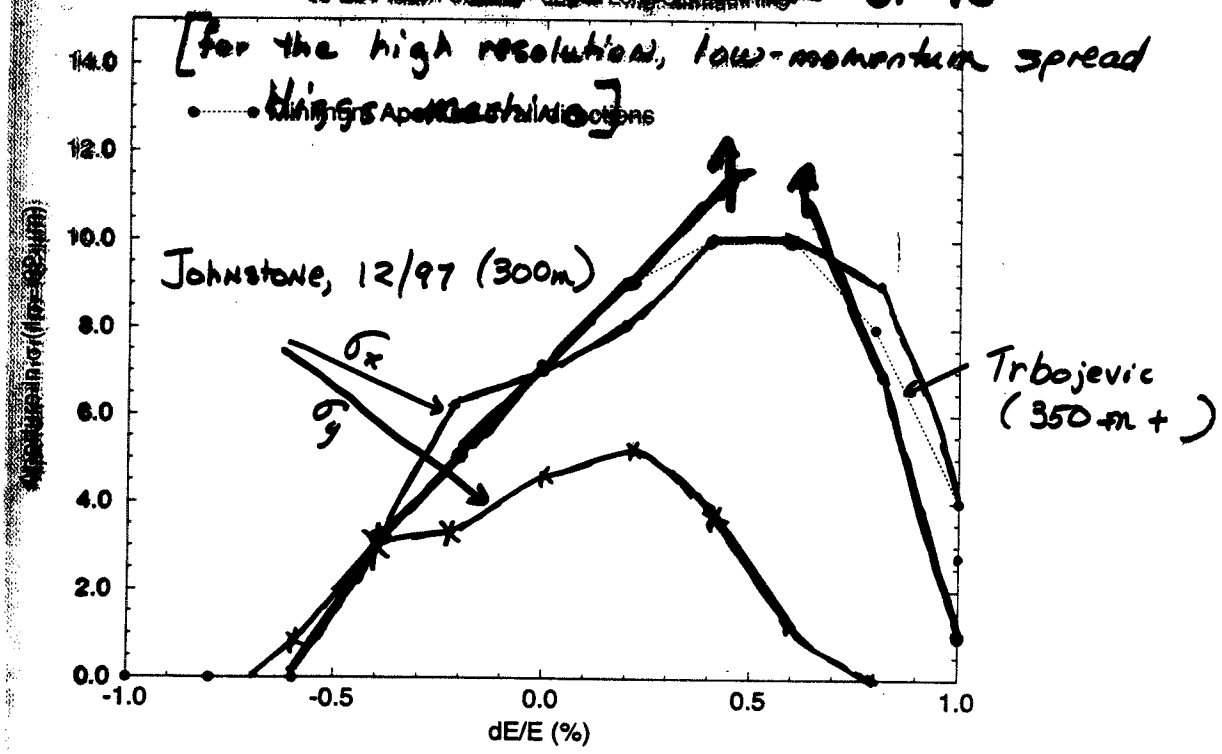

W. WAN

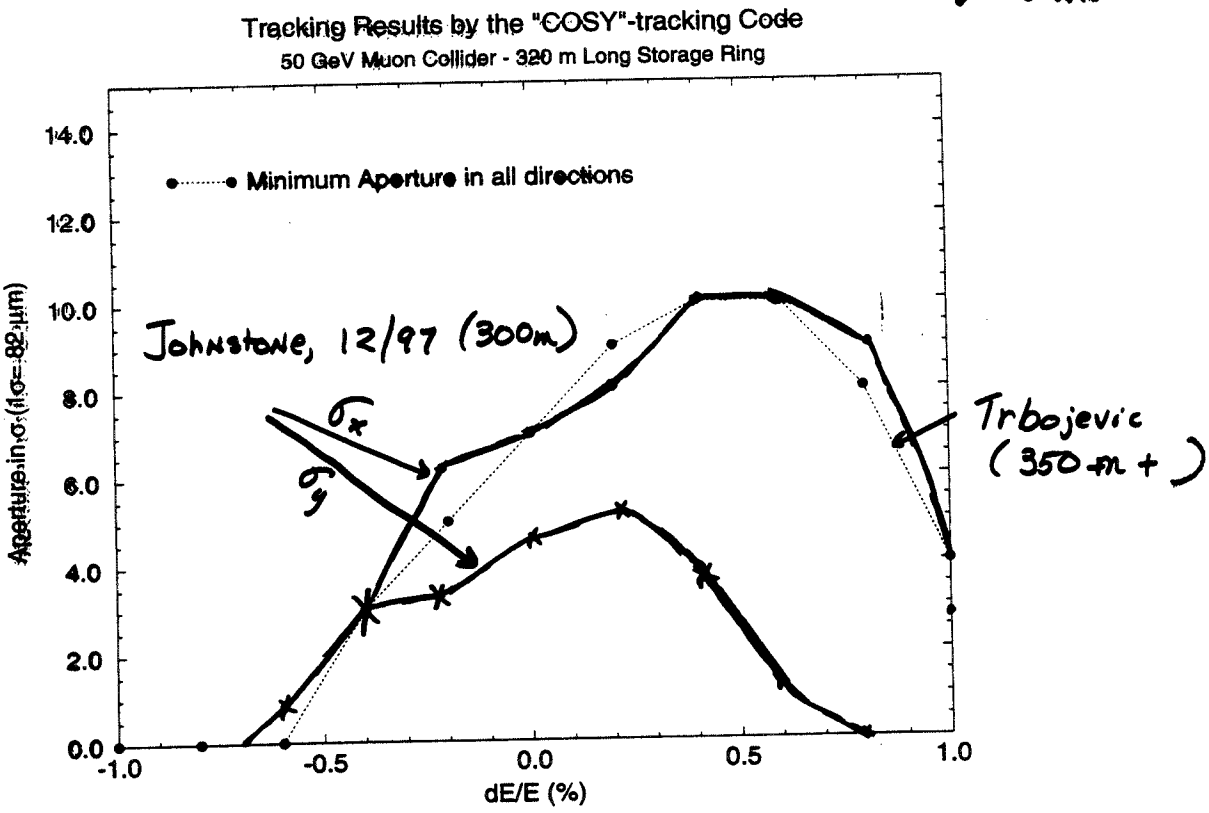

The differences in Dynamic Aperture are not significant

1). Dispersion at horizontal sextupoles is factor of 2 lower in Johnstone design

2). Tunes have not been optimized in Johnstone design.

3) Shorter sextupoles in Trbojevic design

Lattice for 50-50 GeV μ Collider

King Y Ng

Fermilab

12-11-97

I. Some Comments on lattice designed mostly by Dejan + partly by me

1. lattice is not closed yet, now 322.4 m

		Length	Bend angle
IR	2×86.74	173.48 m	162.7°
Arc	5×29.80	149.00 m	197.3°
Total		322.48 m	360.0°

∴ when it is closed, may need to add 20 to 40 m or 340 to 360 m

2. Each plane, 2 families of sextupoles

one for local IR correction ← well matched for nonlinearity cancellation

one for arc ← not matched

∴ if the sextupoles in arc are removed, aperture should be larger.

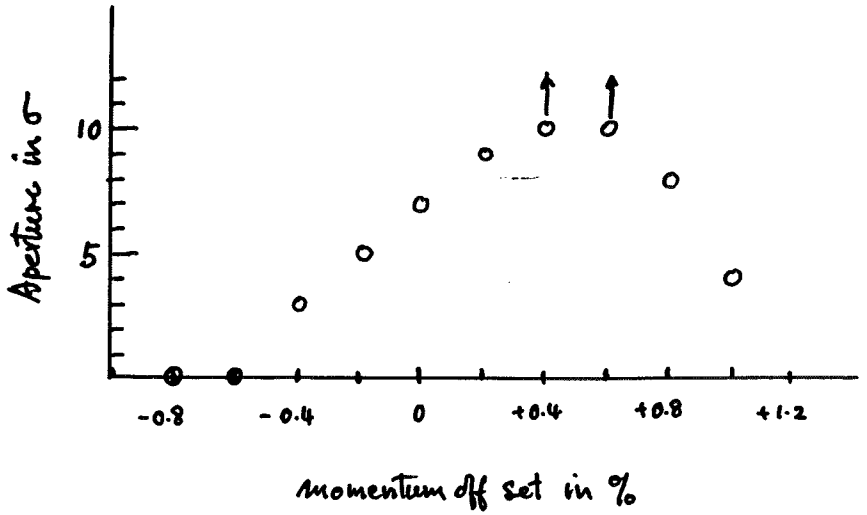

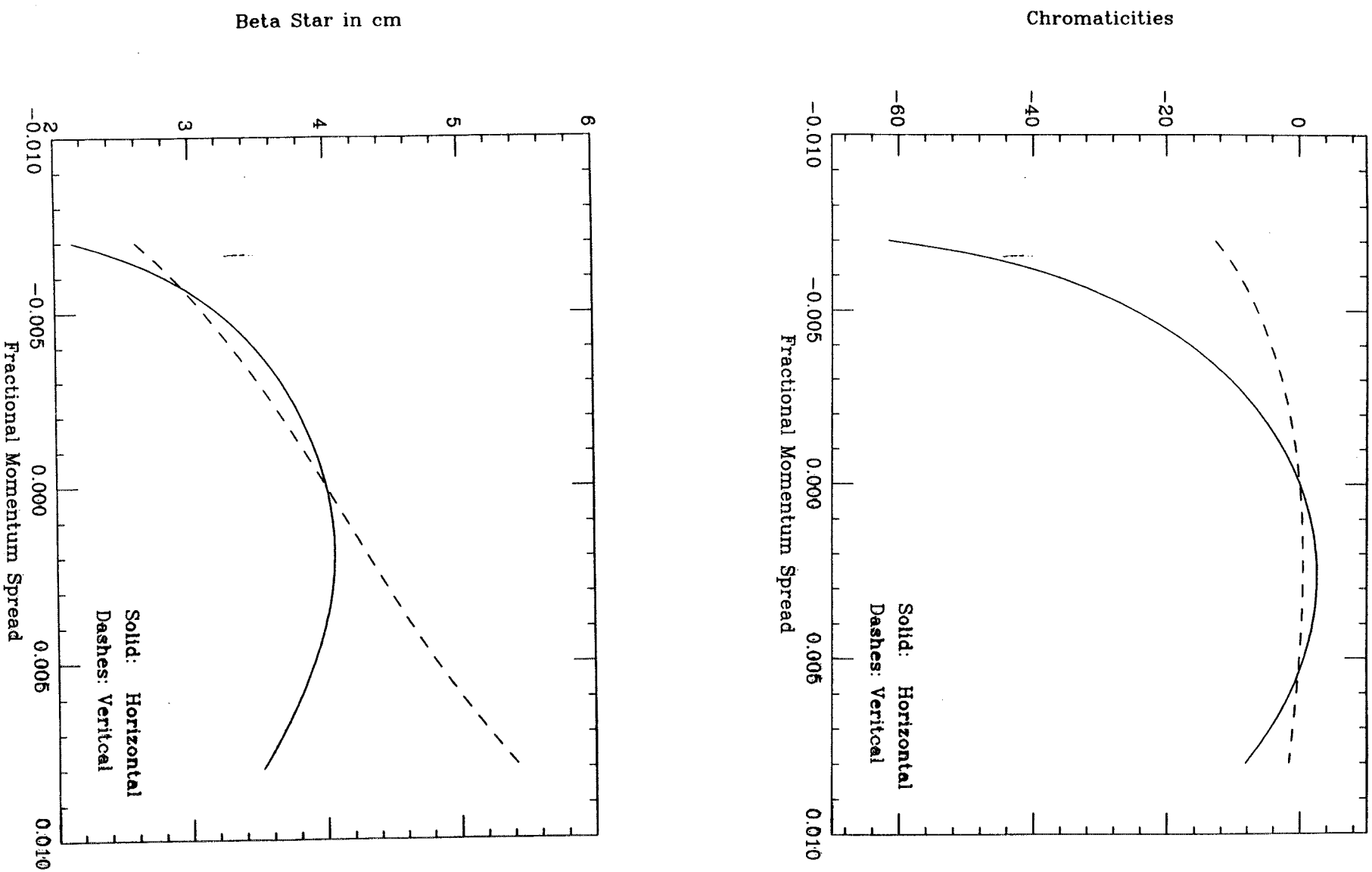
Chromaticities
0
−20
−40
−60
−0.010
−0.005
0.000
0.005
0.010
Fractional Momentum Spread
Solid: Horizontal
Dashes: Veritcal

Beta Star in cm
6
5
4
3
2
−0.010
−0.005
0.000
0.005
0.010
Fractional Momentum Spread
Solid: Horizontal
Dashes: Veritcal

II Problems in lattice

1. What we have now is the aperture of the base lattice

   If we add higher-order field error
   misalignment
   fringe field

   Aperture will be reduced.

   For the Tau-Charm factory lattice (Beijing) (~380m), it was pointed out by KEK that the aperture has been very much reduced by fringe field.

2. Chromaticities as fcn. of momentum off set are bad.

   Higher-order chromaticities can't be cancelled by only 1 family of sextupoles in each plane

   β^* as fcns of momentum spread are bad.

   Need 3 families of sextupoles in each plane

   But no space to place sextupoles in limited number of FMC modules.

---

50 GeV + 50 GeV $p\bar{p}$ collider

Injected bunch has $\sigma_\delta = 0.0010$ $\sigma_z = 0.04\,m$

Synchrotron tune $\nu_s = \frac{|\eta|\sigma_\delta}{\omega_0 \sigma_z}$

Rf voltage $V_{rf} = \frac{2\pi\beta^2 E \nu_s^2}{|\eta| h} \approx \frac{|\eta|}{h} E \left(\frac{\sigma_\delta}{\sigma_z}\right)^2 \frac{2\pi R^2}{c^2} = \frac{|\eta|}{h} \frac{E}{2\pi} \left(\frac{C\sigma_\delta}{\sigma_z}\right)^2$

Let bucket height be $\hat{\delta}$, then

$$\frac{\hat{\delta}}{\sigma_\delta} = \frac{\lambda_{rf}}{\pi\sigma_z} = \frac{C}{\pi h \sigma_z} \quad \text{or} \quad h = \frac{C}{\pi\sigma_z}\frac{\sigma_\delta}{\hat{\delta}}$$

Assume $\hat{\delta}/\sigma_\delta = 5$ $C = 380\,m \Longrightarrow h = 604.79$

Take $h = 605$, then

$$V_{rf} = 1187.2\,|\eta|\ MV$$

V_{rf} (MV)	$\lvert\eta\rvert$	γ_t	ν_s
1	0.000843	34.5	0.00127
5	0.00421	15.4	0.00637
10	0.00843	10.9	0.0127
15	0.01264	8.9	0.0191
20	0.01684	7.7	0.0255

$f_0 = 0.7882\,MHz$

$h = 605$

$f_{rf} = 477.3\,MHz$

$$\alpha_0 = \frac{1}{\gamma_t^2} = \frac{1}{C}\sum_i D_i \theta_i$$

IR will increase C without increasing θ_i by much so will help α_0 to become smaller.

III Another approach

1. Use FODO cells instead of FMC modules

Can put into the arc ~ 30 FODO cells

each of length ~ 9-10 m

phase advance = 90°

I have tried to build these cells, the quad gradients and dipole strength are quite reasonable

Now we can place 3 families of sextupoles to cancel 2nd order chromaticity as well as to assure β^* <u>not</u> a fcn. of momentum spread.

2. Use unequal β^*

for example $\beta^*_y = 4\,cm.$ $\beta^*_x = 40\,cm.$

will lose luminosity by $\frac{1}{2}$ (bad)

<u>Good things.</u>

- chromaticities will be much lower and can be easily corrected.
- Hopefully, may not need local correction
  ∴ shorten ring's circumference & gain back some luminosity
- If the bunch length be shortened, one may consider $\beta^*_y = 2\,cm$ $\beta^*_x = 20\,cm$ & gain back all luminosity.
- For NLC, background at IP will be much smaller for flat beam.
  We need to study this for μ-collider
  If this is also true, the background dipole can be shortened, 1st quad can be pushed in, chromaticities will be further reduced.

Estimation:

1st quad at 5m, 2nd quad at 6m

$\beta^* = 0.04m. \Rightarrow \beta \approx \frac{s^2}{\beta^*} = 625m$ at 5m.

$5\sigma = 4.58$ cm. 2cm shielding

quad. aperture = 6.58 cm.

For 8T pole tip field,

$$\text{max quad gradient} = \frac{8}{0.0658} = 122 \text{ T/m}$$

For a 1m quad $k = \frac{B'l}{Bq} = \frac{122}{166.7} = 0.73\ m^{-1}$

At 5m $\alpha = -\frac{s}{\beta^*} = -125$

To bend α to +125, quad strength required is

$$\Delta\alpha = -\frac{2s}{\beta^*} = k\beta_{5m.} \approx \frac{ks^2}{\beta^*}$$

$$\therefore k = -\frac{2}{s} = -0.4\ m^{-1}$$ (less than max strength)

Chromaticity

$$\xi = \sum \frac{k\beta}{4\pi} \sim -\frac{1}{4\pi}\frac{2}{s}\frac{s^2}{\beta^*} = -\frac{s}{2\pi\beta^*} = -20$$

$\therefore \xi_{1R} \sim -40$ vs. ~ -100 if $\beta_x^* = \beta_y^* = 0.04$ m.

Example 1

Use a doublet: 1st quad changes α to $-\alpha$ in 1st plane
2nd quad changes α to $-\alpha$ in 2nd plane

s (m)	0	5	6	
β(m)	0.04	628	400	$\xi = -3.98$
α	0	−125, +125	+100, −199.6	
$\gamma(m^{-1})$	25	25, 25	25	
β(m)	0.40	62.9	160.8	$\xi = -7.54$
α	0	−12.5, −37.7	−60.2, +60.2	
$\gamma(m^{-1})$	2.5	2.5, 22.56	22.56	

1st quad strength $k = -0.40\ m^{-1}$

2nd quad strength $k = +0.75\ m^{-1}$ due to smaller β

Example 2

Use a doublet, each of strength $|k| = 0.6\ m^{-1}$

s (m)	0	5	6	
β (m)	0.04	625	225	$\xi = -22$
α	0	$-125, +250$	$+150, -15$	
γ (m^{-1})	25	25, 100	100	

β (m)	0.40	62.9	203.6	$\xi = -6.7$
α	0	$-12.5, -50.24$	$-90.4, +31.7$	
γ (m^{-1})	2.5	2.5, 40.2	40.2	

When optimized, should get $\xi_x \cong \xi_y \cong -30$

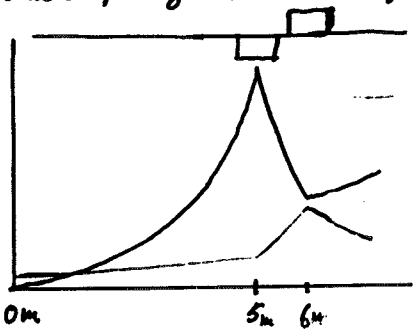

JHF

Y. Mori
KEK-Tanashi

-Japan Hadron Facility-

Interdiciplinary facility based on 50-GeV high intensity proton accelerator comlex

Accelerator complex:

3-GeV rapid cycling proton synchrotron
50-GeV high intensity proton synchrotron

* K-arena	50GeV	Neutrino oscillation Symmetries violation Hypernuclei High density nuclear matter
* E-arena	3GeV	Unstable nuclei
* M-arena	3GeV	Muon physics
* N-arena	3GeV	Spallation neutron source

JHF 50GeV Proton Synchrotron Complex

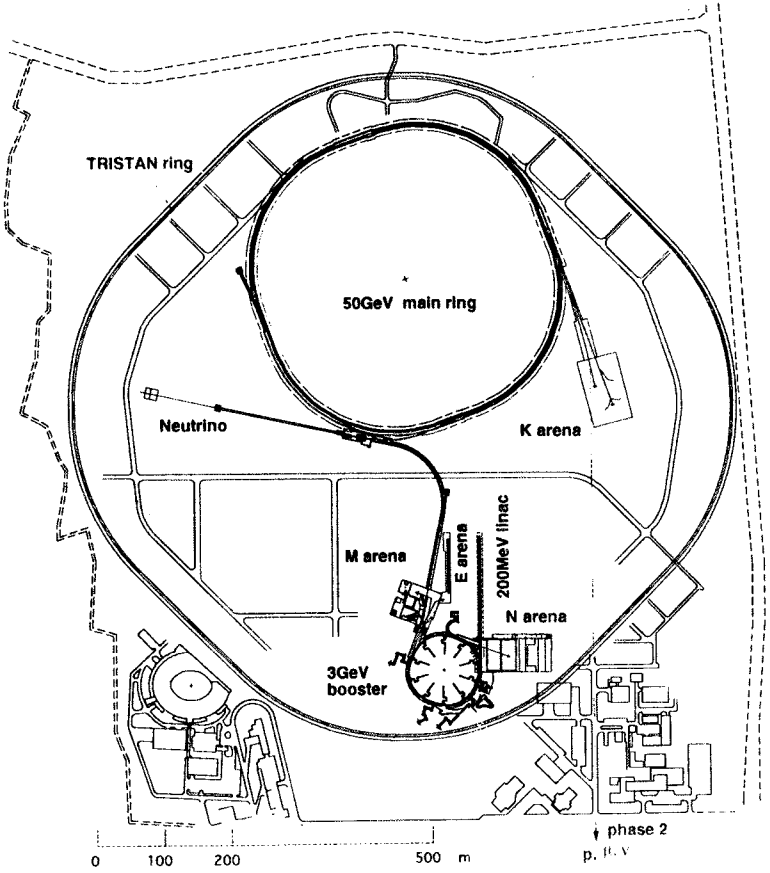

Accelerator Complex

- **200-MeV linac** — **high brightness**

accelerated particle	H^- ion
peak beam current	>30(50) mA (25Hz, 400μs)
structures	RFQ + DTL + ACS

- **3-GeV booster** — **rapid cycling**

intensity	5×10^{13} ppp
repetition rate	25Hz
beam power	0.6 MW → 1.2MW ↗ >2M
RF frequency	1.99-3.43MHz
RF voltage	389kV
circumference	339.4m (KEK-PS tunnel)

- **50-GeV main ring** — **transition free(negative α)**

intensity	2×10^{14} ppp
acceleration cycle	0.3Hz -> > 1Hz
RF frequency	3.43-3.51MHz
RF voltage	270kV
momentum compaction	~ -10^{-3}
circumference	1442m (north site of KEK)

Parameters

Circumference	1445 m
Average Radius	229.979 m
Injection Energy	3 GeV
Extraction Energy	50 GeV
Particle Per Pulse	2×10^{14}
Revolution Period	
at Injection	4.9629 ms
at Extraction	4.8209 ms
Repetition Rate	0.3 Hz
Injection	0.12 s
Acceleration	1.9 s
parabola	0.1 s
linear	1.7 s
parabola	0.1 s
Slow Extraction	0.7 s
Decreasing Field	0.7 s
Average Current	9.4 mA
Circulating Current	
at Injection	6.86 A
at Extraction	7.06 A
Bunching Factor	
at Injection	0.273
at Extraction	0.038

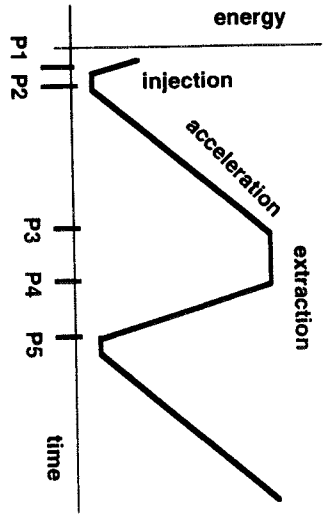

P1 - P2(injection)	0.12 s
P2 - P3(acceleration)	1.9 s
P3 - P4(extraction)	0.7 s
P4 - P5	0.7 s
total	3.42 s
slow extraction of 50GeV	
duty factor	0.20
average current	9.4μA

Distinctive Features

(a) BEAM OPTICS — Small Beam Loss

Lattice

*Imaginary Transition-gamma Lattice

Slow Beam Extraction

*Preseptum + Dyn. Bump (1/3-, 1/2-integer resonance)

(b) HARDWARES

RF System

*New Type of RF Cavity Magnetic Alloy(MA) Core, R&D

High Field Gradient >75kV/m

No Frequency Tuning Q=1~2

Magnet Power Supply

*Converter-chopper Scheme > IGBT PS, R&D, ~1MW, World Largest!

Suppress Reactive Power

High Speed Control

*Double-fed Adjustable Flywheel Generator(DAFG)

Suppress Active Power

Imaginary Transition-gamma Lattice

Transition Energy

$\eta = \alpha - \frac{1}{\gamma_t^2} = 0 \quad , \alpha = \frac{\Delta L}{L} \Big/ \frac{\Delta p}{p}$: momentum compaction factor

no phase stability

non-linear effects: Johnsen effect,Umstatter effect

instabilities: Keil-Schnell criterion

----> **"beam loss"**

If ordinary FODO lattice is applied to 50-GeV PS,

$\alpha_p \approx \frac{1}{\nu_x^2} > 0$ $\Rightarrow \gamma_t \approx \nu_x$

cf. $\gamma_t \approx \nu_x \approx \frac{R}{\bar{\beta}} \approx 20$ (R=200m, $\bar{\beta}$=10m)

Transition Energy ~ 20GeV

Imaginary Transition-gamma Lattice

momentum compaction: $\alpha = \frac{1}{C}\oint \frac{D(s)}{\rho(s)} ds$

$\alpha < 0$: **negative dispersion at B-magnet**

$\Longrightarrow$ **imaginary** γ_t

$$\alpha = \frac{\nu^2}{R}\sum_k \frac{|a_k|^2}{\nu^2 - k^2}$$

$$\text{where } a_k = \frac{1}{2\pi}\oint \frac{\beta^{n/2}(\phi)}{\rho(\phi)} \exp(-ik\phi) d\phi$$

If $\nu < K$,

a_k (K - *th harmonic modulation*, $k = \pm K$) $\Rightarrow$ $\alpha < 0$

" If ν is slightly less than K, the term k=±K in eq. is large and negative , and can be made to cancel the leading term k=0."

Imaginary Transition-gamma Lattice

(1) *β–modulation* * trim Q

*β, D : modulated: LARGE APERTURE

(2) *ρ–modulation* missing B magnet section

* small β - modulation: SMALL APERTURE

* large ring

Momentum Compaction Factor in ρ-modulation

$$\alpha = \frac{\nu^2}{R}\sum_k \frac{|a_k|^2}{\nu^2 - k^2} \approx \frac{1}{\nu^2}\left[1 + \frac{2\sin^2(\xi\pi)}{\pi^2}\left(\frac{1}{1-\xi}\right)^2 \frac{\nu^2}{\nu^2 - n^2}\right]$$

$$\phi > 2\pi\sqrt{\nu^2\left\{1 + \frac{2\sin^2\xi}{\pi^2}\left(\frac{1}{1-\xi}\right)^2\right\}}$$

$$\xi = \frac{L_e}{C}$$

where

C = Total Length of Unit Module,

Le = Length of Missing Bending Magnet Section.

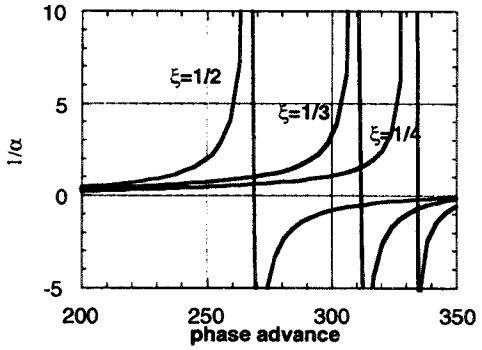

Imginary Transition-gamma Lattice

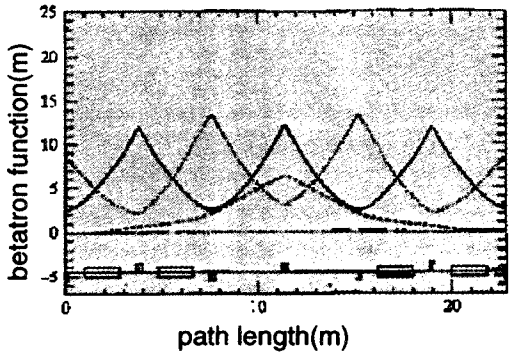

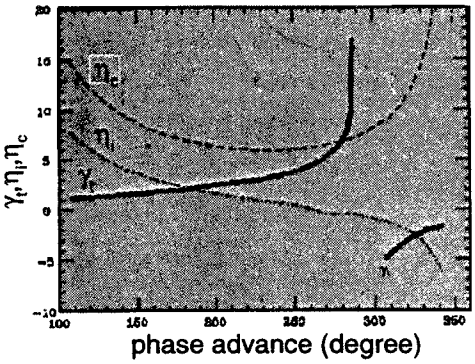

RF System

A high-intensity medium-energy proton synchrotron

A large RF accelerating voltage is needed because,

***large ring radius**

***fast rate of change of the dipole magnetic field**

Effective RF Field Gradient (RF Voltage per Unit Length) should be raised as high as possible.

***The total length of the RF cavities becomes short.**

***Impedance seen by the beam becomes small.**

Conventional ferrite-loaded accelerating cavity suffers from,

a)μQf-value (≈shunt impedance per unit length), decreases along with the RF magnetic field strength.

b)Low Curie temperature, which is typically 100-200°C,limits use at the high RF field gradient.

c)High loss effect at the static magnetic field limits use at a high RF magnetic field.

d)Cavity with the high Q-value ferrite may excite the longitudinal coupled-bunch instability through a de-tuning process for curing high beam loading or in the parasitic mode.

Magnetic Alloy

A high-permeability soft magnetic alloy, such as FINEMET and METGLAS has become available for applying the RF cavity, recently.

Characteristics of MA:

(1) The μQf-value remains constant at a high RF magnetic field of more than 2 kG.
(2) A high Curie temperature, typically 570°C for FINEMET.
(3) No frequency tuning loop is necessary in the cavity control system because of its low Q-value (Q~1). This substantially widens the stable operating region of the cavity loading phase angle under heavy beam loading.
(4)The longitudinal coupled-bunch instability may be reduced, since the Q-value of the cavity is low.
(5) Fabrication of a large core is possible because the core is formed by winding the very thin tapes.

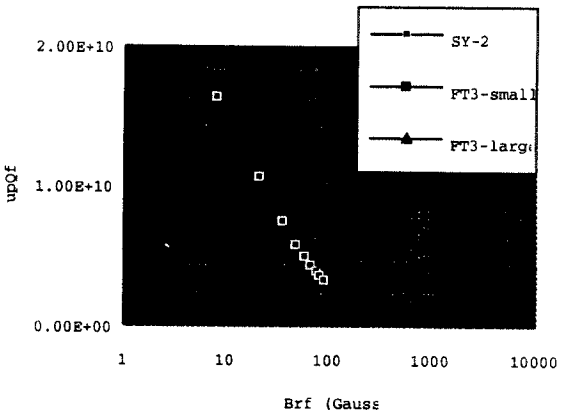

Typical characteristics of Ni-Zn ferrite and Magnetic Alloy(FINEMET).

Power Density vs. Effective Field Gradient

Average power density for a toroidal core is given by,

$$\bar{p} = \frac{W_L}{V} = \frac{2}{4\pi\mu_0 Qf\left(r_0^2 - r_i^2\right) \times \ln\left(\frac{r_2}{r_i}\right)} \times \left(\frac{V_g}{l}\right)^2 ,$$

where $\left(\frac{V_g}{l}\right)$ is an Effective Field Gradient(EFG).

a)Ferrite
EFG is less than ~15kV/m.
b)Magnetic Alloy
EFG can be more than 75kV/m !

MA consumes RF power but not so much for high intensity operation because the beam power is relatively large.

Relative Loading $y = I_b/I_c < 1$

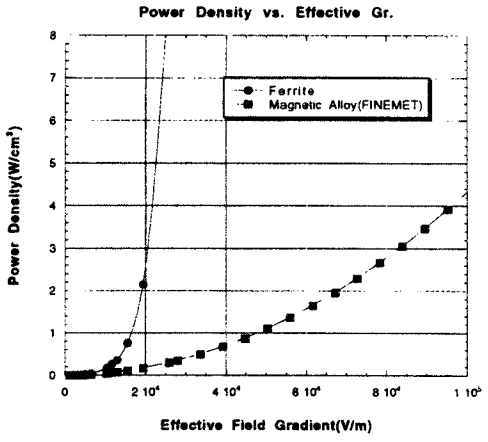

TEST CAVITY

*Single core (O.D=580mm,I.D=250mm, t=25mm)

*Direct water cooling

*RF power :30kW max.(B-class)

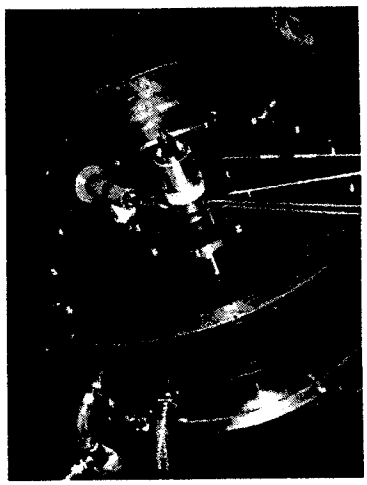

Achieved:

EFG = 220kV/m ! (5.5kV/core)

limited by RF amp.

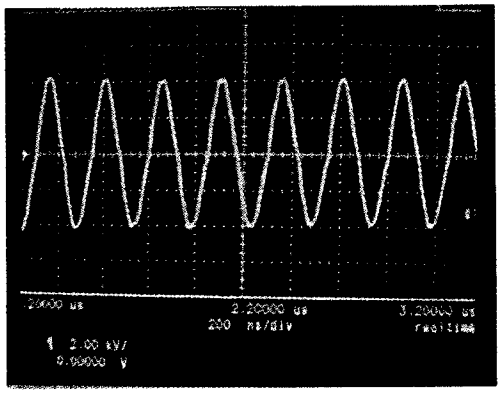

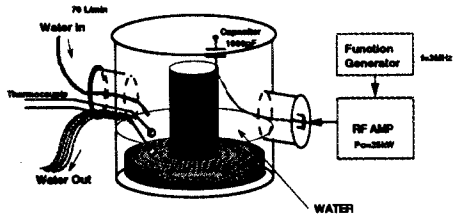

Schematic View of MA-loaded Cavity

Single Gap MA-loaded Cavity

RF Voltage	**16-20kV**
No. of Cores	**4-6**
Shunt Impedance	**500-750 Ω**
Q	**1-2**
Total Length	**30-40 cm**

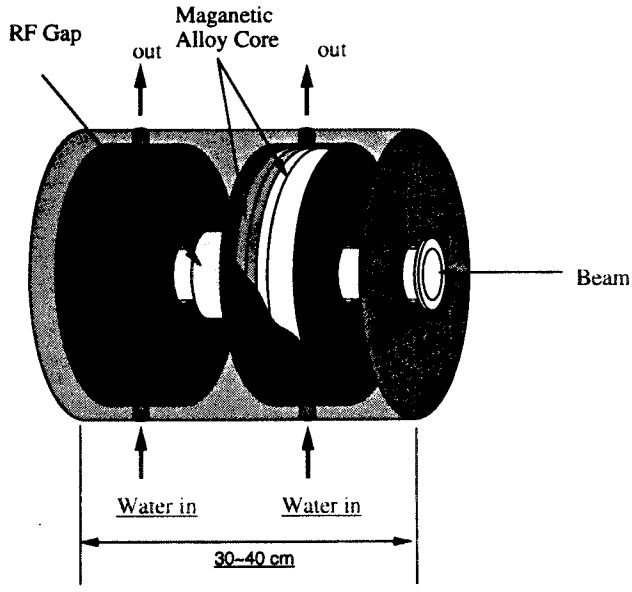

30kW cavity

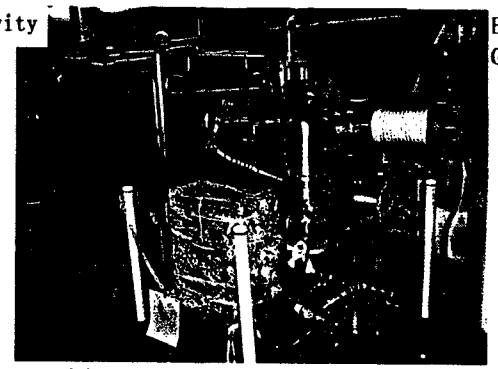

Electron Gun

30kW cavity and beam loading test system. The cavity has two acceleration gaps. Max. 24 cores can be installed in the cavity. Only 6 cores were installed for the following experiments.

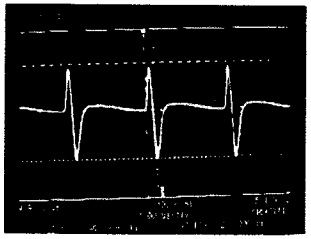

Typical RF voltage for the barrier bucket operation. Maximum voltage was 9 kV .

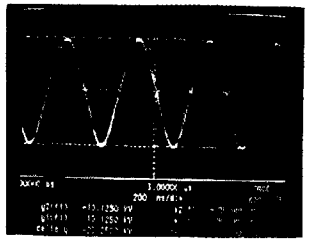

Maximum voltage of 10.1kV was obtained for the pulse operation.

"Barrier Bucket Cavity" 9-10kV/gap Achieved !!

KEK-BNL Collaboration

@ AGS

<to be installed in March '98>

MA cavity vs. Ferrite cavity

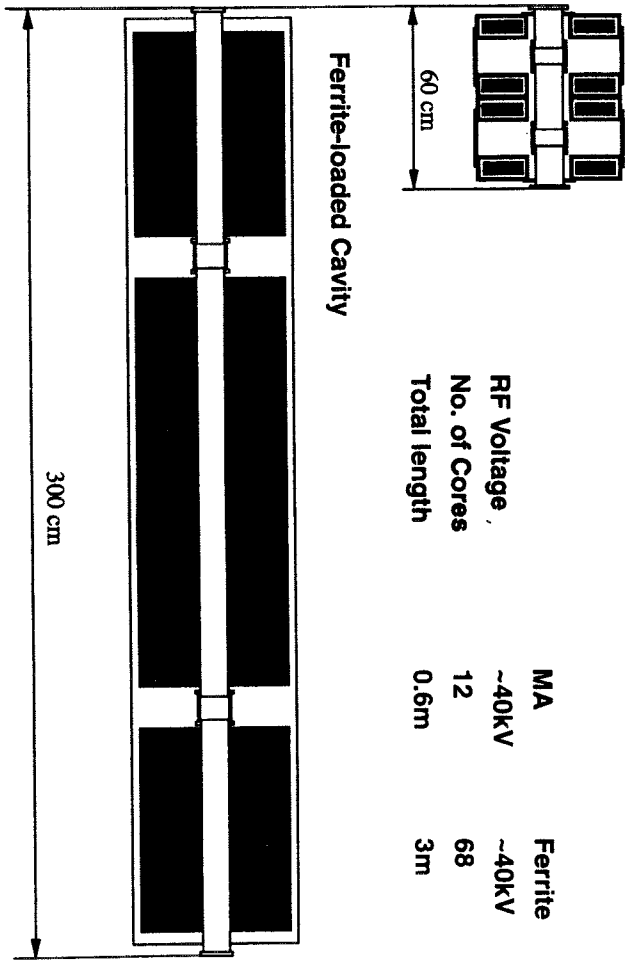

	MA	Ferrite
RF Voltage	~40kV	~40kV
No. of Cores	12	68
Total length	0.6m	3m

Beam Loading Compensation

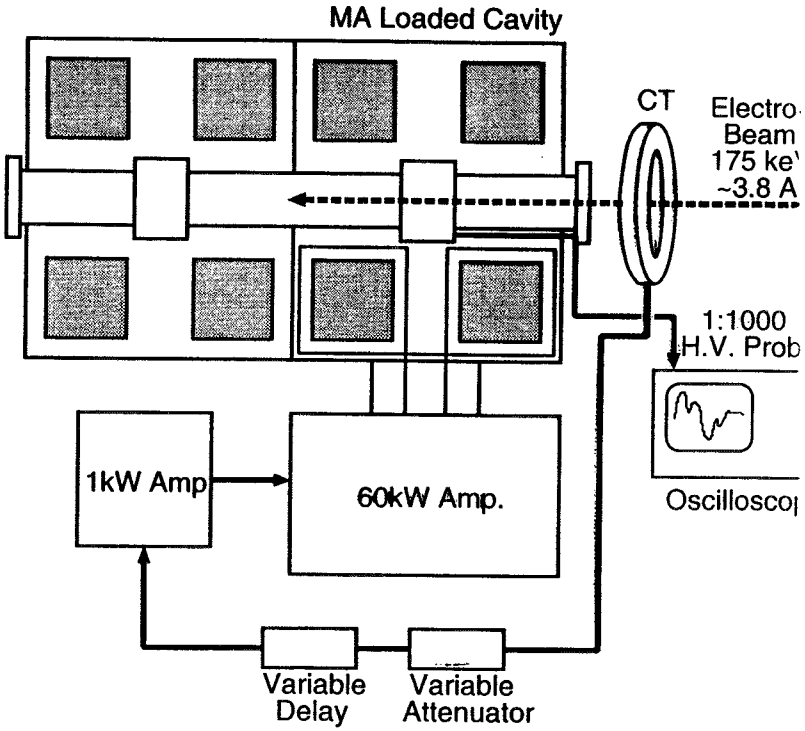

One-turn Delay Feedback
(Feedforward)

Low Q (≒1) ⇒ Wide Band

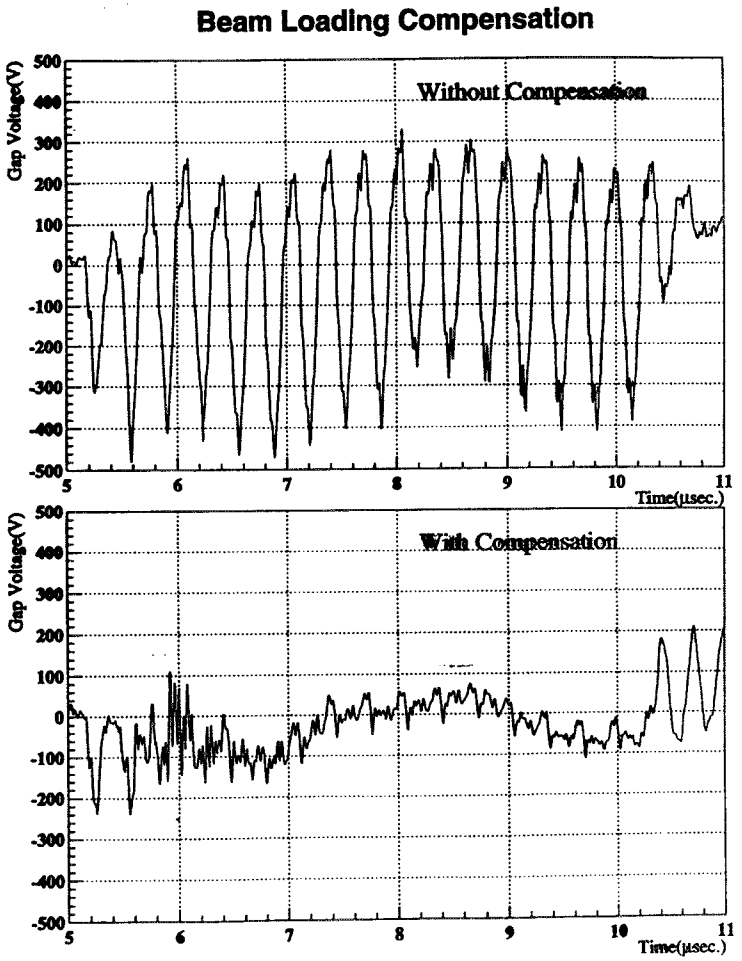

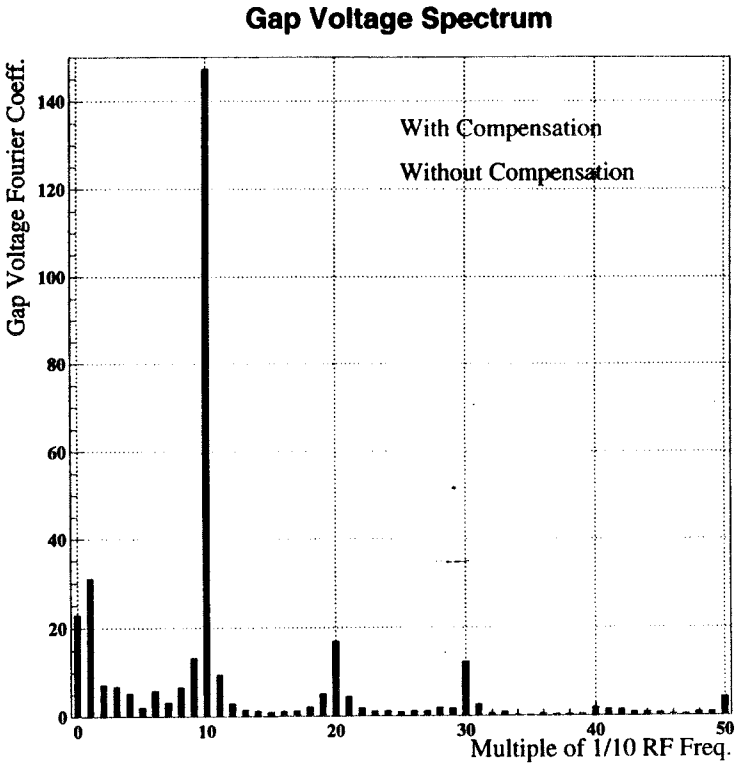
Gap Voltage Spectrum
Gap Voltage Fourier Coeff.
140
120
100
80
60
40
20
0
With Compensation
Without Compensation
0
10
20
30
40
50
Multiple of 1/10 RF Freq.

ULTIMATE LUMINOSITY MUON COLLIDER
(problems and prospects)

A.Skrinsky
Budker Institute of Nuclear Physics
Novosibirsk

San Francisco
December 1997

GENERAL SCHEME of MUON COLLIDER

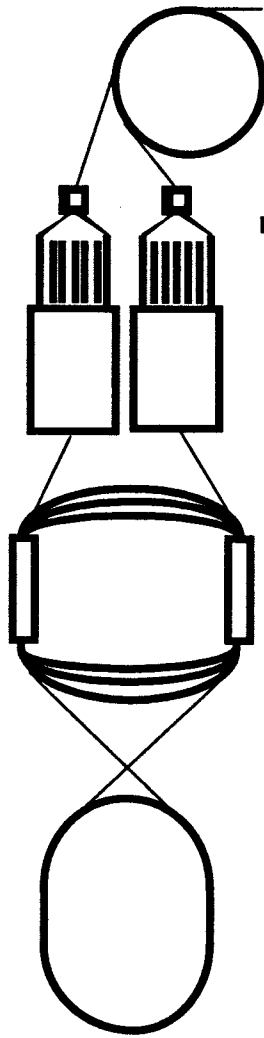

proton injector

proton synchrotron

proton-to-pion target/collection system

pion-to-muon decay channels

preliminary ionization cooling
& single polarized +/- muon bunches
formation

+/- muon accelerator

muon collider

Let us remind first the primary importance of the final stage of ionization cooling for the reaching the highest possible muon collider luminosity.

If at this stage normalized transversal emittance $\varepsilon_{neqtran}$ and longitudinal emittance $\varepsilon_{neqlong}$ were reached, the ultimate luminosity would be: $(\beta_{0\,coll} \equiv \sigma_{longcoll})$

$$L_{\mu\mu\,max}(\beta_\mu, \kappa_{long}) = \frac{N_\mu^2}{4\cdot\pi}\cdot\frac{\gamma_{coll}^2}{\varepsilon_{neqtran}(\beta_\mu, \kappa_{long})\cdot\varepsilon_{neqlong}(\beta_\mu, \kappa_{long})}\cdot\Delta_{Ecoll}\cdot N_{tN}\cdot f_0$$

With the equilibrium emittances reachable (below) and optimal parameters for muon collider

(E_μ= 5 TeV + 5TeV N_μ=1*10^{12} H_{coll}=10 T f_0=15 s^{-1}) Δ_{Ecoll}=0.3%

in dependence of cooling energy E_μ and fraction of cooling decrement transfered to the longitudinal direction κ_{long}:

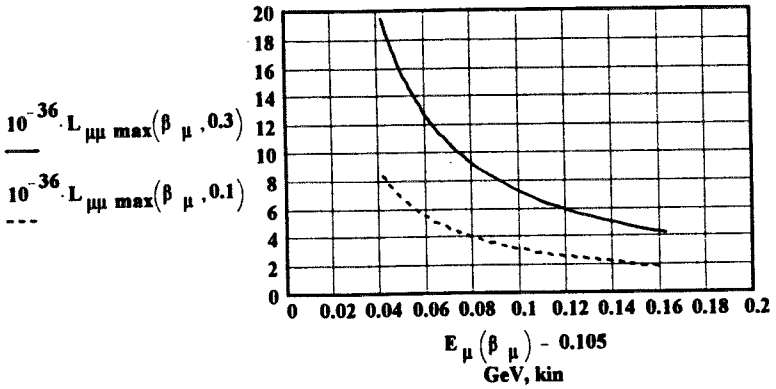

But if calculate the beta-value at collision, assumed as always here to be equal to the muon bunch length, we would get 10 to 20 microns!

Such bunch length and beta-function look impractical; if we limit these values as $\beta_{coll}=\sigma_{longcoll}$, the following formula for "practical" maximum luminosity should be valid:

$$L_{\mu\mu}(\beta_\mu, \kappa_{long}) = \frac{N_\mu^2}{4\cdot\pi}\cdot\frac{\gamma_{coll}^{\frac{3}{2}}}{(\varepsilon_{neq6}(\beta_\mu, \kappa_{long}))^{\frac{1}{2}}\cdot\sigma_{longcoll}^{\frac{1}{2}}}\cdot\Delta_{Ecoll}^{\frac{1}{2}}\cdot N_{tN}\cdot f_0$$

For reasonable limit β_{coll}= 300 microns:

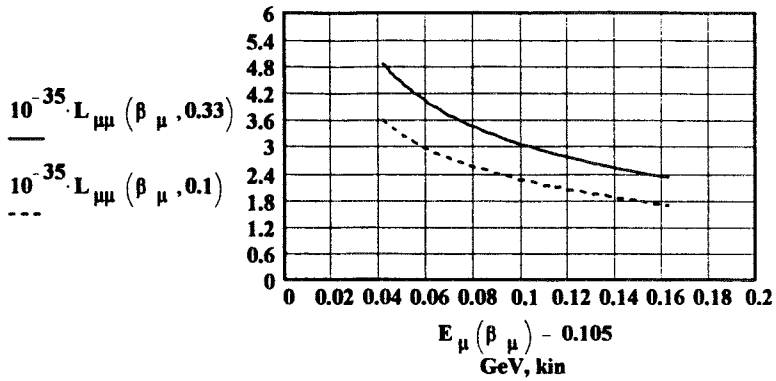

Less than the ultimate one - but still quite good.

Albeit, equilibrium normalized emittance enters the maximal luminosity directly. And the aim of final ionization cooling is to reach minimum of

$$\varepsilon_{neq6}\,.$$

Next problem: to transform this 6-dimensional emittance - properly (below).

Final cooling stage.

$$P_{fr}(\beta_\mu) = 4\cdot\pi\cdot r_e^2\cdot m_e\cdot c^2\cdot N_e\cdot\frac{c}{\beta_\mu}\cdot\left[\ln\left[\frac{2\cdot m_e\cdot c^2\cdot\beta_\mu^2}{I\cdot\left[1+\frac{2}{\sqrt{1-\beta_\mu^2}}\cdot\frac{m_e}{M_\mu}+\left(\frac{m_e}{M_\mu}\right)^2\right]\cdot(1-\beta_\mu^2)}\right]-\beta_\mu^2\right]$$

$$\delta_{\Sigma 0}(\beta_\mu) = \frac{2\cdot P_{fr}(\beta_\mu)\cdot\sqrt{1-\beta_\mu^2}}{(M_\mu\cdot c^3)\cdot\beta_\mu^3}\cdot\left(\frac{1+\beta_\mu^2}{2}\right)+\frac{(1-\beta_\mu^2)^{\frac{3}{2}}}{(M_\mu\cdot c^3\cdot\beta_\mu^2)}\cdot\left(\frac{d}{d\beta_\mu}P_{fr}(\beta_\mu)\right)$$

The "cooling length" for 6-emittance in lithium:

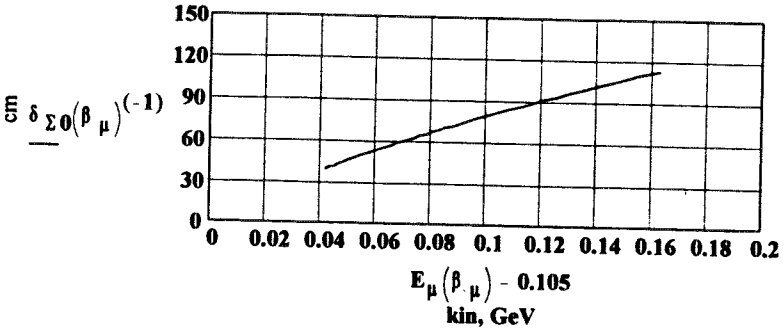

Transversal cooling - straightforward.
For longitudinal direction - more complexity.
"Naturally", when the longitudinal damping is caused by direct dependence of energy losses on muon energy, at kinetic energies above 200 MeV the longitudinal cooling length is 5 times longer than a transversal one; and ionization cooling even transforms into anti-damping below 100 MeV.

The "natural" length of longitudinal cooling:

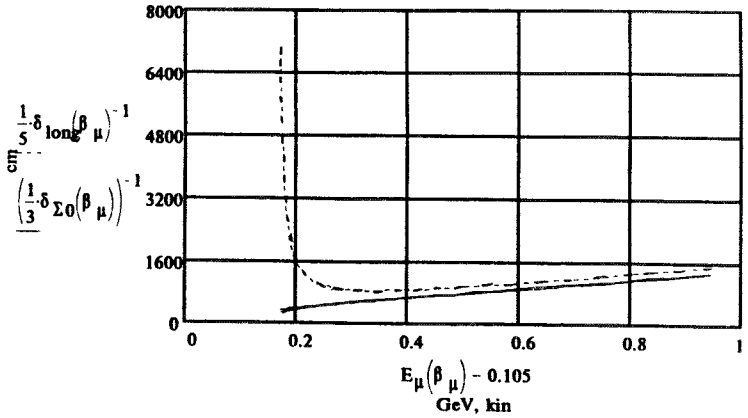

Hence, it is obligatory to redistribute the decrements sum in favour of longitudinal degree of freedom.

This is especially clear when looking on the equilibrium relative energy spread (due to balance of struggling and cooling):

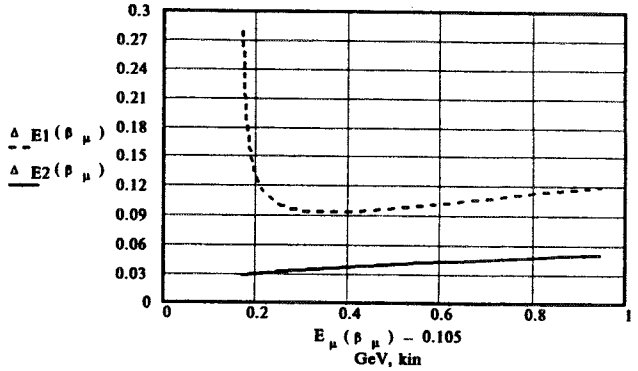

First (upper) line - "natural" decrement; second - upon redistribution.

The final stage of ionization cooling is the crucially important and the most difficult part of the whole cooling problem.

The task is to reach minimal 6-dimension emittance of muon beam.
For this stage it means:

- **to arrange the strongest transversal and longitudinal focusing;**
- **to cool all 3 degrees of freedom simultaneously;**
- **to distribute the decrements sum "equally" to all 3.**

The optimal solution for transversal emittances is -
to use a high current carrying (liquid) lithium thin cylinder.

Surface magnetic field - 10 Tesla.
Lithium cylinder diameter - 1 mm.

$$H_{max} := 1 \cdot 10^5 \qquad a_{li} := 0.05 \qquad \beta_{li}(\beta_\mu) := \sqrt{\frac{10^9 \cdot E_\mu(\beta_\mu) \cdot a_{li}}{300 \cdot H_{max}}}$$

$$\varepsilon_{neqtran}(\beta_\mu, \kappa_{long}) := 4 \cdot \pi \cdot r_\mu^{\,2} \cdot N_e \cdot Z \cdot L_c \cdot \frac{\sqrt{1-\beta_\mu^{\,2}}}{\beta_\mu^{\,3}} \cdot \left(\frac{1-\kappa_{long}}{2} \cdot \delta\Sigma 0(\beta_\mu)\right)^{(-1)} \cdot \beta_{li}(\beta_\mu)$$

Transversal equilibrium radius in cylinder:

$$a_{eq}(\beta_\mu, k_\phi) := \beta_{li}(\beta_\mu) \cdot \frac{\varepsilon_{neqtran}(\beta_\mu, k_\phi)}{\beta_\mu \cdot \gamma_{\mu cool}(\beta_\mu)}$$

$a_{eq}(0.73, 0.3) = 0.011$ **- compare to** a_{li} **!**

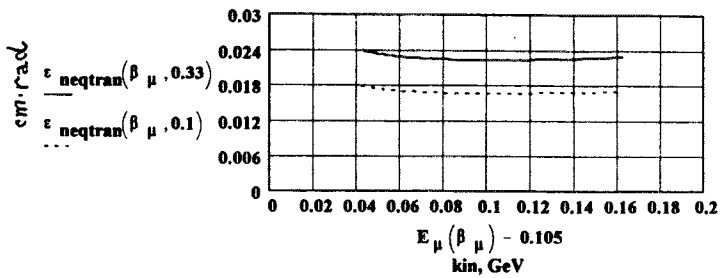

Hence, transversal emittance is almost constant for reasonable cooling energies.

Transversal + longitudinal cooling.

Possible solution for the final stage simultaneous cooling - to transform the current carrying cylinder in to

lithium-beryllium helix

with "teeth like" boundary between these two metals
(more of high density beryllium at larger radius of the spiral - where the muon energies are higher).

(H_{max1} - external bending field)

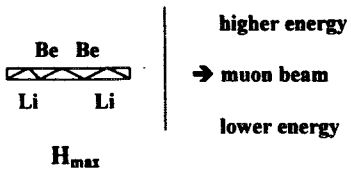

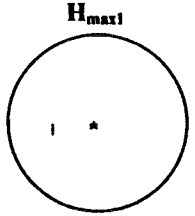

Axial view of the helix

$H_{max1} := 0.5 \cdot 10^5$ Gs

$$r_{helix}(\beta_\mu) := \frac{E_\mu(\beta_\mu) \cdot \beta_\mu \cdot 10^9}{300 \cdot H_{max1}} \qquad r_{helix}(0.82) = 10.029 \text{ cm}$$

$$dE_{dx}(\beta_\mu) := \frac{P_{fr}(\beta_\mu)}{\beta_\mu \cdot c} \cdot \frac{1}{2 \cdot m_e \cdot c^2} \cdot 10^{-3} \qquad dE_{dx}(0.9) = 1.065 \cdot 10^{-3} \text{ GeV/cm}$$

$\lambda_{RF} := 10$ cm $k_\phi := 3 = \frac{eV_{0RF}}{dE_{dx}}$

$$K(\beta_\mu) := \frac{1}{\gamma_{\mu cool}(\beta_\mu)^2} \left| 1 - \left(\frac{\beta_H(\beta_\mu)}{r_{helix}(\beta_\mu)} \right)^2 \cdot \gamma_{\mu cool}(\beta_\mu)^2 \right| \qquad K(0.73) = 0.463$$

Equilibrium relative energy spread in such helix:

$$\Delta E(\beta_\mu, \kappa_{long}) := \sqrt{2 \cdot \pi \cdot r_e^2 \cdot \left(\frac{m_e}{M_\mu} \right)^2 \cdot N_e \cdot \left(2 - \beta_\mu^2\right) \cdot \left(\kappa_{long} \cdot \delta \Sigma 0(\beta_\mu)\right)^{(-1)}}$$

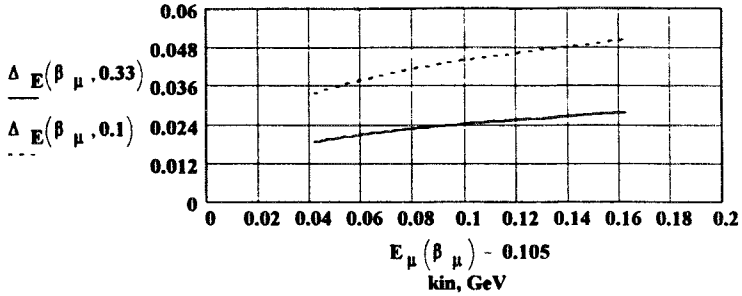

Equilibrium bunch length and longitudinal emittance:

$$\sigma_{longcool}(\beta_\mu, \kappa_{long}) := \sqrt{\frac{E_\mu(\beta_\mu) \cdot \lambda_{RF} \cdot K(\beta_\mu)}{2 \cdot \pi \cdot dE_{dx}(\beta_\mu) \cdot \sqrt{k_\phi^2 - 1}}} \cdot \Delta E(\beta_\mu, \kappa_{long})$$

$\sigma_{longcool}(0.8, 0.33) = 0.114$ cm

$$\varepsilon_{neqlong}(\beta_\mu, \kappa_{long}) := \left(\Delta E(\beta_\mu, \kappa_{long})\right) \cdot \sigma_{longcool}(\beta_\mu, \kappa_{long}) \cdot \gamma_{\mu cool}(\beta_\mu) \cdot \beta_\mu$$

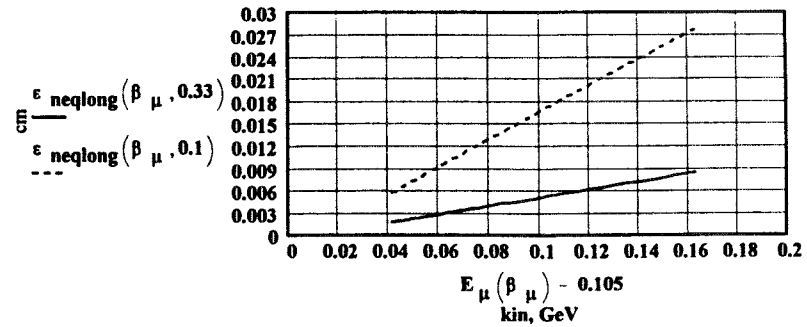

Consequently, equilibrium 6-emittance:

$$\varepsilon_{neq6}(\beta_\mu, \kappa_{long}) = \varepsilon_{neqtran}(\beta_\mu, \kappa_{long})^2 \cdot \varepsilon_{neqlong}(\beta_\mu, \kappa_{long})$$

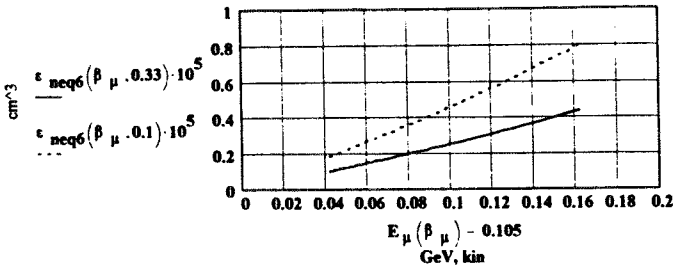

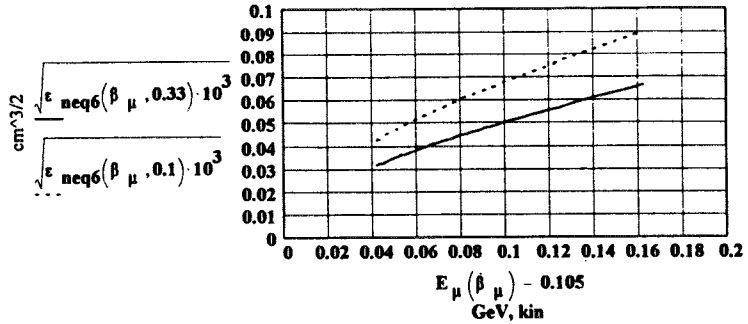

$$k_L(\kappa_{long}) = \sqrt{10^4 \cdot \varepsilon_{neq6}(0.73, 0.333)} \cdot \left(\sqrt{10^4 \cdot \varepsilon_{neq6}(0.73, \kappa_{long})}\right)^{-1}$$

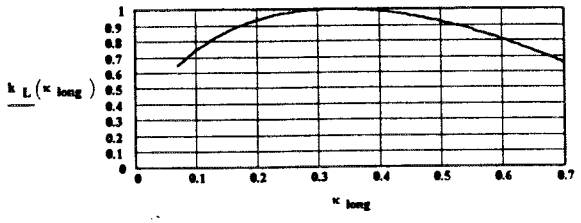

To reach this "practically maximal" luminosity, we need to transfer transversal emittances into longitudinal one (keeping 6-dimension phase space density reached under final cooling as constant as possible!).

For this emittances gymnastic purpose, we need to use combination of dispersive and septum elements, RF accelerating/decelerating structures, delay lines (and not ionization components, which damage 6-density!).
– at "any" convenient energy.

Schematics of the transformation
(in comparison with a bunch monochromatization process):

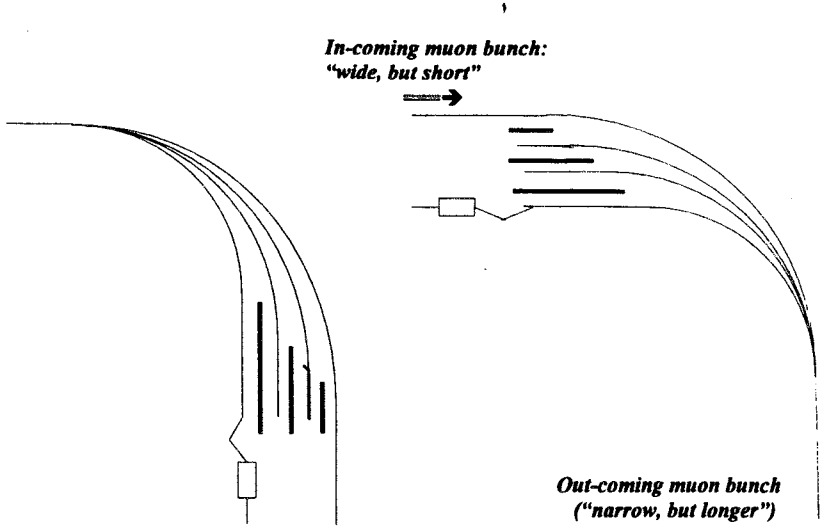

Familiar transformation of the bunch of high momentum spread in to the bunch of the same length with smaller spread, but with proportionally bigger transversal emittance.

The "opposite" transformation of the bunch with big transversal emittance in to the bunch with smaller one but with proportionally bigger momentum spread and longitudinal emittance.

Prevention of muon losses in cooling process.

Losses happen due to:

multiple scattering - the requirement follows: acceptance of the cooling channel should be several times wider than equilibrium one.

single scattering - limits number of "cooling lengths" -

$$\Psi_{tran}(\beta_\mu, \kappa_{long}) = \chi_{life}(H_{max}, \beta_\mu, a_{li}) \cdot \frac{1 - \kappa_{long}}{2} \cdot \delta\Sigma 0(\beta_\mu)$$

$$\Psi_{long}(\beta_\mu, \Delta_{Eacc}, \kappa_{long}) = I(\beta_\mu, \Delta_{Eacc})^{-1} \cdot (\kappa_{long} \cdot \delta\Sigma 0(\beta_\mu))$$

$$\Delta_{Eacc} = \frac{\Delta E_{acc}}{M_\mu \cdot c^2 \cdot (\gamma_\mu - 1)} \qquad T_{max}(\beta_\mu) = \frac{2 \cdot m_e \cdot c^2 \cdot \beta_\mu^2 \cdot \gamma_{\mu cool}(\beta_\mu)^2}{1 + 2 \cdot \gamma_{\mu cool}(\beta_\mu) \cdot \frac{m_e}{M_\mu}} \qquad e_\mu = 0.5 \cdot 10^{-2}$$

$$I(\beta_\mu, \Delta_{Eacc}) \cdot \frac{2 \cdot \pi \cdot r_e^2 \cdot N_A \cdot \frac{Z}{A} \cdot e_\mu}{(\gamma_{\mu cool}(\beta_\mu) - 1)} \int_{\Delta_{Eacc}}^{\left| \frac{2 \cdot e_\mu \cdot \beta_\mu^2 \cdot \gamma_{\mu cool}(\beta_\mu)^2}{(1 + 2 \cdot \gamma_{\mu cool}(\beta_\mu) \cdot e_\mu)(\gamma_{\mu cool}(\beta_\mu) - 1)} \right|} \frac{1}{z^2} \left| 1 - \beta_\mu^2 \frac{z}{\frac{2 \cdot e_\mu \cdot \beta_\mu^2 \cdot \gamma_{\mu cool}(\beta_\mu)^2}{(1 + 2 \cdot \gamma_{\mu cool}(\beta_\mu) \cdot e_\mu)(\gamma_{\mu cool}(\beta_\mu) - 1)}} \right| dz$$

$$\Psi_{tot}(\beta_\mu, \Delta_{Eacc}, \kappa_{long}) = \begin{cases} \Psi_{tran}(\beta_\mu, \kappa_{long}) & \text{if } \frac{2 \cdot m_e \cdot c^2 \cdot \beta_\mu^2 \cdot \gamma_{\mu cool}(\beta_\mu)^2}{1 + 2 \cdot \gamma_{\mu cool}(\beta_\mu) \cdot \frac{m_e}{M_\mu}} \cdot \left[\left[M_\mu \cdot c^2 \cdot (\gamma_{\mu cool}(\beta_\mu) - 1) \right]^{-1} \right] < \Delta_{Eacc} \\ \left(\frac{1}{\Psi_{tran}(\beta_\mu, \kappa_{long})} + \frac{1}{\Psi_{long}(\beta_\mu, \Delta_{Eacc}, \kappa_{long})} \right)^{-1} & \text{otherwise} \end{cases}$$

(Losses due to muon decay is not very limiting:

$$\Psi_{life}(\beta_\mu, \kappa_{long}) = c \cdot \kappa_{long} \cdot \delta\Sigma 0(\beta_\mu) \cdot \frac{\beta_\mu}{\sqrt{1 - \beta_\mu^2}} \cdot \tau_{\mu 0} \qquad \Psi_{life}(0.73, 0.33) = 531.563 \quad)$$

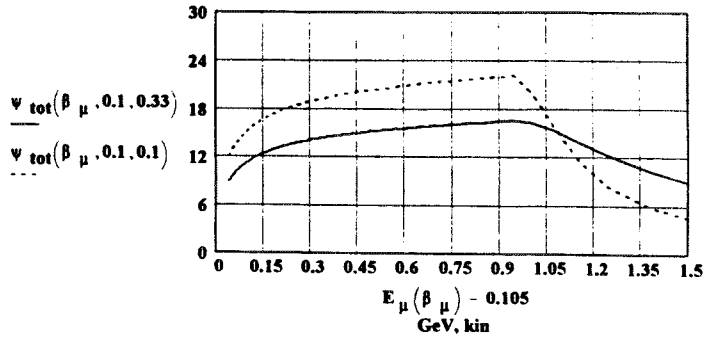

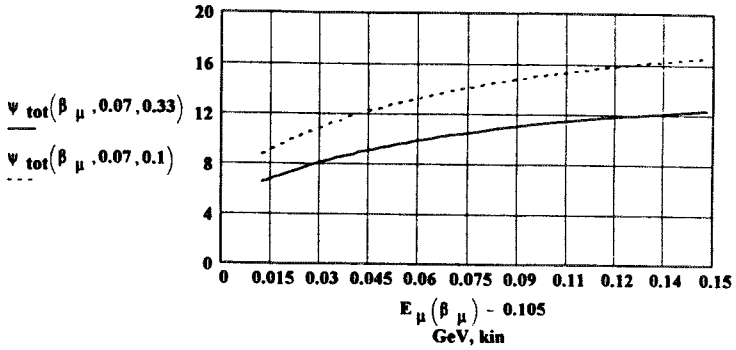

Multi-channel proton/pion conversion system:

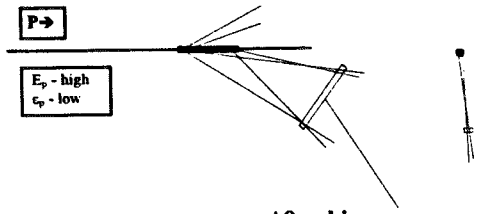

$\Delta\theta_\pi$ - big
$\Delta\phi_\pi$ - small!

Hence, in a single channel:

θ-emittance is big;
ϕ-emittance is very small.

(Maybe, it is reasonable to arrange multi-sectioned target:

This could be especially useful at high proton energy - 100 GeV?)

Hence, possible solution - many pion channels with one transversal emittance being very small.

In this direction, we can split each pion broad spectrum beam - in to several ones of +/- 5 % momentum spread.

As a result, at the exit of multi-channel proton-to-pion conversion system we have many independent pion beams with at least one transversal emittance quite small. These beams can easily be transported straight away of the target space, and the following channel gymnastics will happen in reasonably free room.

The next step is to arrange in each channel the energy dispersion in this smaller emittance direction, and than to direct each of the +/- 5% momentum spread pion beams in a separate strong focusing decay channels.

Such narrow momentum spread pion beams (with very small emittance in one direction), upon passing about 2 decay lengths (proportional to the pion energy in each channel, around $15*\beta_\pi*E_\pi/E_{\pi 0}$ meters), generate muon beams of momentum spread about +/- 30%, with strong correlation of muon spin direction and its momentum.

At the figure the dependence of relative muon momentum in lab system on polar angle of decay θ in CMS is shown, for pion kinetic energies 300 MeV (solid line) and 60 MeV (dotted line).

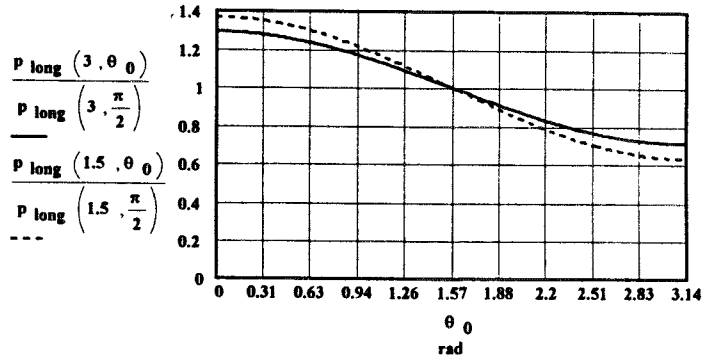

Consequently, for every particular muon beam:
cut away the middle 30% of muon spectrum;
separate upper and lower parts of muon spectrum
with opposite helicities in to 2 sub-channels.

The next phase - to shift the energy in each muon channel by RF acceleration/deceleration to the energy optimal for ionization cooling (around 100 MeV).
Then - several stages of:
preliminary cooling + combining of several muon bunches in one + next preliminary cooling + ...

All the upper μ^+ (μ^-) bunches will be combined in the "first" bunch and all the lower μ^+ (μ^-) the "second" one, and 4 bunches will be cooled down to lowest 6-emittances.

Afterwards, we reverse helicity of the second at the later stage upon acceleration to 45 GeV (by additional non-accelerating turn) and than combine both beams in one (1 μ^- bunch + 1 μ^+ bunch) - and we shall get
70% longitudinal polarization degree muon beam
of 70% of full intensity and dubbled ultimately small 6-emittance
- the same for each particular beam -
and the luminosity would rise 2.8 times.

(90 GeV for muons are equivalent to 440 MeV for electrons)

Helicities of colliding bunches are modulated at relative frequency

$$\nu_{spin} = \frac{E_{GeV}}{90} .$$

At integer spin resonances remain the same all the time.
At half-integer resonances the helicities reverse at consequent turns.

Relative helicities (from ++/-- to +-/-+) at the interaction region can be controlled by choosing a proper injection path (maybe, by additional non-accelerating turn of one beam at, say, 45 GeV) - to acquire proper angle between spin and velocity.

There are no losses in polarization degree at cooling stage (and almost no angle appears between spin and velocity).

Polarization losses (second term) due to energy spread in muon collider:

$$\zeta_{\mu eq} = 1 - \frac{\left(2\cdot\pi\cdot\nu_{synch}^{-1}\cdot\frac{E_{coll}}{0.9\cdot 10^5}\cdot\Delta E_{coll}\right)^2}{2} .$$

To half-turn muon helicity - full turn of muon trajectory at $\frac{90}{2} = 45$ GeV

$\Longrightarrow$ corresponds to $\int H\cdot s\, ds = \frac{45\cdot 10^9\cdot 2\cdot\pi}{300}\cdot 10^{-6} = 942.478$ Tesla·meter

MAIN FORMULAS:

A requirement - $\beta_{coll} = \sigma_{longcoll} = 3$ mm (?)

$$L_{\mu\mu}(\beta_\mu, \kappa_{long}) = \frac{N_\mu^2}{4\cdot\pi}\cdot\frac{\gamma_{coll}^{\frac{3}{2}}}{(\varepsilon_{neq6}(\beta_\mu, \kappa_{long}))^{\frac{1}{2}}\cdot\sigma_{longcoll}^{\frac{1}{2}}}\cdot\Delta_{Ecoll}^{\frac{1}{2}}\cdot N_{tN}\cdot f_0$$

$$N_{tN} = \frac{q_e\cdot H_{coll}\cdot\tau_{\mu 0}}{2\cdot\pi\cdot M_\mu\cdot c\cdot 2}$$

$$L_{\mu\mu 2}(\beta_\mu, \kappa_{long}) = \frac{N_\mu^2\cdot q_e\cdot\tau_{\mu 0}}{1.2\cdot 10^4\cdot M_\mu\cdot c}\cdot\frac{1}{(\varepsilon_{neq6}(\beta_\mu, \kappa_{long}))^{\frac{1}{2}}}\cdot\frac{\gamma_{coll}\cdot eV_{0MV}^{\frac{1}{4}}\cdot\nu_r^{\frac{1}{2}}}{\lambda_{RFcoll}^{\frac{1}{4}}}\cdot H_{coll}^{\frac{5}{4}}\cdot f_0$$

$$\sigma_{longcoll} = 0.6\cdot 10^4\cdot\sqrt{\frac{\lambda_{RFcoll}\cdot\gamma_{coll}^2}{eV_{0MV}\cdot H_{coll}\cdot\nu_r^2}\cdot\Delta_{Ecoll}}$$

$$\varepsilon_{nlongcoll} = \gamma_{coll}\cdot\sigma_{longcoll}\cdot\Delta_{Ecoll}$$

$$\varepsilon_{neqtraneff}(\beta_\mu, \kappa_{long}) = \frac{\varepsilon_{neqtran}(\beta_\mu, \kappa_{long})\cdot\varepsilon_{neqlong}(\beta_\mu, \kappa_{long})^{\frac{1}{2}}}{\gamma_{coll}^{\frac{1}{2}}\cdot\Delta_{Ecoll}^{\frac{1}{2}}\cdot\sigma_{longcoll}^{\frac{1}{2}}}$$

$$\nu_{synch} = \sqrt{\frac{eV_{0MV}}{3\cdot 10^{-4}\cdot H_{max}\cdot\lambda_{RFcoll}\cdot\nu_r^2}}$$

$$\zeta_{\mu eq} = 1 - 0.8\cdot 10^{-8}\cdot\frac{\gamma_{coll}^2\cdot\nu_r^2\cdot\lambda_{RFcoll}\cdot H_{coll}\cdot\Delta_{Ecoll}^2}{eV_{0MV}}$$

$$\xi_{coll}(\beta_\mu, \kappa_{long}) = \frac{r_\mu}{4\cdot\pi}\cdot\frac{N_\mu\cdot\gamma_{coll}^{\frac{1}{2}}\cdot\sigma_{longcoll}^{\frac{1}{2}}\cdot\Delta_{Ecoll}^{\frac{1}{2}}}{\varepsilon_{neqtran}(\beta_\mu, \kappa_{long})\cdot\varepsilon_{neqlong}(\beta_\mu, \kappa_{long})^{\frac{1}{2}}}$$

"OPTIMIZED OPTIONS"

$N_\mu = 1\cdot 10^{12}$

High energy 5 TeV + 5 TeV :

$\gamma_{coll} = 50000$ $E_{coll} = 5.25\cdot 10^6$ MeV

$H_{coll} = 0.8\cdot 10^5$ $R_{coll} = 2.188\cdot 10^5$ cm $N_{tN} = 1.12\cdot 10^3$

$\Delta_{Ecoll} = 0.000015$ $\nu_r = 40$ $eV_{0MV} = 16$ $\lambda_{RFcoll} = 10$ cm

$\gamma_{coll}\cdot\sigma_{longcoll}\cdot\Delta_{Ecoll} = 0.238$ $\varepsilon_{neqlong}(0.86, 0.33) = 5.008\cdot 10^{-3}$

$L_{\mu\mu 2}(0.73, 0.3) = 9.797\cdot 10^{34}$ $\zeta_{\mu eq} = 0.64$ $\sigma_{longcoll} = 0.314$

Medium energy 1 TeV + 1 TeV :

$\gamma_{coll} = 10000$ $E_{coll} = 1.05\cdot 10^6$ MeV

$H_{coll} = 0.7\cdot 10^5$ $R_{coll} = 5\cdot 10^4$ cm $N_{tN} = 980.394$

$\Delta_{Ecoll} = 0.00003$ $\nu_r = 30$ $eV_{0MV} = 4$ $\lambda_{RFcoll} = 10$ $\nu_{synch} = 4.6\cdot 10^{-3}$

$\gamma_{coll}\cdot\sigma_{longcoll}\cdot\Delta_{Ecoll} = 0.227$ $\varepsilon_{neqlong}(0.86, 0.33) = 5.008\cdot 10^{-3}$

$L_{\mu\mu 2}(0.73, 0.3) = 1.038\cdot 10^{34}$ $\zeta_{\mu eq} = 0.887$ $\sigma_{longcoll} = 0.359$

Low energy 50 GeV + 50 GeV :

$\gamma_{coll} = 500$ $E_{coll} = 5.25\cdot 10^4$ MeV

$H_{coll} = 0.7\cdot 10^5$ $R_{coll} = 2.5\cdot 10^3$ cm

$\Delta_{Ecoll} = 0.002$ $\nu_r = 40$ $eV_{0MV} = 30$ $\lambda_{RFcoll} = 10$ $\nu_{synch} = 0.01$

$\gamma_{coll}\cdot\sigma_{longcoll}\cdot\Delta_{Ecoll} = 1.479$ $\varepsilon_{neqlong}(0.86, 0.33) = 5.008\cdot 10^{-3}$

$L_{\mu\mu 2}(0.73, 0.3) = 9.922\cdot 10^{32}$ $\zeta_{\mu eq} = 0.701$ $\sigma_{longcoll} = 0.327$

ULTIMATE LUMINOSITY at 5 TeV + 5 TeV :

$N_\mu = 5\cdot10^{12}$

$\gamma_{coll} = 50000$ $E_{coll} = 5.25\cdot10^6$ MeV

$H_{coll} = 1\cdot10^5$ $R_{coll} = 1.75\cdot10^5$ cm $N_{tN} = 1.401\cdot10^3$

$\Delta_{Ecoll} = 0.00012$ $\nu_r = 300$ eV $_{0MV} = 16$ $\lambda_{RFcoll} = 10$ $\nu_{synch} = 7\cdot10^{-4}$

$\gamma_{coll}\cdot\sigma_{longcoll}\cdot\Delta_{Ecoll} = 0.217$ $\varepsilon_{neqlong}(0.86, 0.33) = 5.008\cdot10^{-3}$

$L_{\mu\mu\ 2}(0.73, 0.3) = 8.865\cdot10^{36}$ $\zeta_{\mu eq} = -1.619\cdot10^3$ $\sigma_{longcoll} = 0.3$

no polarization!

$\xi_{coll}(0.73, 0.33) = 0.748$ - subject for lithium compensation!

$$k_{bbatten}(\beta_\mu, \kappa_{long}) := \frac{8}{4\cdot\pi\cdot r_e\cdot\frac{N_e}{3}\cdot\sigma_{rcoll}(\beta_\mu, \kappa_{long})^2}$$

$k_{bbatten}(0.73, 0.33) = 0.013$

ULTIMATE MONOCHROMATICITY, 50 GeV + 50 GeV

$N_\mu := 1\cdot10^{12}$

$\gamma_{coll} := 500$ $E_{coll} = 5.25\cdot10^4$ MeV

$H_{coll} := 0.7\cdot10^5$ $R_{coll} = 2.5\cdot10^3$ cm

$\Delta_{Ecoll} := 0.000001$ - requires transfering of longitudinal emittance to transversal ones!

$\nu_r := 10$ eV $_{0MV} := 0.0015$ $\lambda_{RFcoll} := 100$ $\nu_{synch} = 8.452\cdot10^{-5}$

$\gamma_{coll}\cdot\sigma_{longcoll}\cdot\Delta_{Ecoll} = 6.614\cdot10^{-4}$ $\varepsilon_{neqlong}(0.86, 0.33) = 5.008\cdot10^{-3}$

$L_{\mu\mu\ 2}(0.73, 0.3) = 2.346\cdot10^{31}$ $\zeta_{\mu eq} = 0.999$ $\sigma_{longcoll} = 0.293$

Space charge limitation (transversal) at cooling stage:

$$N_{b\mu\ cool}(\beta_\mu, \kappa_{long}, \beta_{loc}) := \frac{2}{r_\mu}\cdot\beta_\mu\cdot\gamma_{\mu\ cool}(\beta_\mu)^2\cdot\frac{\varepsilon_{neqtran}(\beta_\mu, \kappa_{long})\cdot\sigma_{longcool}(\beta_\mu, \kappa_{long})}{\beta_{loc}}$$

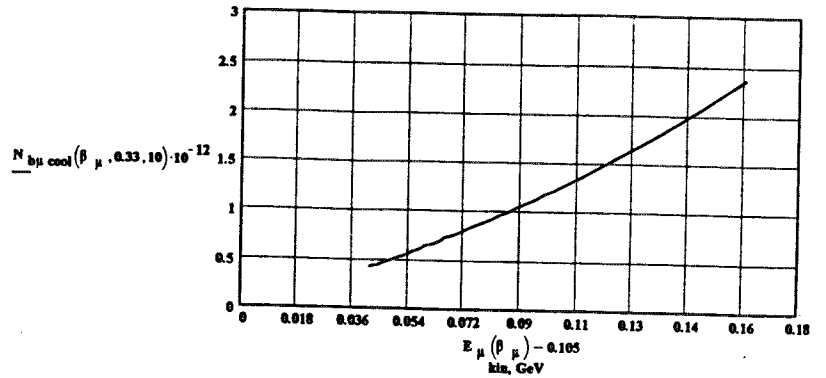

COLLIDER OPTIONS.

MUON^{minus} - PROTON collisions:

the same acceleration chain gives the "same" luminosity;

proton spin shall be vertical at all stages except interaction region;

at both sides of interaction region - spin rotators to transform proton spin to longitudinal direction
(this rotators do not harm muon polarization - too weak!).

Same sign particles collider ($\mu^+\mu^+$, $\mu^-\mu^-$, μ^+p) needs two-stores rings of opposite field.

NEW $\mu^{\pm}$ COOLING FOR $\mu^{\pm}$ COLLIDERS AND POSSIBLE REALIZATION AT JHF/KEK

4th International Conference
on
Physics Potential and Development of $\mu^{+}\mu^{-}$ Colliders

December 10 - 12, 1997
San Fransisco

K. Nagamine

Meson Science Laboratory, Institute of Materials Structure Science,
High Energy Accelerator Research Organization
(KEK - MSL)
and
Muon Science Laboratory, Institute of Physical and Chemical Research
(RIKEN)

- ★ $\mu^{\pm}$ Cooling and $\mu^{\pm}$ Colliders
- ★ New μ^{+} Cooling; Recent Development
- ★ New μ^{-} Cooling; Recent Development
- ★ Intense Ultra- Slow $\mu^{\pm}$ Source Project at JHF/KEK
- ★ Conclusion

$\mu^{\pm}$ COOLING AND $\mu^{\pm}$ COLLIDERS

★Most Important Component for $\mu^{\pm}$ Colliders

Proton Accelerator,
Pion Collector,
$\pi\mu$ Decay Section,
RF Rotation,
Muon Cooling,
Muon Accelerator
Muon Collider Ring

★Muon Cooling

⇨ Muon Source for Further Acceleration

Muons for Advanced Muon Science

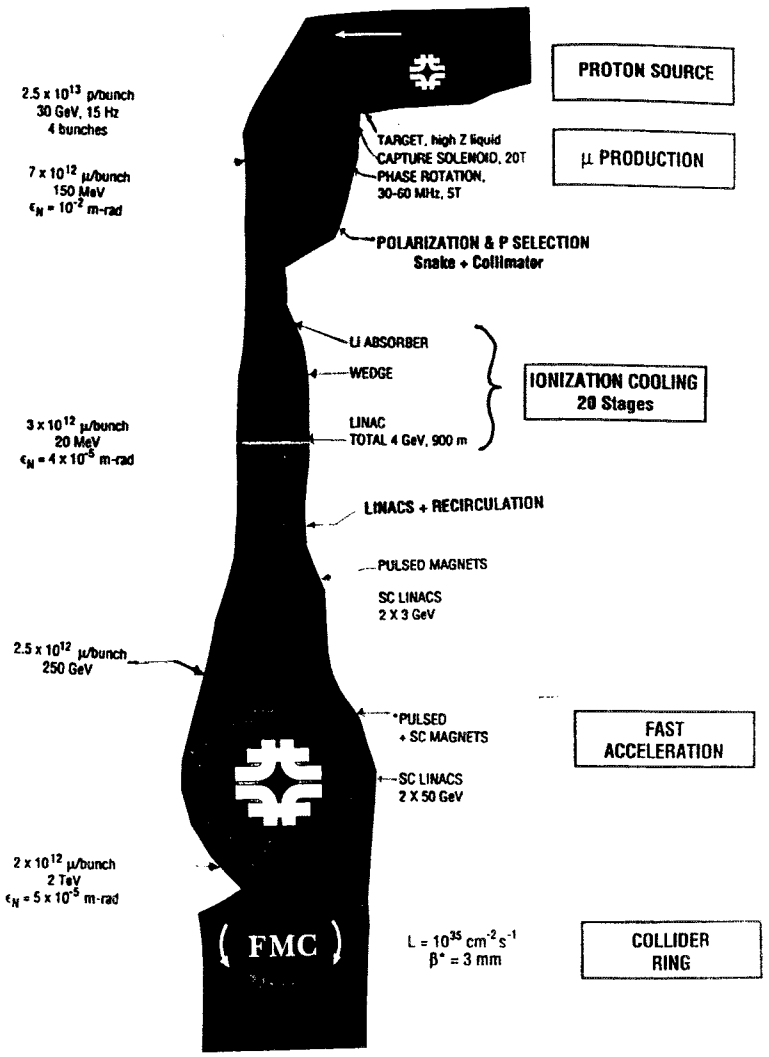

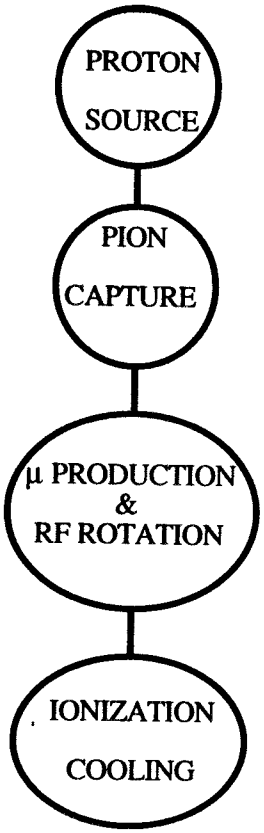

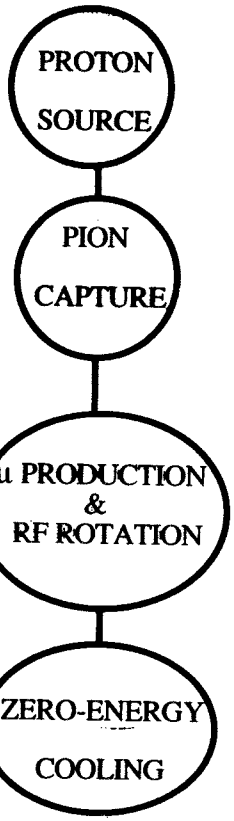

μ^+ μ

3×10^{12} μ/bunch 5×10^{12} μ/s

20 MeV 10 keV

$\varepsilon_N : 4 \times 10^{-5}$ m-rad 8×10^{-8} m-rad

EXCELLENT FEATURES OF ZERO-ENERGY COOLING

1. Extremely Small Transverse Emittance
   Thermal μ^+ (2000 K, 0.2 eV)

   P_t: 6×10^{-3} MeV/c
   d: 10^{-2} m

$$\varepsilon_t(1\ \text{TeV}) = \frac{P_t}{P_p} d = 6 \times 10^{-11}\ \text{rad} \cdot \text{m}$$

   μCF μ^-, (^{3}Heμ^-) from (t^3Heμ) Decay
   P_t : 1 MeV/c
   d : 10^{-2} m

$$\varepsilon_t(1\ \text{TeV}) = \frac{P_t}{P_p} d = 6 \times 10^{-8}\ \text{rad} \cdot \text{m}$$

2. Ready for Acceleration

3. Ready for Other Muon Science Studies

NEW μ^+ COOLING; RECENT DEVELOPMENT

Complete Stopping of High Energy μ^+

and

Re-Emission of Ultra-Slow μ^+

High Brightness, Very Low Emittance
High Intensity

Ionization of Thermal Mu from Hot Metal Surface (KEK)

Slow μ^+ from Degraded μ^+ in Solid Inert Gas (PSI)

GENERATION OF ULTRA-Slow μ^+

Laser Resonant Ionization of Thermal Mu
(UTMSL/KEK)

Slowing Down in Rare Gas Solid (Ar, Kr)
(TRIUMF, PSI)

Phase Space Compression
(PSI)

Ionization Cooling, frictional Cooling
(PSI,UCLA)

Crystal Channeling
(UCLA)

1. THERMAL MUONIUM PRODUCTION IN VACUUM

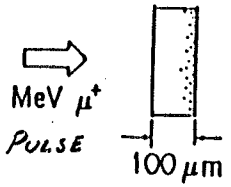

STOPPING μ^+ AT REAR-SIDE OF FOIL W

μ^+ DIFFUSION AND REACHING TO FOIL SURFACE

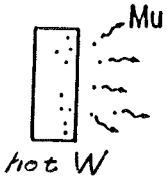

Mu EVAPORATION

2. MUONIUM IONIZATION AND SLOW μ^+ PRODUCTION

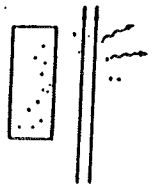

LASER IONIZATION OF Mu

ULTRA-SLOW POSITIVE MUONS AND SURFACE SCIENCE

–Probing Dynamical Surface Layer–

STEPS TOWARDS ULTRA-SLOW μ^+ BEAM AT KEK

1) **Generation of Thermal Muonium (μ^+e^-) from Hot Tungsten in Vacuum — A.P. Mills Jr., K. Nagamine et al. (1986)**

2) **Laser Ionization of Thermal Muonium S. Chu, K. Nagamine et al. (1988)**

3) **Ultra-Slow μ^+ Beam Production by Muonium Laser Ionization at Primary Proton Beam K. Nagamine, Y Miyake, et al. (1995)**

祝　Steve Chu
ノーベル物理学賞(1997)

ミュオニウム(1S-2S)レーザー共鳴実験のため
KEK 中間子に滞在(1987 年 1 月-8 月)

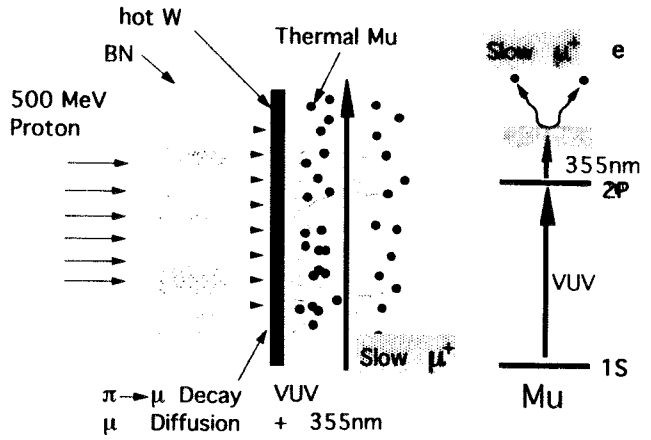

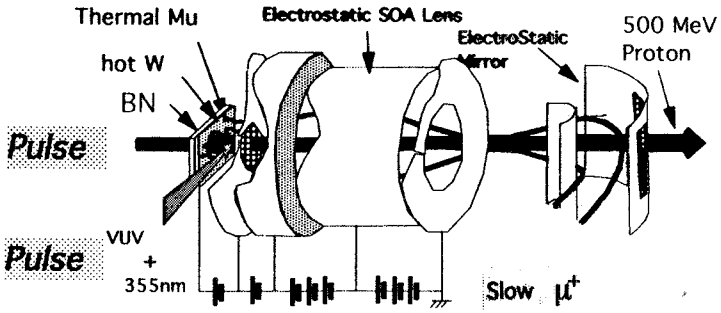

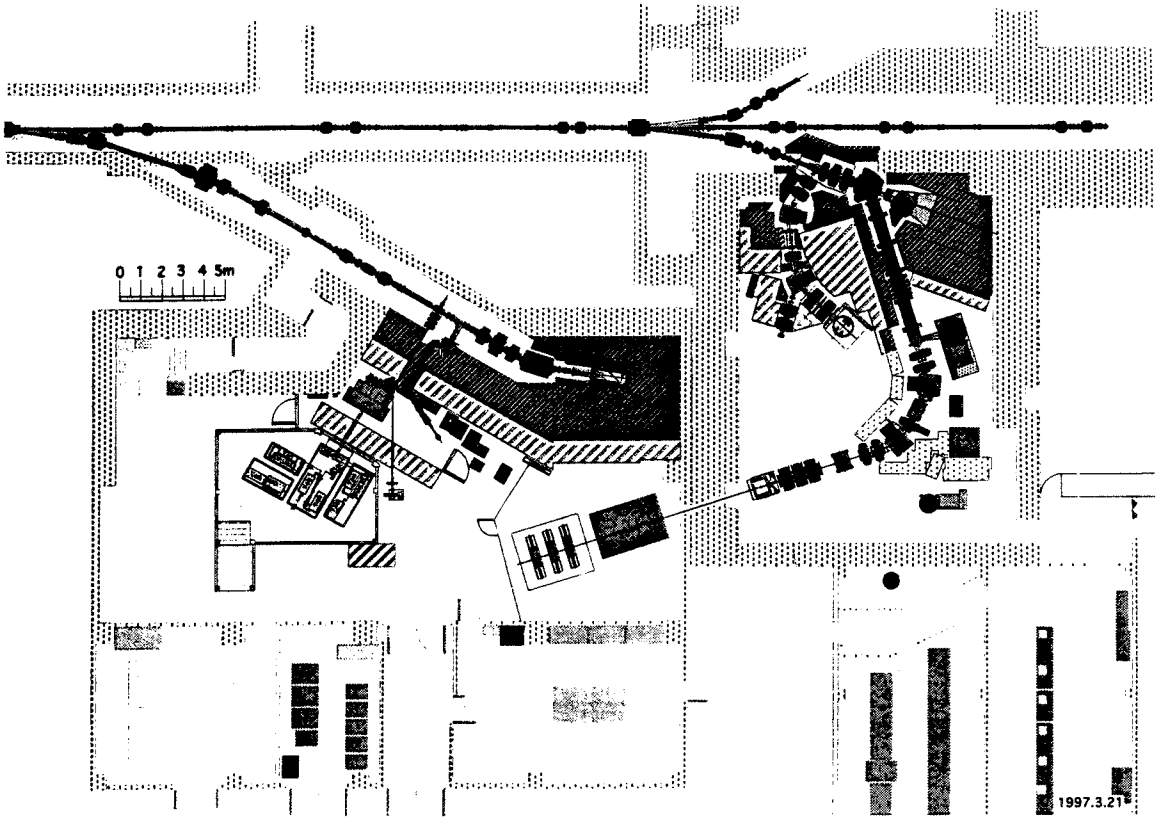

PROBING 10Å THICK SURFACES WITH 10 keV μ^+

μSR Pattern

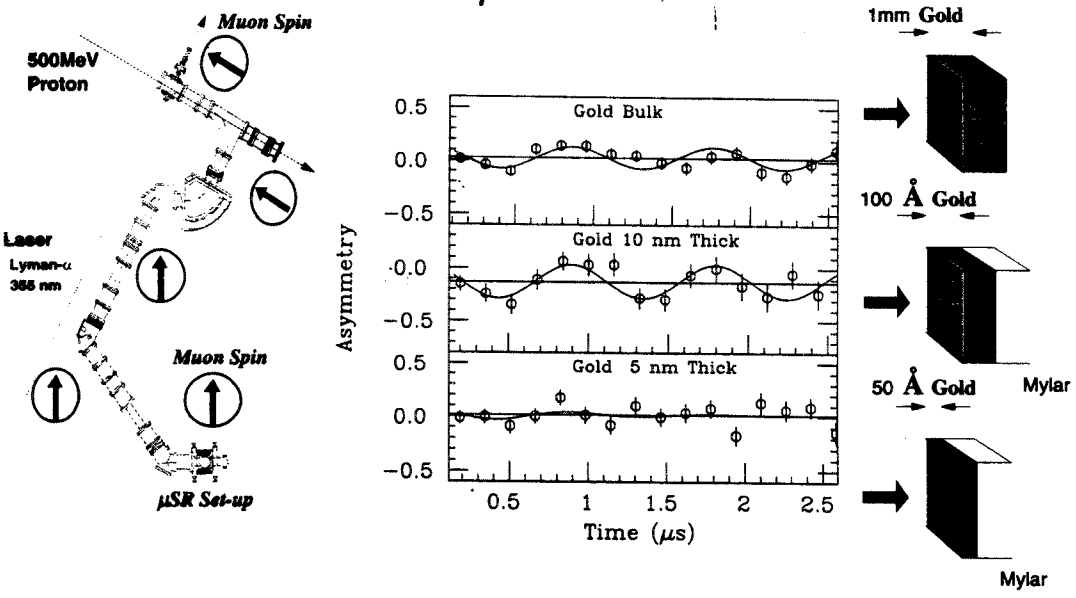

Table 1 Ultimate Intensity of ULTRA- SLOW μ^+

$N_{Mu} = I_p \times N_{\pi+} \times N_{st\mu} \times \varepsilon_{Mu}$

$N_{\mu+} = N_{Mu} \times \varepsilon_{ioni} \times \varepsilon_{coll}$

	500 MeV, 3.8μA, 1 mn BN 50 μm hot W Laser/Optics (07/94)	1 GeV, 200 μA Laser/Optics(12/95)	10 x BN 10 x hot W	Sintered W Laser/Optics(99)
I_p (p/s)	2.4×10^{13}	$\rightarrow 1.3 \times 10^{15}$		
$N_{\pi+}$ (π^+/p)	2.0×10^{-4} (8.7 mb)	$\rightarrow 1.5 \times 10^{-3}$	$\rightarrow 1.5 \times 10^{-2}$	
$N_{\pi\mu}$ (/π^+)	2.2×10^{-3} (Monte-Carlo)		$\rightarrow 2.2 \times 10^{-2}$	
$\varepsilon_{M\mu}$ (/stμ)	1×10^{-2} ($\lambda_{d.l.}$/50 μm)			$\rightarrow 0.5$
N_{Mu} : (/s)	1.1×10^{-2}	4.2×10^{7}	8.4×10^{9}	4.2×10^{11}
ε_{ioni}	4×10^{-5} (H-LRIS)	$\rightarrow 0.1$		$\rightarrow 0.5$
ε_{coll}		$\rightarrow 0.1$		
N_μ (/s)	4.4 (13) exp.	1.3×10^{6}	2.6×10^{8}	2.2×10^{10} (6.5×10^{10})

→JHP

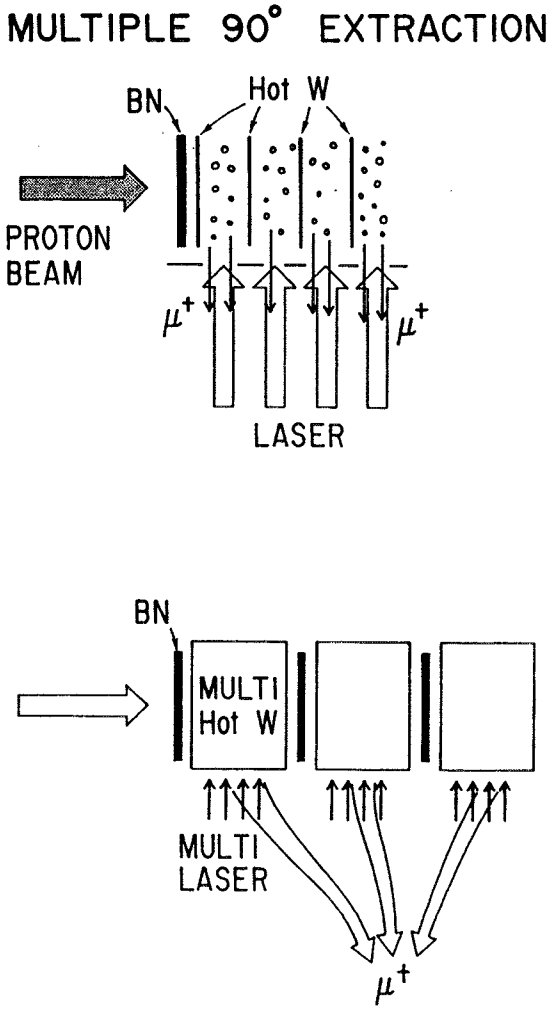

CHANGE OF THE SCHEME

μ^+

★Original

Proton → Multiple Zero-Energy Source → Acceleration & Muon Science Use

1 GeV, 200 μA
1.3×10^{15} /s

2×10^{10} /s

★New Scheme

Proton → Pion Capture → Muon Production & RF Rotation

3 GeV, 200 μA
1.3×10^{15} /s

4×10^{13} /s

2×10^{13}

→ Multiple Zero-Energy Source → Acceleration & Muon Science Use

5×10^{12} /s

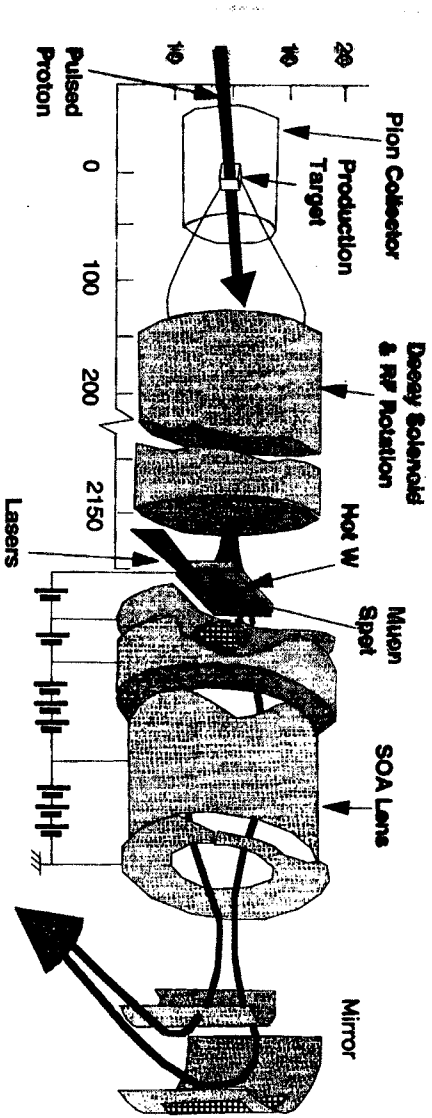

Slow μ^+

10 keV

$\sim10^{12}$ μ/s

$\sim10^{-7}$ m-RAD

NEW μ^+ COOLING; RECENT DEVELOPMENT

Complete Stopping of High Energy μ^-

and

Re-Emission of Ultra-Slow μ^-

Difficulty due to μ^- Atom Formation

eV ($d\mu$) from Solid $H_2(D_2)$ (TRIUMF)

keV μ^- from μCF in Solid D-T (KEK/RIKEN)

keV ($^3He\mu$) from Solid $T_2(^3He)$ (RIKEN/KEK)

SLOW μ^- : POSSIBLE IDEAS

RE-EMISSION METHOD

cf. CYCLOTRON TRAP FRICTIONAL COOLING & ACCUMULATION

1) Slow μ^- Production via μCF

K. Nagamine, Proc. Japan Academy 65('89) 225

2) Slow ($d\mu$) Production and Ionization

MULTI-PHOTON IONIZATION, 2.0 keV

3) Slow ($^3He\mu$)+ Source and Stripping

K. Nagamine, Hyperfine Interactions 82('93)539

CONCEPT OF μCF

FUSION IN SMALL MOLECULE AND "CIRCULATION"

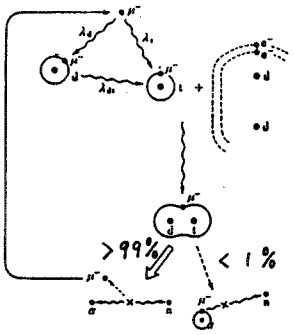

α-STICKING

μ^- Release After μCF

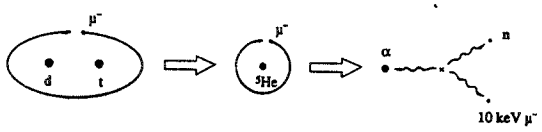

Slow μ^- Generation Via μCF

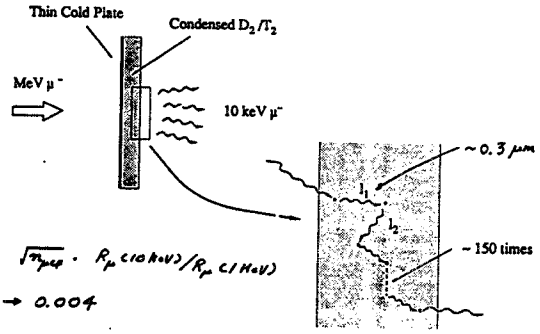

$\sqrt{\frac{m_\mu}{m_e}} \cdot R_\mu(10\,keV)/R_\mu(1\,MeV)$

$\rightarrow$ 0.004

360

RAMSAUER EFFECT ENHANCED
SLOW μ^- VIA μCF

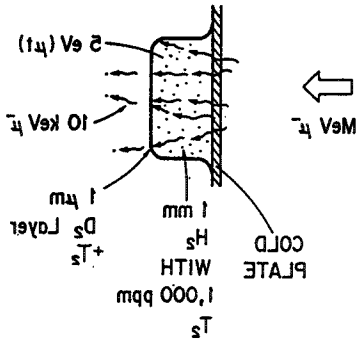

$\sqrt{\frac{m_\mu}{m_e}} \cdot R_\mu(10\,keV)/R_\mu(2\,eV) \cdot E_{R(2)}$ (eV)

RELEASE

$\rightarrow$ 0.11

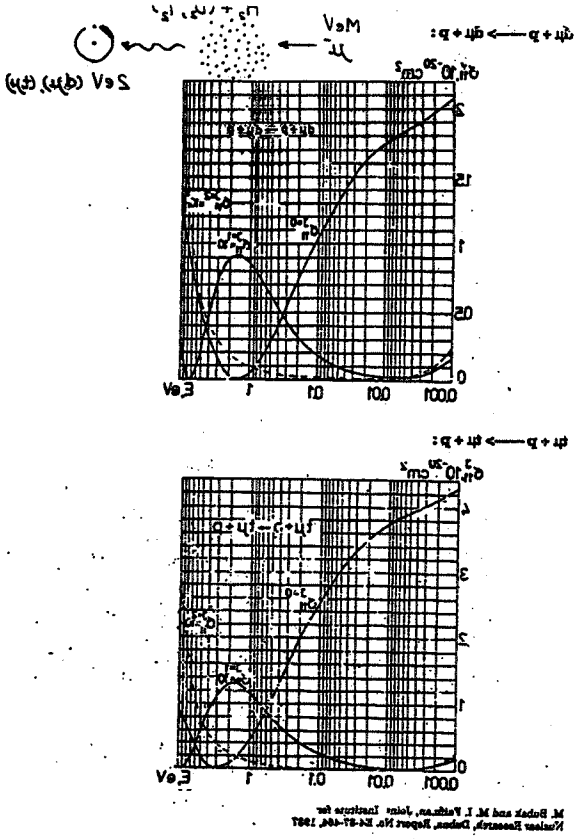

M. Bodak and M. I. Petkau, Joint Institute for Nuclear Research, Dubna, Report No. R4-87-466, 1987

Slow and Monochromatic $(^3He\mu)^+$ Beam

Principle; Formation and Decay of $(d^3He\mu)$ and $(t^3He\mu)$

μ^- Stopping in D_2 with ^3He

$(d\mu) + {}^3He \rightarrow (d^3He\mu) \rightarrow (^3He\mu)(3.2\ keV) + d$

μ^- Stopping in Solid T_2 with Accumulated ^3He

$(t\mu) + {}^3He \rightarrow (t^3He\mu) \rightarrow (^3He\mu) + t$

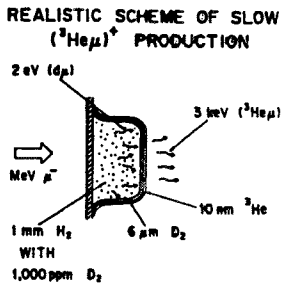

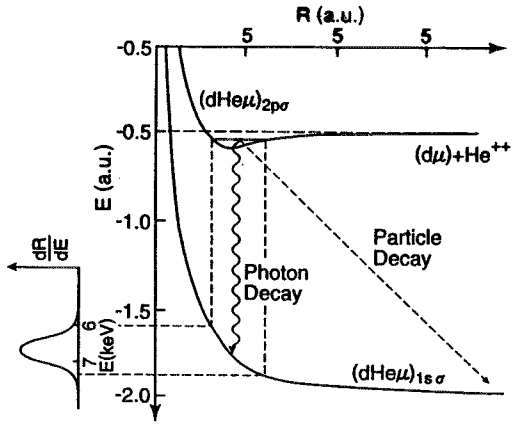

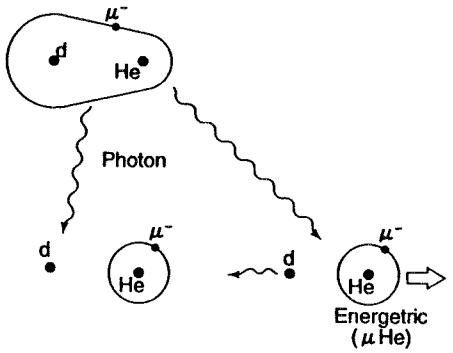

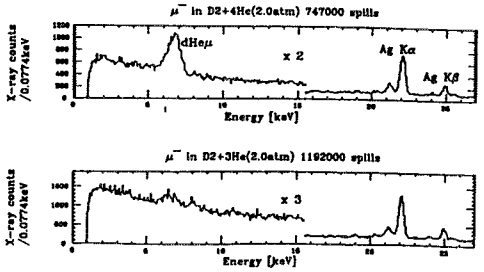

Large Scale Source of $(^3He\mu)^+$ Beam

μ^- Stopping in Multi-layer of Solid T_2 and $(^3He\mu)^+$ Emission

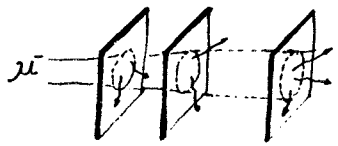

Collection of $(^3He\mu)^+$

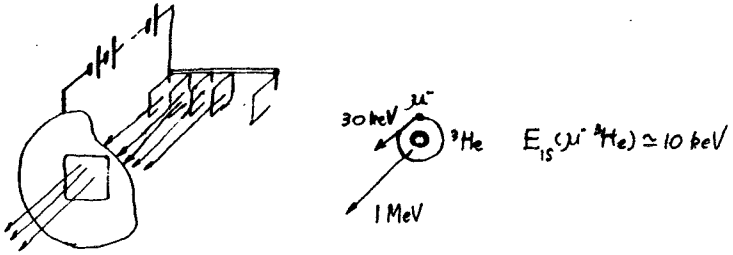

Acceleration to a few MeV and μ^- Detachment

⇨ **Intense Slow μ^- Beam**

INTENSE ULTRA-SLOW $\mu^\pm$ SOURCE PROJECT AT JHF/KEK

IDEA ADOPTED FROM

EARLY STAGE OF $\mu^+\mu^-$ COLLIDERS

LARGE $\pi^\pm$ ACCEPTOR

$\pi \rightarrow \mu$ DECAY SECTION

RF ROTATION

+

ZERO-ENERGY $\mu^\pm$ SOURCE

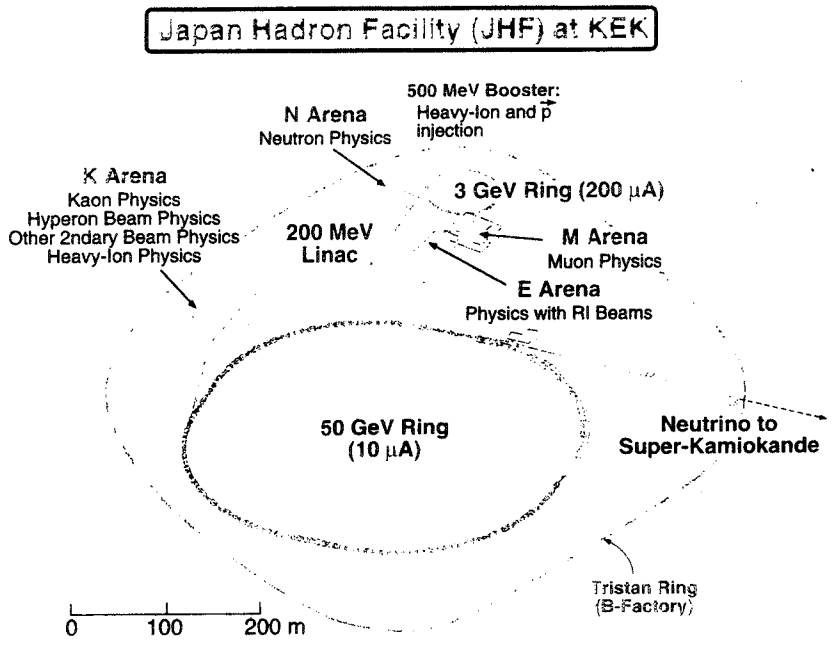

Fig. I.1 Proposed accelerator complex and experimental areas for JHF.

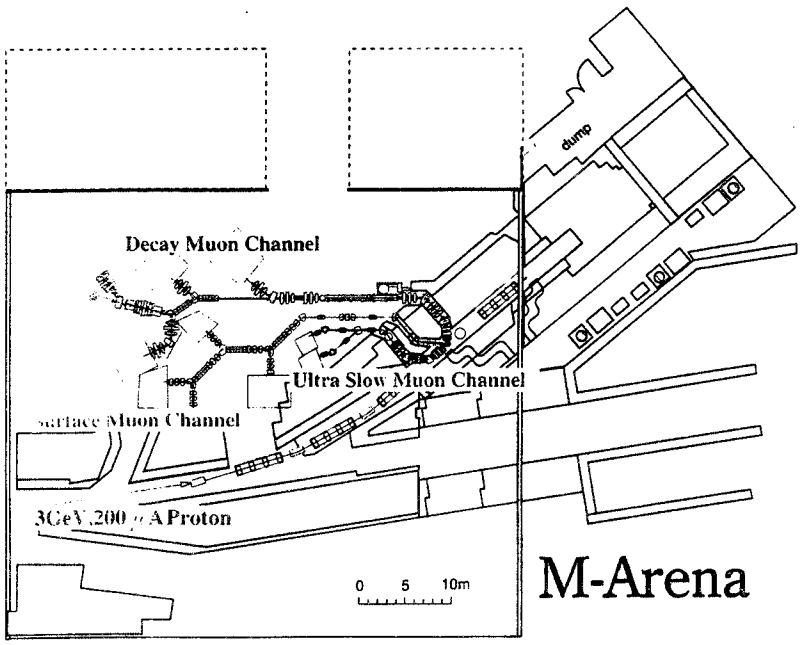

Figure III.3.2. Proposed facility layout of the M-arena at JHF to be installed at the present north counter hall of 12-GeV PS.

NEW SCHEME FOR M-ARENA OF JHF

K. Ishida, A. Bogacz, K. Nagamine

Proton Source	200 μA, 3 GeV	
π-Production Target	3 cm Be	
Pion Collection (1)	28 T, 7.5 cm Bore,	-0.5m ~0.5m
Pion Collection (2)	14 T, 7.5 cm Bore,	-0.5m ~0.5m
Decay Solenoid (1)	7.5T, 15 cm Bore,	1.5m ~51.5m
Decay Solenoid (2)	3.75T, 15 cm Bore,	1.5m ~26.5m

$L_\pi(s^{-1})$ 1.25×10^{15}

$L_\pi(\pi^-, s^{-1})$ 2.05×10^{13} (0.022)

$N_\mu(s^{-1})$ 1.5×10^{13} (0.55) [P.C.1),D.S.(1)]

$\sigma_x = \sigma_y$=5.7cm

$\sigma_x = \sigma_y$=190 mr

p_μ = 221 MeV/c, $\sigma(p_\mu)$ = 85 MeV/c (39%)

$N_\mu(s^{-1})$ 3.1×10^{12} (0.15) [P.C.2),D.S.(2)]

$\sigma_x = \sigma_y$=6.4 cm

$\sigma_x = \sigma_y$=190 mr

$\bar{P}_\mu$ = 138 MeV/c, $\sigma(p_\mu)$ = 49 MeV/c (38%)

15 T Capture Solenoid with Transition to a Small 5 T Channel
Proton Beam @ 150 mr with Scattered Proton Removal

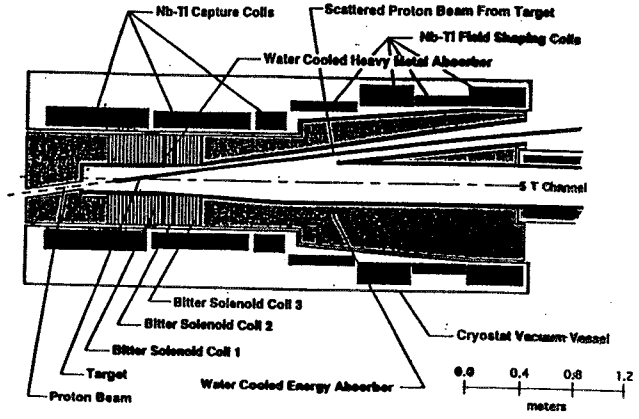

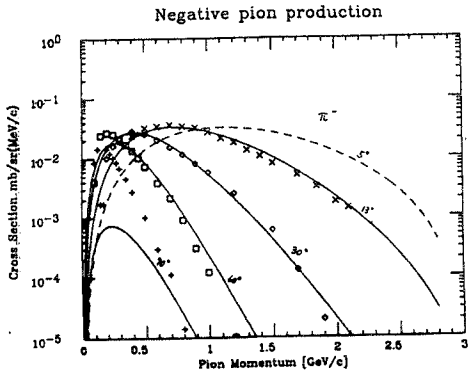

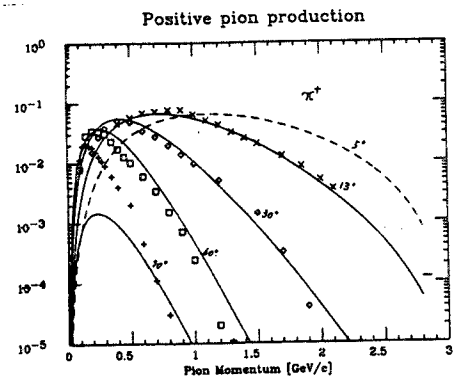

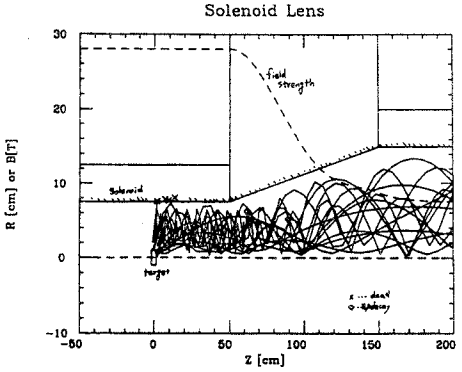

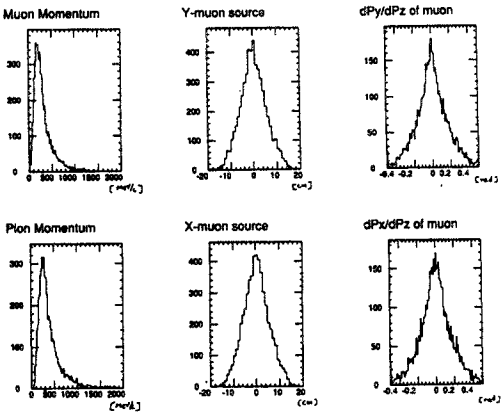

Table 1. Induction Linac Design Parameters

Parameter	Unit	Value
Voltage Gradient	MV/m	1.5
Cell Voltage	kV	50
Cell Length	cm	2
E_{min}	MeV	120
E_{max}	MeV	480
Accel. Length	m	30
Number of Cells		1000
Cell Voltage rise time	ns	40
Pulse Length	ns	100
Rep. Rate	Hz	25
Accel. Gap width	cm	0.5
Total Power per cell	kW	1
Total Power	MW	1

Table 2. Induction Cell Design Parameters

Parameter	Unit	Value
Core material – Metglass 2605SC		
Core outer radius, R_2	cm	48
Core inner radius, R_1	cm	30
Core axial width, w	cm	1.5
Core loss	kJ/m^3	3.8
Maximum core flux swing	Tesla	2.5
Dielectric gap width, g_d	mm	3
Vacuum insulator width, g_v	cm	1
Cell Capacitance	nF	9
Core leakage resistance	Ohms	8
Core leakage current	kA	4
Total Power per cell	kW	1

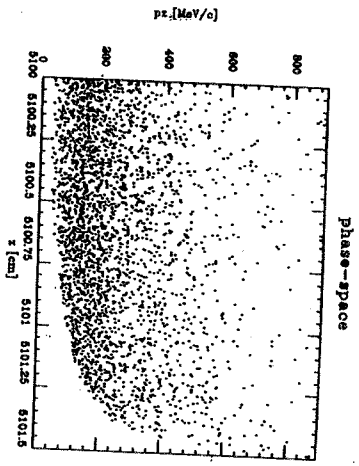

$\bar{P}_\mu$: 197, σ_P : 83 MeV/c

42 %

RF-COMPRESSION

A. Bogacz

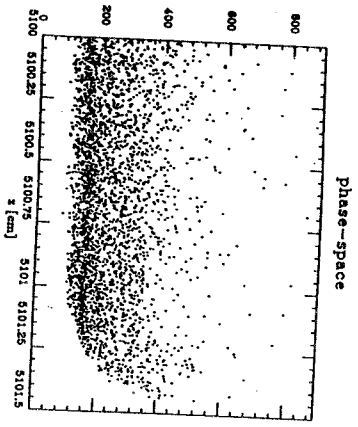

$\bar{P}_\mu$: 218, σ_P : 52 MeV/c

24%

Figure 11

Figure 12

NEW SCHEME FOR KEK-MSL & RIKEN-RAL

	KEK-MSL		RIKEN-RAL	
Proton Source	5μA, 0.5 GeV		200 μA, 0.8 GeV	
π-Production Target	3 cm Carbon			
Pion Collection	14 T, 7.5 cm Bore,		-0.5m ~0.5m	
Decay Solenoid	3.5T, 15cm Bore,		1.5m~21.5m	
$I_p(s^{-1})$	3.1×10^{13}		1.25×10^{15}	
$I_\pi(\pi^- \cdot s^{-1})$	4.3×10^{13}	(0.0014)	2.9×10^{12}	(0.0023)
$N_\mu(s^{-1})$	1.5×10^{13}	(0.35)	7.3×10^{11}	(0.25)
$\sigma_{x,y}$(cm)	6.1			
$\sigma_{x,y}$(mr)	190			
p_μ(MeV/C)	114 ± 40			

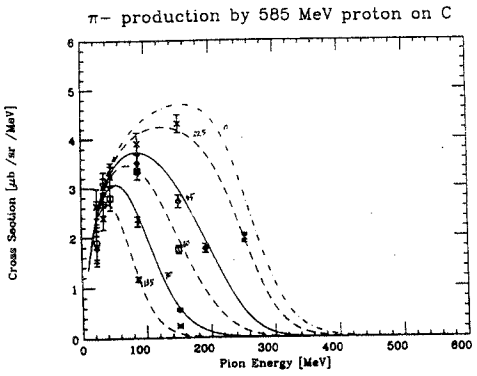
π− production by 585 MeV proton on C
Cross Section [μb /sr /MeV]
Pion Energy [MeV]

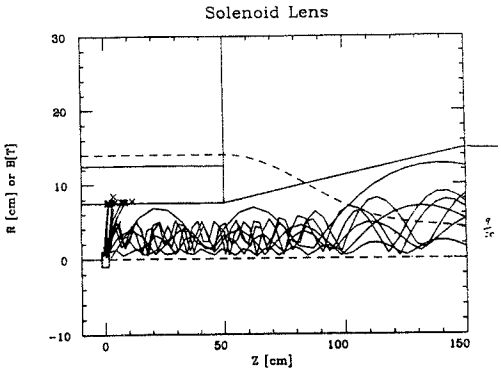
Solenoid Lens
R [cm] or B[T]
Z [cm]

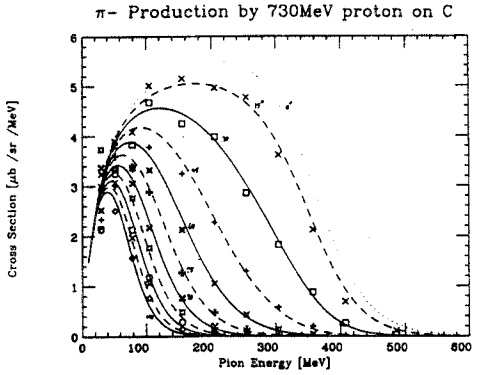
π− Production by 730MeV proton on C
Cross Section [μb /sr /MeV]
Pion Energy [MeV]

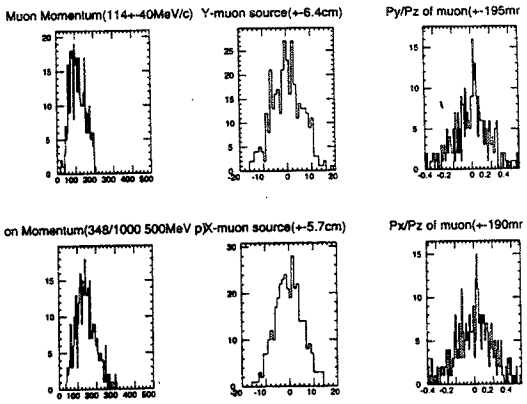
Muon Momentum(114+-40MeV/c)
Y-muon source(+-6.4cm)
Py/Pz of muon(+-195mr
on Momentum(348/1000 500MeV p)
X-muon source(+-5.7cm)
Px/Pz of muon(+-190mr

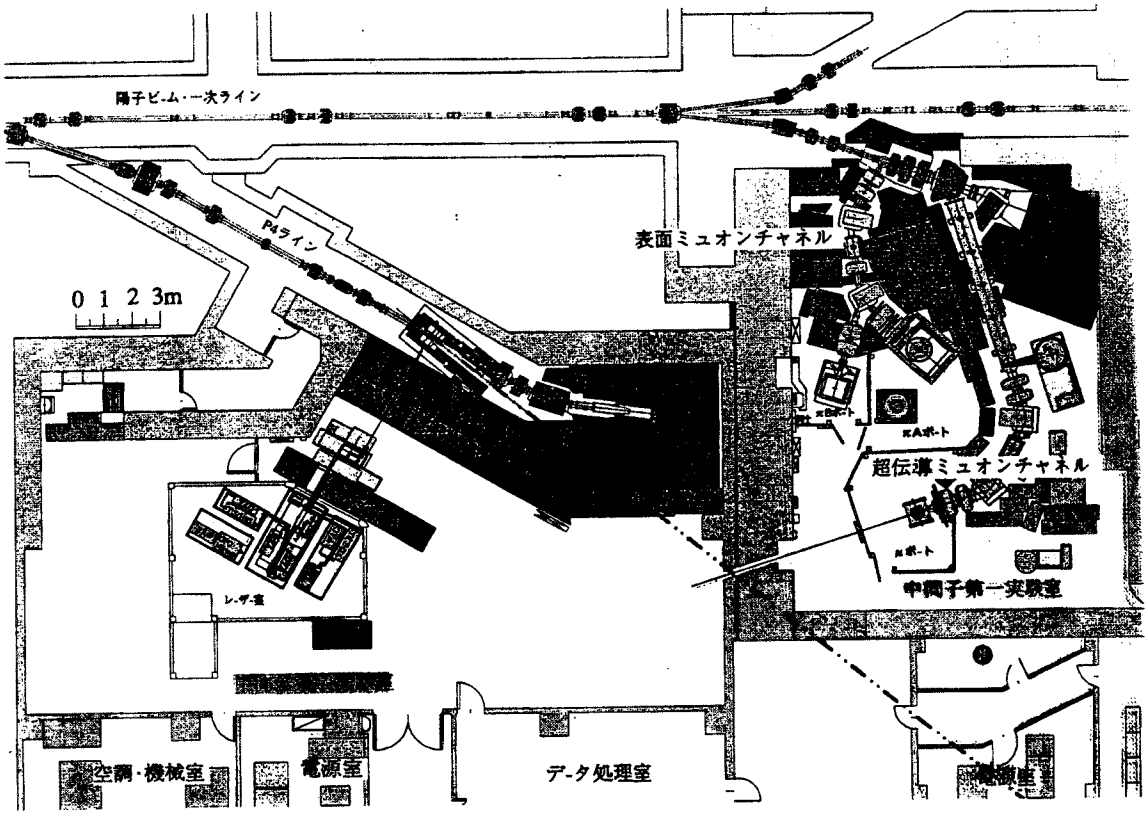
陽子ビーム一次ライン
P4ライン
0 1 2 3m
表面ミュオンチャネル
超伝導ミュオンチャネル
中間子第一実験室
空調・機械室
電源室
データ処理室

CONCLUSION

(DEC.11,1997)

★ Development of Realistic $\mu^{\pm}$ cooling Method is Essentially Important not only for $\mu^{+}\mu^{-}$ Colliders but also for Advanced Muon Science
- μSR for Materials Characterization
- Muon Catalyzed Fusion for Energy Source
- Bio-Medical Applications

★ Realization of Large Solid-Angle Pion Collector is Highly Requested
- Even for Low Energy (below 3 GeV) Proton Accelerator

MUON DYNAMICS IN A TOROIDAL SECTOR MAGNET

Physics Potential & Development of $\mu^+\mu^-$ Colliders
San Francisco, CA

Juan C. Gallardo

Dec. 10-12, 1997

MOTIVATION

- ❑ Longitudinal cooling section (emittance exchange) is needed to compress the beam phase-space to obtain High Luminosity. (compression ration $\approx 10^6$)
- ❑ Bent solenoids (vertical and horizontal), dipoles, wedges (Li,Be)
- ❑ Matching and dynamics require careful design and numerical studies. The codes must be if all possible SYMPLECTIC to eliminate any superfluous dilution of 6D phase-space.

☛ Objective: Single particle HAMILTONIAN formulation of simplified model. This is not a substitute for ICOOL, GEANT,...

FORMULATION

- Approximated Hamiltonian in accelerator frame of reference

$$H = -A_s(1+hx) - hx(1+\delta) - \frac{(1+hx)}{2(1+\delta)}\{(p_x - A_x)^2 + (p_y - A_y)^2\}^{\frac{1}{2}}$$

  s independent variable, $\frac{\vec{p}}{p_o}$, $\vec{A}$ normalized momentum and vector potential, z pulse length and $\delta = \frac{p}{p_o} - 1$.

- $(x, p_x); (y, p_y) \text{and} (z, \delta)$ are canonical variables.

- Metric $d\sigma^2 = dx^2 + dy^2 + (1+hx)^2 ds^2$ for horizontal bending.

Physics Potential & Development of $\mu^+\mu^-$ Colliders. Dec. 10-12, 1997.

- We need the vector potential. The magnetic and electric field are obtained from $\vec{B} = \text{curl}\,\vec{A}$; $\vec{E} = c\beta_o \frac{\partial \vec{A}}{\partial z}$ (recall the metric)

  ⇛ Bend solenoid (horizontal as an example)

$$\vec{A_s} = -\frac{1}{2} B_o \frac{y}{(1+hx)} \vec{e_x} + \frac{B_o}{2h} \ln(1+hx) \vec{e_y}$$

  it satisfy $\text{div}\,\vec{\text{A}} = 0$ and the longitudinal magnetic field is $B_s = \frac{B_o}{(1+hx)}$.

  ⇛ Guiding Dipole $\vec{A}_D = -\frac{1}{2}(1+hx)\vec{e_s}$ to compensate the natural drift due to the toroidal solenoid, but keeping Dispersion.

SYMPLECTIC INTEGRATOR

- The time evolution of a mechanical system is *equivalent* to a transformation in phase space.

CANONICAL TRANSFORMATION

$$(q,p,z,\delta) \qquad \mathcal{M} \qquad (Q,P,Q_\delta,P_\delta)$$

$$s=0 \qquad \Longrightarrow \qquad s=\Delta s$$

The transformation ~~matrix~~ map $\mathcal{M}$ is SYMPLECTIC

Why is it important?

⇛ It gives the correct dynamics. Conserve 6D phase-space

⇛ Increase speed of computations and accuracy.

Physics Potential & Development of $\mu^+\mu^-$ Colliders. Dec. 10-12, 1997.

- The integration of Equation of Motion MUST be done with a *symplectic integrator* otherwise there is the possibility of undesirable phase space dilution.

- É. Forest and K. Ohmi have proposed an explicit procedure to construct first order symplectic integrators.

  The idea is:

  ⇛ Construct a generating function

$$F(x,P,z,P_\delta) = xP + zP_\delta + \Delta s H(x,P,z,P_\delta)$$

  this function generates the correct motion up to order $(\Delta s)^2$.

Using standard procedures:

$$Q = \frac{\partial F}{\partial P} = x + \Delta s \frac{\partial H}{\partial P}$$
$$Q_\delta = \frac{\partial F}{\partial P_\delta} = z + \Delta s \frac{\partial H}{\partial P_\delta}$$
$$p = \frac{\partial F}{\partial x} = P + \Delta s \frac{\partial H}{\partial x}$$
$$\delta = \frac{\partial F}{\partial z} = P_\delta + \Delta s \frac{\partial H}{\partial z}$$

⇛ This set of equations can be inverted exactly; hence we write:

$$Q = f_1(q,p) \equiv q(s+\Delta s)$$
$$P = f_2(q,p) \equiv p(s+\Delta s)$$
$$\ldots$$

The surprising fact is that the equation of motion are algebraic instead of differential equations. The integration is faster and more reliable.

⇛ This approach has been partially implemented in ICOOL (see next talk by R. Fernow)

⇛ Test on model problems with exactly known solutions (6D) (drift,dipole)

SUMMARY

We have presented:

⇛ A single particle (no space-charge) Hamiltonian of a combined bend solenoid and dipole system.

⇛ The model problem is useful for numerical studies of emittance exchange scenarios.

⇛ Lastly, an explicit symplectic integrator of first order which lead to equations of motion that can be inverted exactly.

⇛ Parts of these ideas have been implemented in ICOOL.

A First Look at Emittance Exchange in a Bent Solenoid System

R.C. Fernow
BNL

11 December 1997

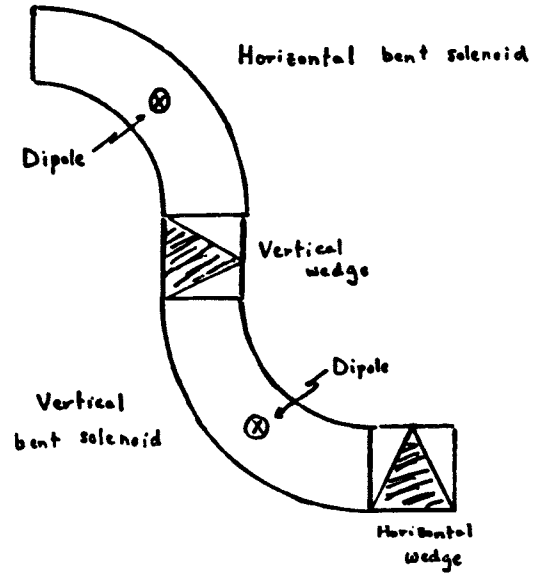

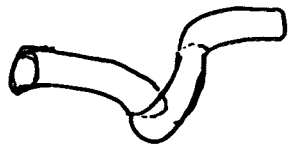

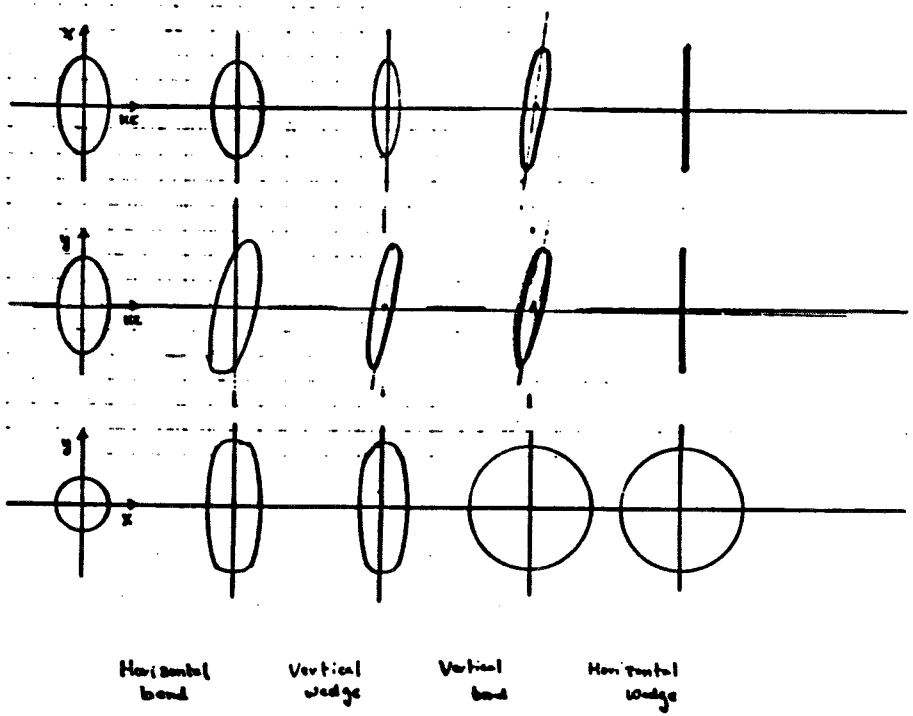

First order equations of motion

$$x'' = h(1 + hx) - \frac{q}{p}[B_y(1 + 2hx) - B_s y']$$

$$y'' = \frac{q}{p}[B_x(1 + 2hx) - B_s x']$$

where h is constant.

Field model

$$B_x(x,y,s) = B_D a_{11} y$$
$$B_y(x,y,s) = B_D (a_{10} + a_{11} x)$$
$$B_s(x,y,s) = B_S(1 - hx)$$

Case 1

o transverse E beam on-axis

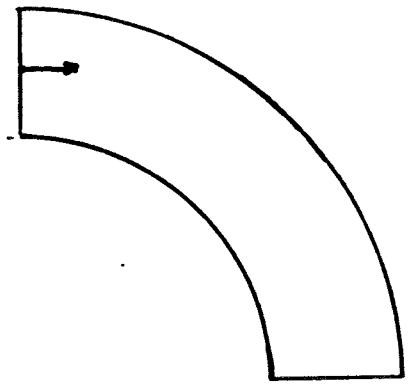

$\Delta p = \pm 10\%$ (full range)

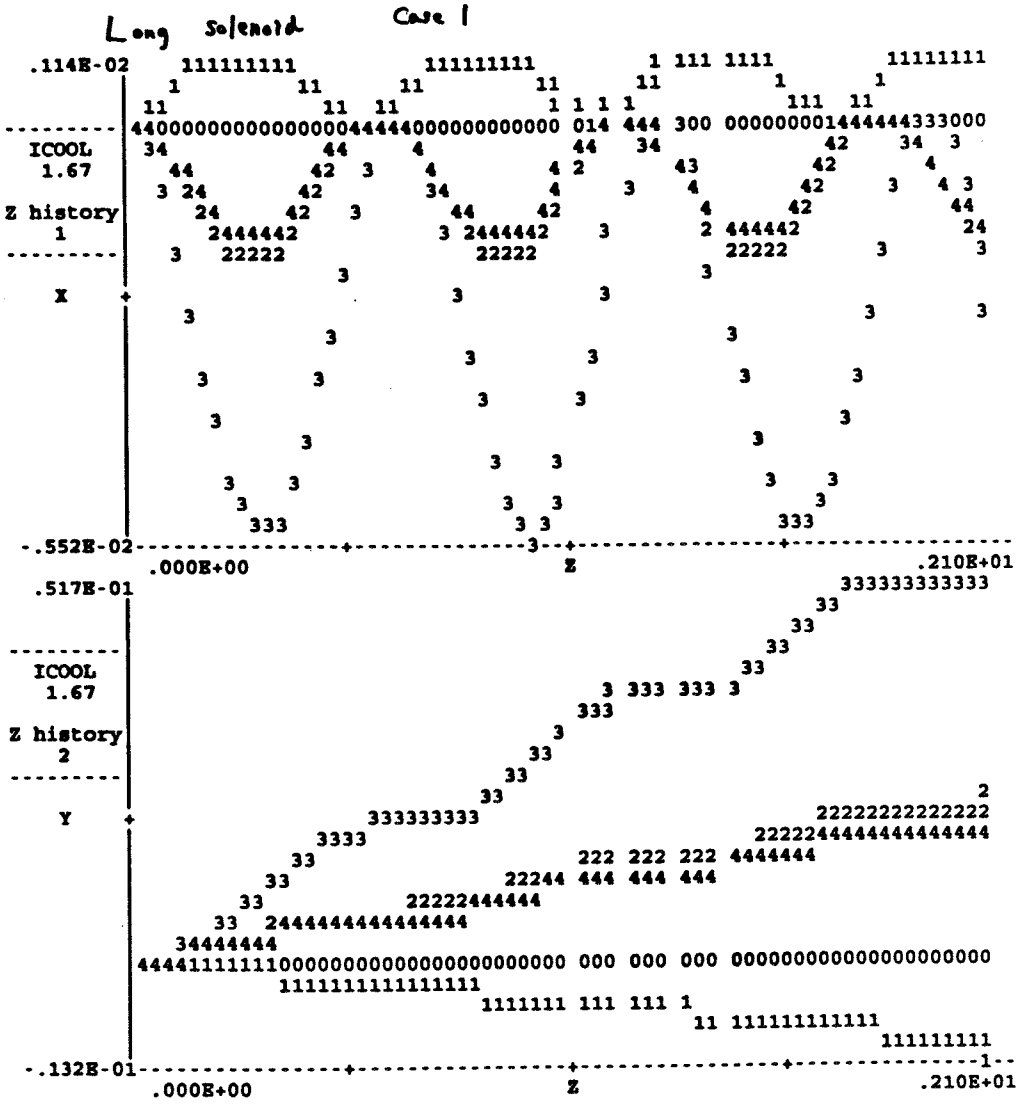

$p = 200$ MeV/c

$B_s = 7$ T

$B_b = -2$ T

Y22

Case 1

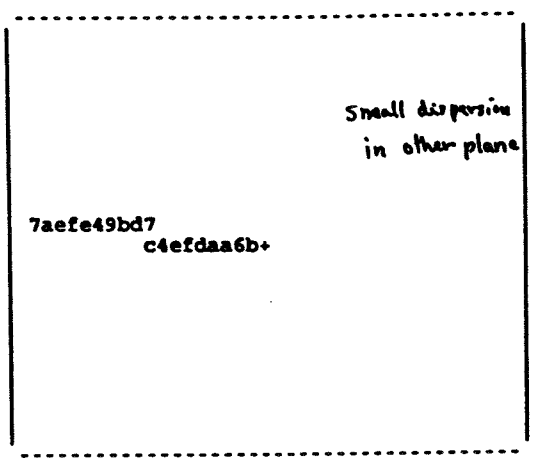

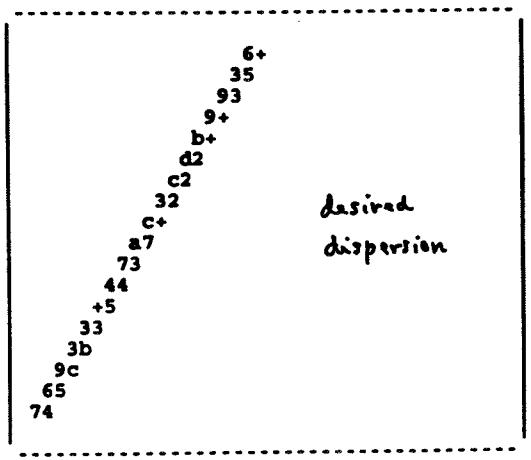


```
ICOOL                    1.67
-----------------------------
plot          =           2
var(x)        =          KE
dest(x)       =           1
var(y)        =           X
dest(y)       =           1

lo x          =    .100E+00
hi x          =    .180E+00
step x        =    .200E-02
lo y          =   -.600E-01
hi y          =    .600E-01
step y        =    .600E-02

contents      =         200
under x       =           0
over x        =           0
under y       =           0
over y        =           0
-----------------------------
```

```
ICOOL                    1.67
-----------------------------
plot          =           5
var(x)        =          KE
dest(x)       =           1
var(y)        =           Y
dest(y)       =           1

lo x          =    .100E+00
hi x          =    .180E+00
step x        =    .200E-02
lo y          =   -.600E-01
hi y          =    .600E-01
step y        =    .600E-02

contents      =         200
under x       =           0
over x        =           0
under y       =           0
over y        =           0
-----------------------------
```

Design criteria

- Larmor wavelength

$$\lambda_L = 2\pi \frac{p}{eB_s}$$

- make solenoid length $L_S = \frac{1}{4}\lambda_L$ to minimize size in the non-dispersive plane and divergence in both planes

- make solenoid length correspond to 90° for geometric convenience

$$L_S = \frac{\pi}{2}\rho$$

- this fixes required dipole strength (dipole sign controls sign of dispersion)

$$B_D = \frac{p}{e\rho}$$

Case 1

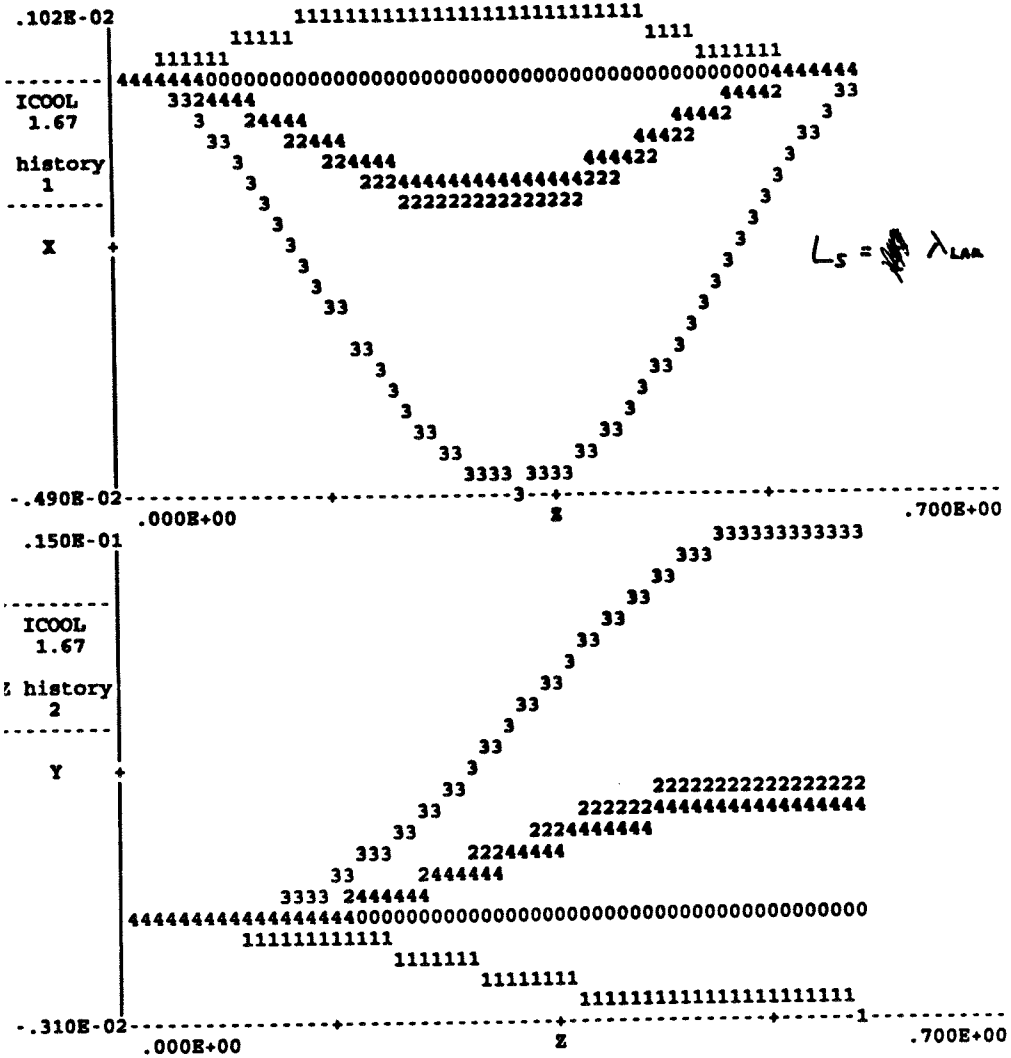

$L_s = \lambda_{LAR}$

$p = 200$ MeV/c

$B_s = 7$ T

$B_0 = -1.75$ T

Case 1

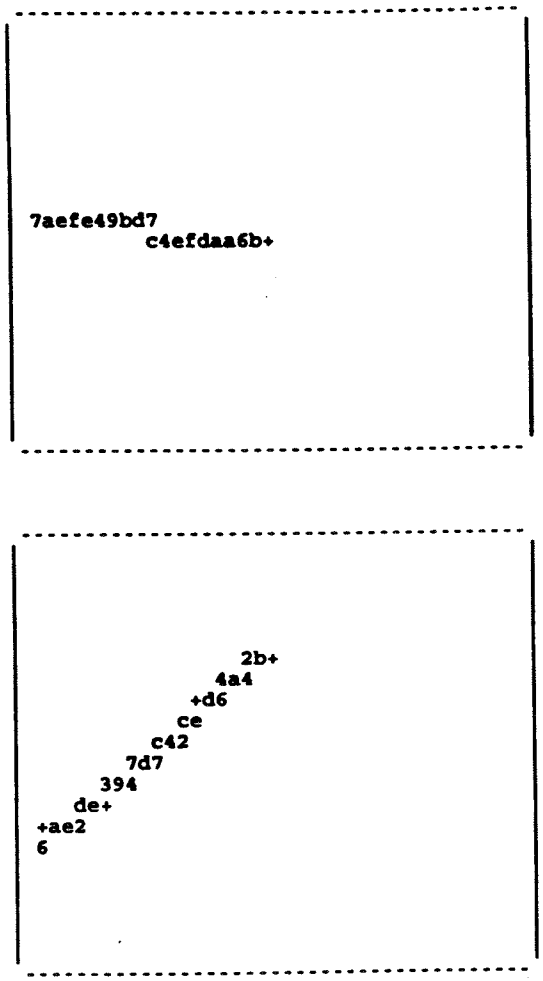

ICOOL	1.67
plot	2
var(x)	KE
dest(x)	1
var(y)	X
dest(y)	1
lo x	.100E+00
hi x	.180E+00
step x	.200E-02
lo y	-.300E-01
hi y	.300E-01
step y	.300E-02
contents	200
under x	0
over x	0
under y	0
over y	0

ICOOL	1.67
plot	5
var(x)	KE
dest(x)	1
var(y)	Y
dest(y)	1
lo x	.100E+00
hi x	.180E+00
step x	.200E-02
lo y	-.300E-01
hi y	.300E-01
step y	.300E-02
contents	200
under x	0
over x	0
under y	0
over y	0

Case 2

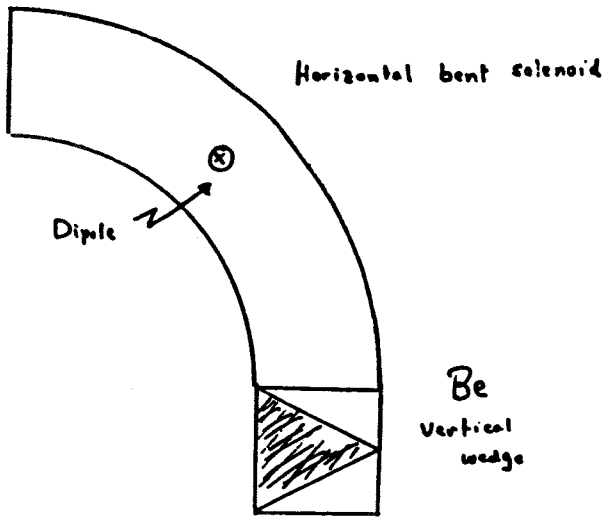

p = 200 MeV/c

B_s = 7 T

B_D = −1.75 T

Δp = ± 10%

- adjust wedge dimensions to remove dispersion

Wedge design equations

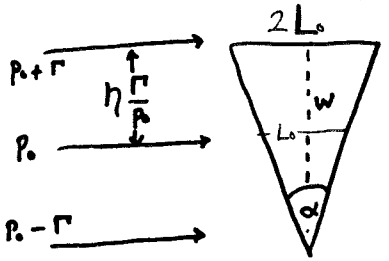

$$\frac{\overline{dE}}{dz} L_o = \Gamma_E$$

$$w = 2\eta \frac{\Gamma}{p_o}$$

$$h = f(\epsilon, m.s.)$$

$$\tan\frac{\alpha}{2} = \frac{2L_o}{2w}$$

Ideal conditions

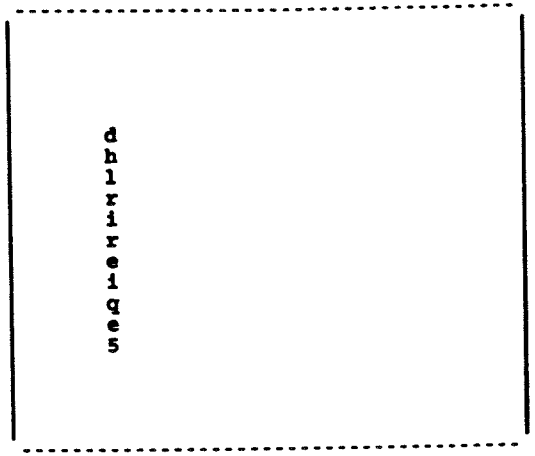

$\alpha = 125°$

$L_o \simeq 8$ cm

ICOOL	1.67
plot	6
var(x)	KE
dest(x)	2
var(y)	Y
dest(y)	2
lo x	.800E-01
hi x	.160E+00
step x	.200E-02
lo y	-.300E-01
hi y	.300E-01
step y	.300E-02
contents	200
under x	0
over x	0
under y	0
over y	0

Cour 2

The real world !

Scattering

Straggling

beam size

beam radial divergence

beam angular momentum

Com 2

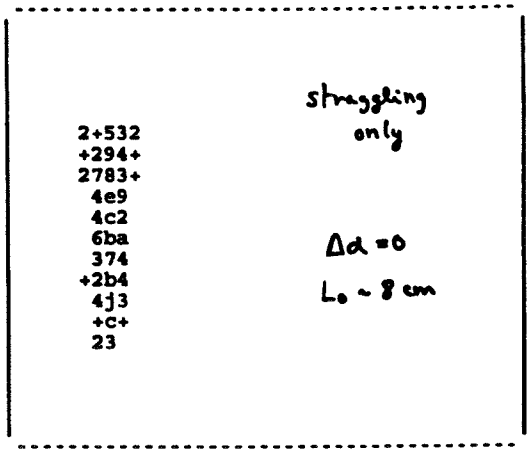

ICOOL	1.67
plot	6
var(x)	KE
dest(x)	2
var(y)	Y
dest(y)	2
lo x	.800E-01
hi x	.160E+00
step x	.200E-02
lo y	-.300E-01
hi y	.300E-01
step y	.300E-02
contents	200
under x	0
over x	0
under y	0
over y	0

425

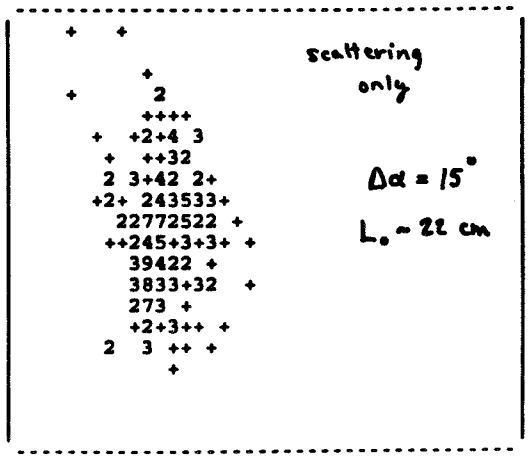

ICOOL	1.67
plot	6
var(x)	KE
dest(x)	2
var(y)	Y
dest(y)	2
lo x	.600E-01
hi x	.140E+00
step x	.200E-02
lo y	-.400E-01
hi y	.400E-01
step y	.400E-02
contents	200
under x	0
over x	0
under y	0
over y	0

426

Com 2

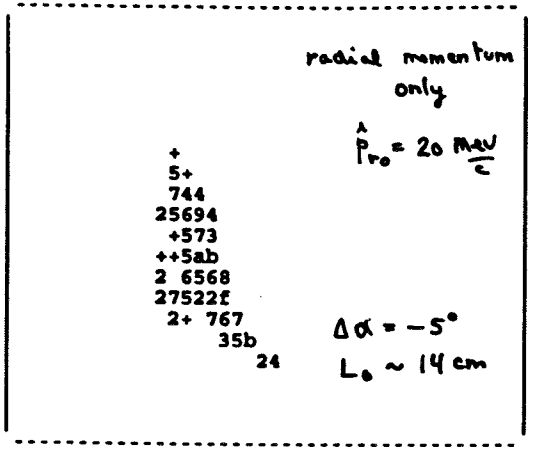

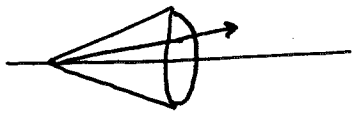

ICOOL	1.67
plot	6
var(x)	KE
dest(x)	2
var(y)	Y
dest(y)	2
lo x	.500E-01
hi x	.130E+00
step x	.200E-02
lo y	-.400E-01
hi y	.400E-01
step y	.400E-02
contents	200
under x	0
over x	0
under y	0
over y	0

Case 3

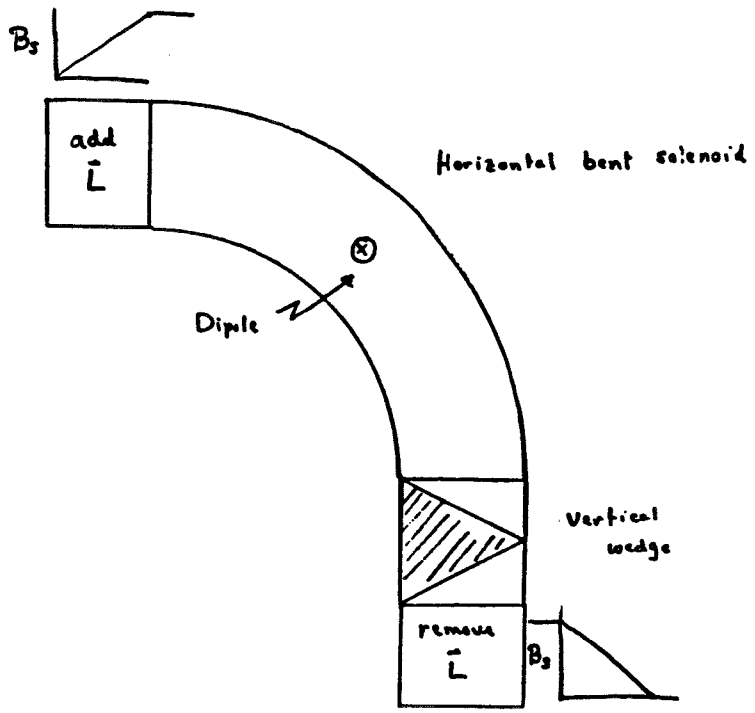

Case 3

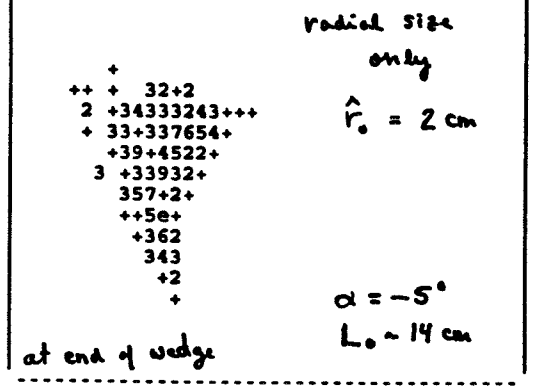

ICOOL	1.67
plot	9
var(x)	KE
dest(x)	3
var(y)	Y
dest(y)	3
lo x	.500E-01
hi x	.130E+00
step x	.200E-02
lo y	-.400E-01
hi y	.400E-01
step y	.400E-02
contents	200
under x	0
over x	0
under y	0
over y	0

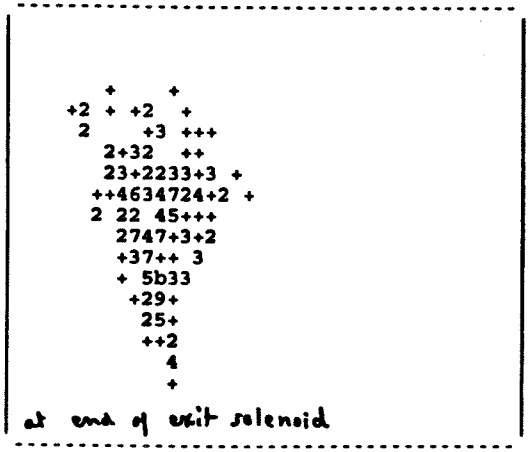

ICOOL	1.67
plot	10
var(x)	KE
dest(x)	4
var(y)	Y
dest(y)	4
lo x	.500E-01
hi x	.130E+00
step x	.200E-02
lo y	-.400E-01
hi y	.400E-01
step y	.400E-02
contents	200
under x	0
over x	0
under y	0
over y	0

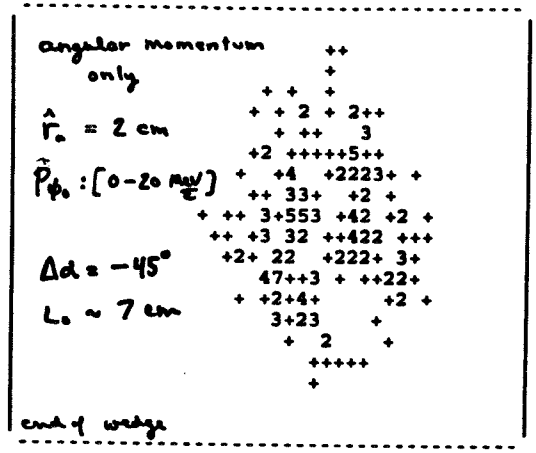

Case 3

ICOOL 1.67

plot	9
var(x)	KE
dest(x)	3
var(y)	Y
dest(y)	3
lo x	.500E-01
hi x	.130E+00
step x	.200E-02
lo y	-.400E-01
hi y	.400E-01
step y	.400E-02
contents	200
under x	0
over x	0
under y	0
over y	0

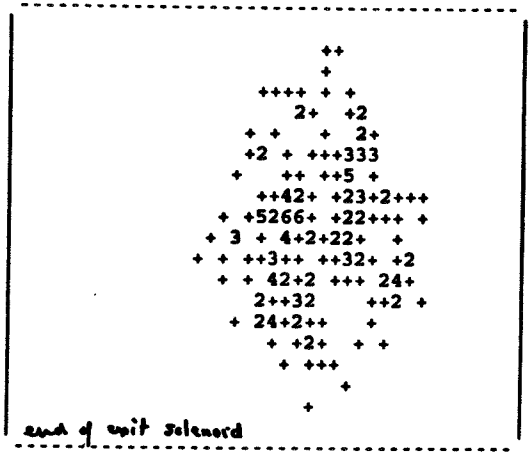

ICOOL 1.67

plot	10
var(x)	KE
dest(x)	4
var(y)	Y
dest(y)	4
lo x	.500E-01
hi x	.130E+00
step x	.200E-02
lo y	-.400E-01
hi y	.400E-01
step y	.400E-02
contents	200
under x	0
over x	0
under y	0
over y	0

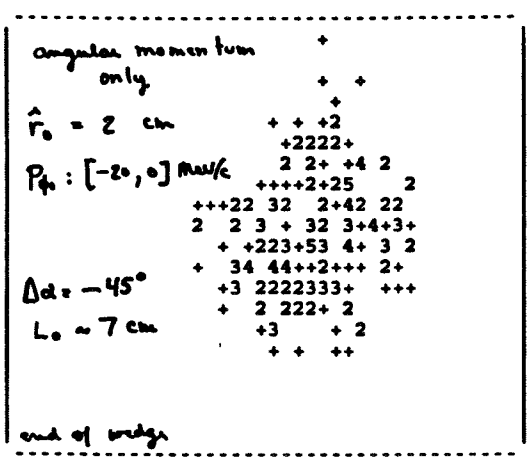

Case 3

ICOOL 1.67

plot	9
var(x)	KE
dest(x)	3
var(y)	Y
dest(y)	3
lo x	.500E-01
hi x	.130E+00
step x	.200E-02
lo y	-.400E-01
hi y	.400E-01
step y	.400E-02
contents	200
under x	0
over x	0
under y	0
over y	0

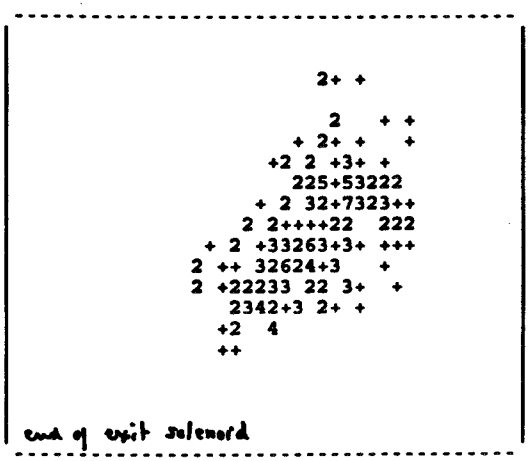

ICOOL 1.67

plot	10
var(x)	KE
dest(x)	4
var(y)	Y
dest(y)	4
lo x	.500E-01
hi x	.130E+00
step x	.200E-02
lo y	-.400E-01
hi y	.400E-01
step y	.400E-02
contents	200
under x	0
over x	0
under y	0
over y	0

// Conclusions

- 1st order simulation under ideal conditions give
  expected dispersion from the bent solenoid
  expected reduction in momentum spread

- scattering, straggling, and transverse emittance effects all reduce the efficiency of the exchange process

- design optimization is in progress
  → 2nd order simulation is probably necessary
  → hope to have design by BNL cooling workshop in January

Ionization Cooling for μ^+-μ^- Colliders- II (~Fermilab)

David Neuffer

Fermilab

December 1997

Outline

Introduction:
- Cooling process, cooling equations,
- Cooling requirements,
- Cooling scenario overview

Simulations of ionization cooling
- **-Simucool results**
  - wedges,
  - Li lens,
  - ring cooler

Recent developments:
- Match, wedge transport design,
- Feasibility study,
- Li lens program

Cooling Simulations program – P. LeBrun
- Geant, Icool, Parmela, Simucool

Cooling Experiment – S. Geer

Summary; discussion

Table 1: Parameter list for μ^+-μ^- Colliders

Parameter	Symbol	Higgs ??	500GeV	4TeV
Collision Energy	$2E_\mu$	100	500	4000 GeV
Energy per beam	E_μ	50	250	2000 GeV
Luminosity	$L=f_0 n_s n_b N_\mu^2/4\pi\sigma^2$	5×10^{31}	1×10^{33}	$10^{35}cm^{-2}s^{-1}$
Source Parameters				
Proton energy	E_p	16	16	30 GeV
Protons/pulse	N_p	$2\times5\times10^{13}$	$4\times2.5\times10^{13}$	$4\times3\times10^{13}$
Pulse rate	f_0	15	15	15Hz
μ-production acceptance	μ/p	0.2	0.2	.2
μ-survival allowance	N_μ/N_{source}	0.32	0.3	.333
Collider Parameters				
Collider radius	R	60	150	1000m
Number of μ /bunch	$N_{\mu\pm}$	3.2×10^{12}	1.5×10^{12}	2×10^{12}
Number of bunches	n_B	1	1	2
Storage turns	$2n_s$	1000	1800	1800
Normalized emittance	ε_N	10^{-4}	10^{-4}	5×10^{-5}m-rad
μ-beam emittance	$\varepsilon_t=\varepsilon_N/\gamma$	2×10^{-7}	4×10^{-8}	2.5×10^{-9}m-rad
Interaction focus	β_0	4	2	0.3 cm
Beam size at interaction	$\sigma=(\varepsilon_t\beta_0)^{1/2}$	90	30	2.1 μm

Beam Cooling Requirements

Beam from source and rf rotation:

$\varepsilon_{\perp,N} \cong 0.015$ m-rad (7 cm $\times$70 mrad); $\delta p/p \sim 10\%$, $\delta z \sim 1$ m
at $p_\mu \cong 300$ MeV/c
up to 7×10^{12} μ's/bunch - need ~3×10^{12} μ's/bunch after cooling

Cool by ~5 $\times$ 10^5 :

Beam at **2$\times$2 TeV** Collider:
$\varepsilon_{\perp,N} \cong 0.00005$ m-rad; $\delta p/p \sim 0.12\%$, $\delta z \sim 3$mm at $p_\mu \cong 2$ TeV/c

Beam at **250$\times$250 GeV** Collider:
$\varepsilon_{\perp,N} \cong 0.00006$ m-rad; $\delta p/p \sim 0.12\%$, $\delta z \sim 1$cm at $p_\mu \cong 0.2$ TeV/c

Beam at **50$\times$50 GeV** Collider:
$\varepsilon_{\perp,N} \cong 0.00009$ m-rad; $\delta p/p \sim 0.12\%$, $\delta z \sim$4cm at $p_\mu \cong 50$ GeV/c

Beam at **50$\times$50 GeV** Collider – **(small $\delta p/p$ mode)**:
$\varepsilon_{\perp,N} \cong 0.00032$ m-rad; $\delta p/p \sim 0.003\%$, $\delta z \sim$13cm at $p_\mu \cong 50$ GeV/c

Cool before μ-decay : $\tau_\mu = 2.2$ μs; $c\tau_\mu$ =660m

μ^+-μ^- Collider Scenario Overview

μ^+-μ^- source - ~KAON-class p-driver (10^{14} at 15 Hz) produces ~0.1μ/p ($p + X \rightarrow \pi \rightarrow \mu$)

μ^+-μ^- cooling - cools muons by ~10^6 in ~ 3μs using ionization cooling

μ^+-μ^- acceleration - recirculating linacs and/or rapid-cycling synchrotrons (0.1 $\rightarrow$ 2000 GeV/c)

μ^+-μ^- collider - storage ring ~2000 turns/pulse, σ=2μ, $\Delta\nu$ = 0.05, high-L detector

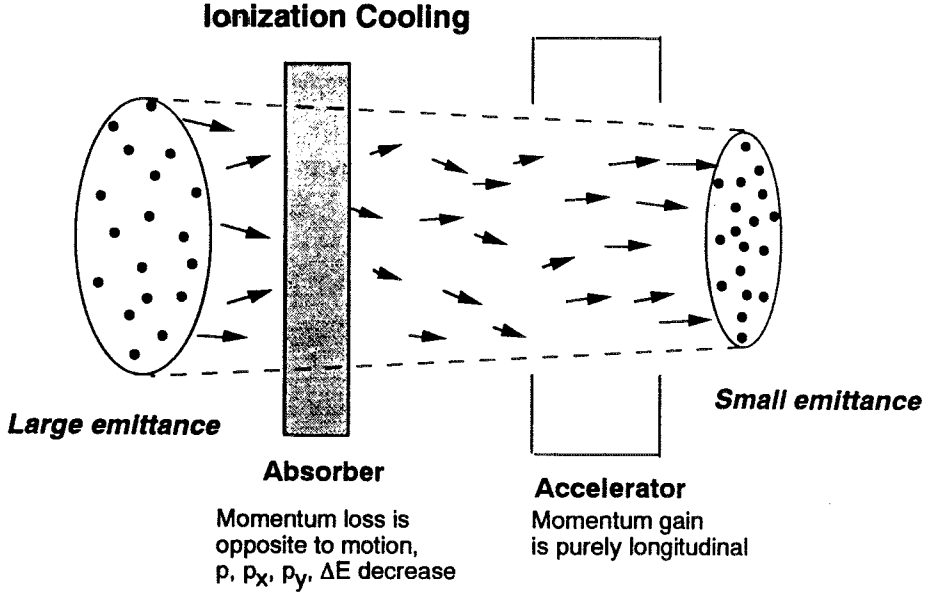

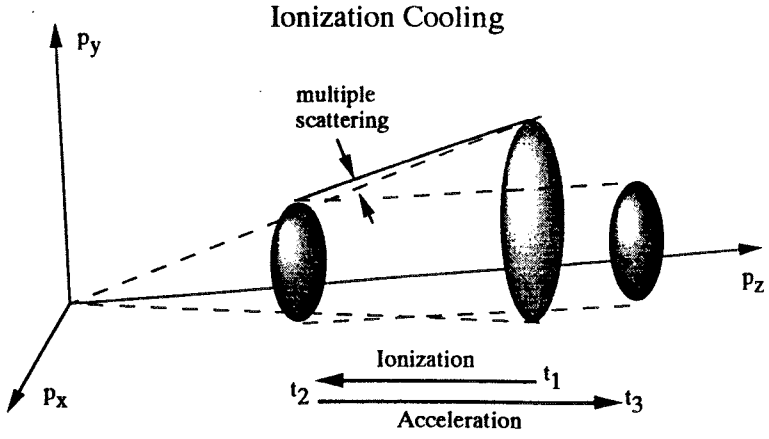

Beam Cooling Equations

Transverse emittance cooling:

$$\frac{d\varepsilon_N}{ds} = -\frac{1}{\beta^2 E}\frac{dE}{ds}\varepsilon_N + \frac{\beta_\perp E_s^2}{2\beta^3 m_\mu c^2 L_R E}$$

Energy cooling:

$$\frac{d\sigma_E^2}{ds} = -2\frac{\partial \frac{dE}{ds}}{\partial E}\sigma_E^2 + 4\pi\left(r_e m_e c^2\right)^2 n_e \gamma^2\left(1-\frac{\beta^2}{2}\right)$$

From transverse cooling:

want $\beta_\perp$ small at absorber (1m → 1cm)
⇒ strong-focusing;
want L_R large in absorber ⇒ low-Z (Be or Li)

From longitudinal cooling:

for $\partial(dE_\mu/ds)/\partial E > \sim 0$ ⇒ $E_\mu > \sim 0.2$ GeV
⇒ (dispersion + wedge absorbers)

since $(\Delta E_\mu)^2 \propto \gamma^2$ and $E_{cool} \propto \gamma$ ⇒ **E_μ minimal**

Transverse-longitudinal emittance exchange

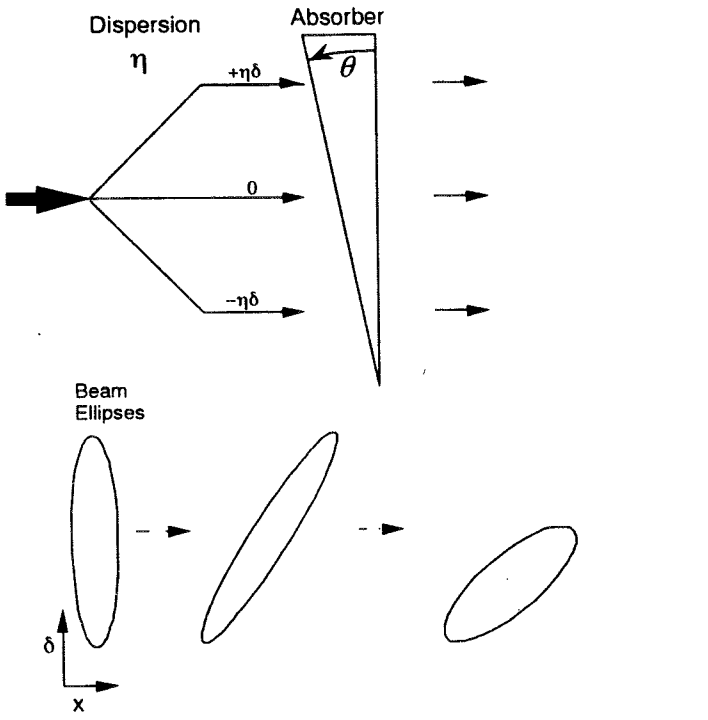

Dispersion:

$$x \rightarrow x + \eta\delta$$

$$\delta \rightarrow \delta - \frac{\frac{dE}{ds}\tan\theta}{E}x = \delta - \delta' x$$

(η, δ are in δE/E units)

Beam Cooling Scenario for feasibility study

I-Initial Cooling section

-reduce $\delta p/p$ to < 5%
-reduce bunch length to <~10cm
-Keep transverse emittance < 0.01 m-rad

II-Intermediate cooling regime

- reduce bunch lengths to ~cm scale
- reduce transverse emittances to < 0.0008

III-Final Cooling Region

-minimize transverse emittance (to ε_N< 0.0001 m-rad)
-keep bunch length, $\delta p/p$ moderately small

Cooling Methods

I-Initial Cooling section

- wedges within capture/decay solenoid
- thick Be absorbers with solenoid transports
- wedges with rf buncher for bunch compression
- Ring cooler

II-Intermediate cooling regime

- SOSO/FOFO cooling modules
- Ring cooler
- wedges within solenoid transports, rf bunching

III-Final Cooling Region

-Li lens → low energy Li lens / reverse wedge for minimal cooling

Ring Cooler - V. Balbekov

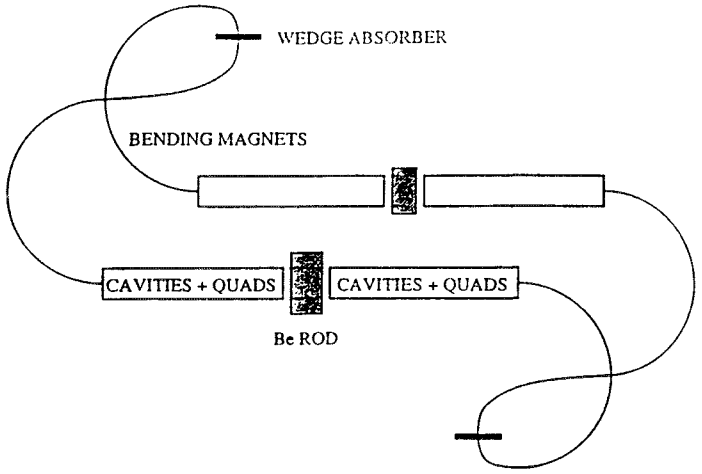

Figure 3: Schematic of ring cooler

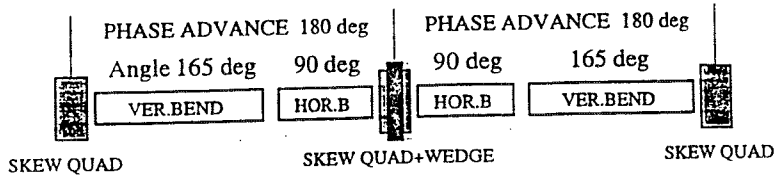

Figure 4: Bending section of the cooler

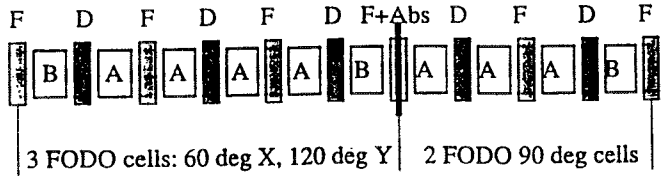

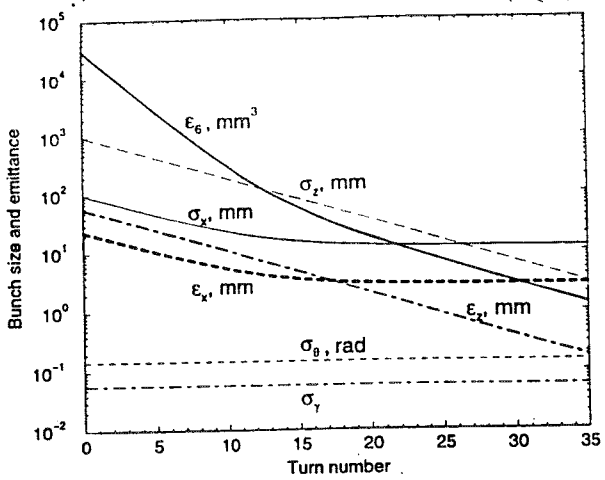

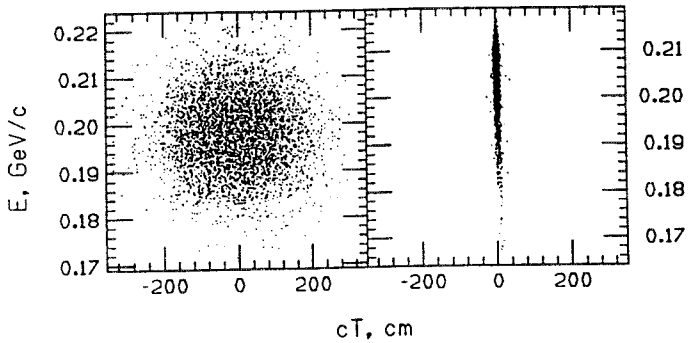

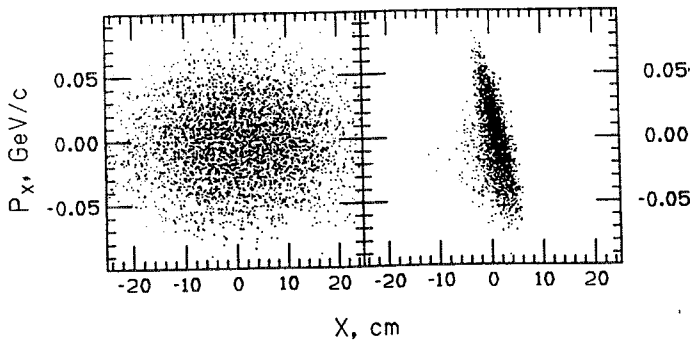

Final Cooling Section (possible parameters):

B'(T/cm)	R(cm)	L (m)	P_{beam} (MeV/c)	ε_t cooling (cm)	I(MA)
10	1	1.2	280→150	0.070→0.046	0.5
20	0.6	1.2	280→150	0.046→0.031	0.36
20	0.6	1.2	280→150	0.031→0.022	0.36
40	0.4	1.2	280→150	0.022→0.016	0.32
40	0.4	1.2	240→70	0.016→0.009	0.32

These parameters would avoid very high gradient, small aperture Li lens; gradients are actually less than previously achieved in solid Li lens (15 cm long)

total reacceleration rf required is ~650MV

Higher gradient would still be desired (80→160→ ?? T/m)

Last step would require rf debunching to reduce δp, in order to avoid beam loss as momentum becomes small.

If no wedges, longitudinal emittance will dilute by at least ~2×

Li lens R&D

Because focussing and absorber are the same device, and very strong focussing is possible; Li lens is ideal cooling material

High rep. Rate (15 Hz) + high field of cooling ⇒ Liquid lens

Fermilab Li lens R&D Plan

- Develop with BINP (Silvestrov et al.) a 15 cm long, 10 T/cm liquid Li lens for p-bar production

- Design a 10 T/cm 1 m long Li lens for ionization cooling.

Design of 40T/m Li lens should also be initiated.
(Design is substantially B,r dependent)

Proceed to construction on cooling Li lens(es)

Insert in cooling experiment

High lens power (~0.5 MW/m scale)
(final cooling section would need ~5m)
⇒ New power supply/pulser design
(shorter pulses, high power, 15Hz)
High pressure pump for Li

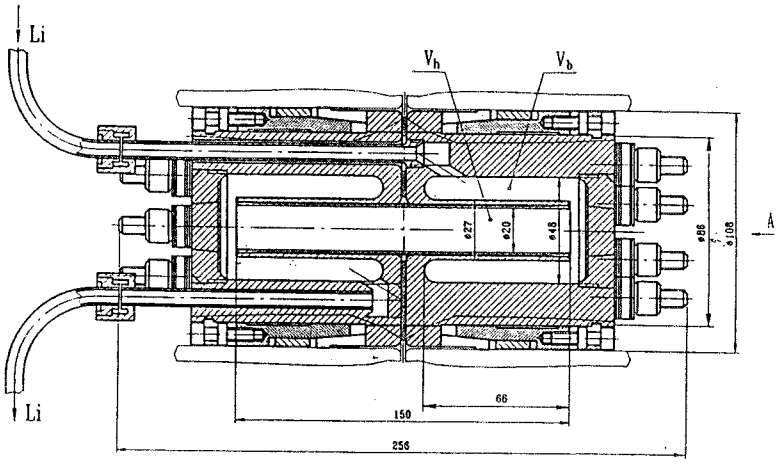

Fig.7 Lens with big buffer volume: V_h =50 cm^3, V_b =166 cm^3.

LITHIUM CURRENT CARRYING COOLING ROD

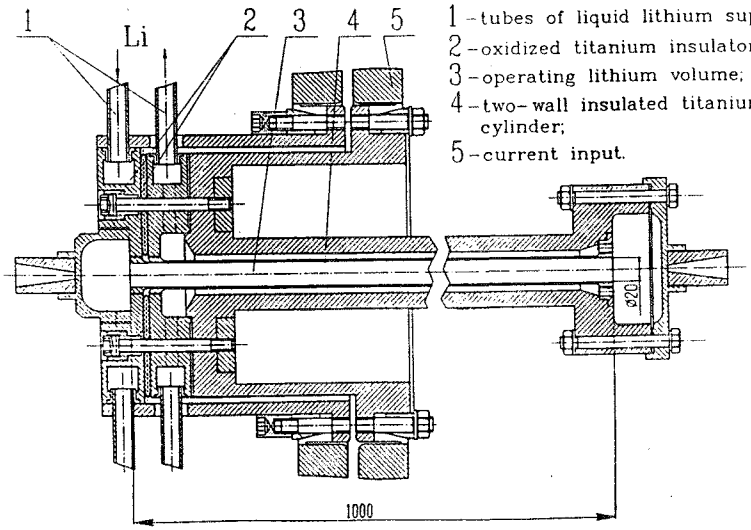

Simucool beam-cooling simulations

References:

A. Van Ginnekin, NIM A 362, 213 (1995)
A. Van Ginnekin and D. Neuffer, NIM A ?, ? (1997/8)
A. Van Ginnekin and D. Neuffer, PAC97 proceedings (1997)

Features:

Accurate representation of beam-material interactions:

Ionization loss - μ-e (w/ fluctuations, Bhabha J=1/2 scattering, restriction threshold)

Coulomb scattering- μ-A (multiple scattering, large angles, Incoherent)

High-energy processes (bremstrahlung, pair production, deep inelastic)

Can include beam transport, including transport with magnetic fields

Does not (yet) include rf-cavities, realistic acceleration model

Not developed for multi-user code extensions

SIMUCOOL Beam Cooling simulation studies

A - single steps from complete scenarios

1 - Absorber at low-β^* focus (FOFO or FDFD focus)
large ε, small ε cases, E-dependence, Be, Li, LiH, H absorbers

2 - Absorber in Be (or Li) lens

3 - Absorber within solenoid
difficulties with toroidal motion

4 - Wedge absorbers
- ΔE - x exchange (reduce ΔE, increase ε_N)

5 - End-point cooling ($E \rightarrow 20$ MeV/c)
$\varepsilon_N \rightarrow 5\times10^{-5}$ m-rad; ε_L increases
- anti-wedges at low energy, low-E beam in Li lens

B - Multistep cooling simulations

1. FOFO lattice

2. Multistep Be and Li Lens - cools ε_T from 0.01 to 0.000086 m-R

3. Ring Cooler - 10—30 turn; cools by 100—10000 ×

Wedge Cooling (δp-ε_t exchange):

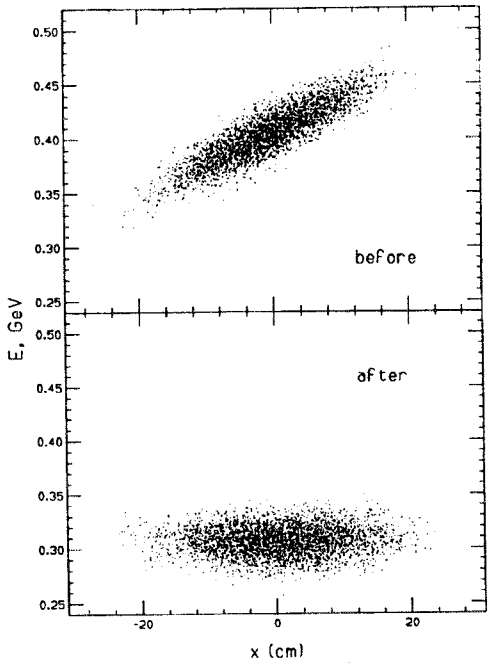

Simulation conditions (wedge only):

$\overline{P}$ = 391 → 340 MeV/c; η = 1m → ~ 0
δP = 28.6 → 13.9 MeV/c
ε_x = 1.5→2.76 cm-rad, ε_y 1.5→1.34 cm-rad
$\varepsilon_{6\text{-}D}$ = × 0.78

Multiple Lens-absorber simulations show cooling by large factors:

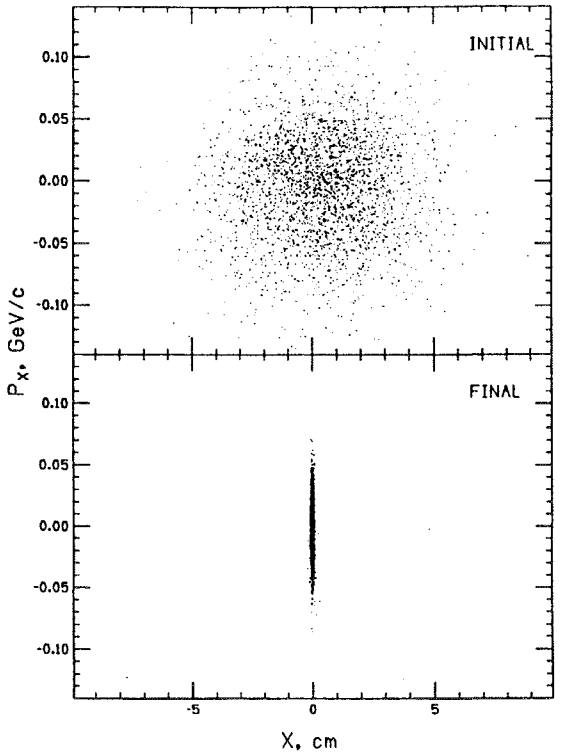

$\varepsilon_{t,N}$ cools from 0.01 to 0.00009 m; little beam loss, limited ε_L growth

Li lens R&D

Because focussing and absorber are the same device, and very strong focussing is possible; Li lens is ideal cooling material

High rep. Rate (15 Hz) + high field of cooling ⇒ Liquid lens

Fermilab Li lens R&D Plan

- Develop with BINP (Silvestrov et al.) a 15 cm long, 10 T/cm liquid Li lens for p-bar production

- Design a 10 T/cm 1 m long Li lens for ionization cooling.
Design of 40T/m Li lens should also be initiated.
(Design is substantially B,r dependent)

Proceed to construction on cooling Li lens(es)

Insert in cooling experiment

Liquid Li lens design challenges

High lens power (~0.5 MW/m scale)
(final cooling section would need ~5m)
⇒ New power supply/pulser design
(shorter pulses, high power, 15Hz)
High pressure pump for Li

Recent Beam Transport studies (W. Wan)

Design of transport for multiple Li lens
Focus to small β^* for cooling
Tapered entrance/exit to lens possible ...
Solenoid based solution

Transport for wedges
Solenoids, n= ½ dipoles, phase-space rotation solenoids
x- and y- wedges, but motion is planar

Cooling Simulation Studies

P. LeBrun

Systematic development of simulation and optimization tools
for cooling scenario development
and to support cooling experiment

Ideal cooling simulation:

- includes all energy-loss physics (nongaussian tails, etc.)
- includes all beam optics (nonlinear fields, coupling, rf acceleration)
- includes space charge & wakefields
- optimizes beam and elements for cooling scenarios

Inventory existing codes and capabilities

GEANT, ICOOL, SIMUCOOL, PARMULA. ...

Set up code repository for multi-person use and development- GEANT, ICOOL

Update codes to improve functionality

Geant - update double-precision, improve energy-loss model
ICOOL(R. Fernow)
SIMUCOOL - add long solenoids, rf model

Cooling Experiment Proposal – S. Geer

Dear Kirk;

I had an opportunity to reflect a bit on the idea of the "RF wedge" and its role in cooling. Before I begin, have you read the recent manuscript by Dave Neuffer "Phase Space Exchange in Thick Wedge Absorbers fo Ionization Cooling"? I believe the development Dave follows is the key to a successful understanding of ionization cooling. I say this because we all, at an instinctive level, relate to cooling systems we know and love, whether it be radiation, stochastic, or electron cooling. In these systems, the orbit functions such as beta, alpha, dispersion, etc. are determined by periodicity conditions in a circular ring. Such is not the case in our present linear system. We can (and do) change the orbit functions with the energy loss foils, as Dave demonstrates. This misunderstanding has led some of us (including me) to an unnecessarily restrictive way of thinking about the problem.

I also want to point out that a deflecting mode cavity provides in its center exactly what you wanted by going off center through an accelerating cavity.

Now, as to the $100 misunderstanding. Since I don't know the details of the bet, I am led to wonder what Earnest was thinking of. Even in Ken Robinson's paper in 1957, Ken stated that the horizontal betatron oscillations in an AG electron synchrotron can be radiation cooled (slowly) by fully coupling them with the vertical oscillations, which then are cooled less slowly. A postdoc of mine, Craig Holt, showed in all generality in the early 80's that vertical motion can be cooled by cooling horizontal motion and coupling them. I believe (according to Valery Balbekov) that Kolomenky and Lebedev showed that horizontal and longitudinal oscillations could be radiation cooled together by coupling them with a --- guess what?— deflecting mode cavity operating at a synchrobetatron resonance! Others have reinvented this on occasion.

What the cavity (in a beam with a correlation between position and momentum i.e. dispersion) does is couple the modes together. What it does not do is "trade" or turn longitudinal phase space into transverse phase space (violating Courant's theorem given at the Hans Bethe 60th hoedown). In a cooling ring one can think of a coupled particle first with large betatron amplitude being damped, transfering into longitudinal oscillation, not being damped, back into (less) large betatron amplitude, being damped, back into a smaller longitudinal oscillation , etc. Both end up being damped. Note that depending on the phase difference between transverse and longitudinal oscillations, the longitudinal might either grow or diminish. You can think of this as an expression of Courant's theorem (and in a larger sense, the Poincare invariants) . In this case, it might be that larger coupling and therefore cooling is achievable than in the circular accelerator. The detailed mechanism in the absence of a synchrobetatron resonance needs to be described more carefully.

Notice that all is not rosy, however. The motion is not linear for large phase oscillations, and in fact for large phases, the momentum spread is increased, not reduced. This is a problem not shared by the wedge absorber, which reduces the momentum spread irrespective of the arrival time. Therefore one would expect to use the RF wedge only after sufficient longitudinal cooling that the bunches are narrow. Also, it is clear that a deflecting mode cavity is not easier or cheaper than an easily adjustable absorber. Some more study might clarify its role.

If you agree, I will say something about this at San Francisco.

Let me know what you think.

Fred

FRED MILL, FNAL

Dear Kirk McDonald,

I am finally taking a few moments to read the material you sent me on Monday. It deserves a careful answer, so please do not take this quick note as definitive or final. I would like to think about it a little more. However, let me begin by making a few quick observations:

(a) The "theorem" in Courant's paper is actually a formulation of the first Poincare invariant,

dq^dp = dQ^dP

for the linear case. However, Poincare's theorem on differential invariants is much more general; it does *NOT* assume a linear dynamic. This discouragingly suggests that the popular wisdom on the impossibility of trading transverse and longitudinal phase space may indeed be correct -- not because of Courant but because of Poincare. However, I'm still only 92% satisfied about this. (Something about dispersion bothers me at the moment. I'll try to formulate it more precisely and get back to you later.)

There is a (false) story about the Wright brothers. The experts of their time were ridiculing them for believing that heavier than air flight was possible. Some were in attendance at Kitty Hawk. After the flight had ended, they approached the brothers, and one said, "Oh, well ... if you're going to do *that* ... ."

Incidentally, the final paragraphs in Courant's paper -- about extraction not violating this theorem because it is a nonlinear process -- are qualitative and seem a little shaky to me. The phase space under consideration seems to change in the middle of the argument. (I have to make this more firm before calling it an "objection.")

(b) Regarding the example that you sent, what you intend is a mapping of phase space coordinates before entering the capacitor onto coordinates after leaving the capacitor -- like <f|S|i> in QM. However, the third equation, z' = z, does not belong to this map. The z-coordinates are fixed by the positions of the "before" and "after" planes. (I probably could explain this better at a blackboard. It is hard to wave one's arms effectively while typing on a keyboard.) What you really want instead is

-E' = -E - V
t' = F(x, y, t; p_x, p_y, -E)

where I am formally emphasizing that -E, rather than E or p_z, is the coordinate conjugate to t. (See Eq. 3.45 on p. 130 of "Intermediate Dynamics ...".) Here, t and t' refer to the time at which the particle passes through the "in-plane" and "out-plane" respectively. In the limit of an infinitely thin capacitor, t' = t. Of course, dE'/dE = 1. (The symplecticity of the RF map is worked out in pp.53-56; see also pp.159-163.)

If, instead, you take your map to be a "time-advance map" over a time-interval delta-t, then you still should not write z' = z or E' = E + V. These indicate to me that it is the Poincare map, not the time-advance map, that you are writing.

(c) On the definition of "linear": let z = (x, y, z, ...) be a set of coordinates. A map z_final = F(z_initial) is "linear" when F(c*z) = c*F(z) for any number c. Constant acceleration is the simplest example of a nonlinear dynamical system. (S.Ulam said once that the term "nonlinear dynamics" is about as meaningful as "non-elephant zoology." At least, I think it was Ulam who said that. Put crudely -- and almost, but not quite, correctly -- nonlinear dynamics means everything except the harmonic oscillator.)

This does not completely answer your question. I'll try to think a little more about it if I can, and I'll study your Web page also.

Incidentally, thank you for reading my book. I'd appreciate learning of errors that you find.

Regards,
Leo Michelotti

Three Bypasses of ~~Data Flow Bottle Neck~~

Bottle Neck of Data Flow in Neutrino-Higgs Factory and Device R&D of QMC-QMD based on EEEE Laws for PPPP

Jing SHEN

Institute of High Energy Physics, Chinese Academy of Sciences
P.O.Box 918(6), Beijing 100039, P.R.C.

Dec. 4, 1997

* **QMC-QMD** Quantum Muon Colliders-Quantum Muon Detectors
* **EEEE** Electric Electronics Engineering and Economy
* **PPPP** Progress of Particle Physics Projects

* **Quantum Dirac waveguide**:
  Cooling spectrum, Beta waveband shifter, Steering and undulating radiations.
* **Quantum doped fiber amplifier**:
  Cherenkov/scintillation imaging calorimeter, 1 pixel/1 fiber non-PMT readout.
* **Parallelism readout electronics & photonics**:
  Small granule-large array, new topology of MLPS for imaging, crossing links.
* **Electronic collimator, detector sharing collider's extra-duty of background**:
  Inverse PET triggering, and active devices instead of tungsten nose.

* AGS-SLA leap opened SM, but **lag behind Livingston law at Higgs of SM-SUSY**
* Bit rate growth of FEE-DAQ **lags behind imaging pixels growth of event/bkgrd**
* **Moore law & beyond**, Nucl. disarmament are making these **two lags leap back.**

1 Problems of realistic and advancing lepton colliders

1.1 Muon colliders

1.1.1 "Unforeseen losses during the 25 stages of cooling"
1.1.2 "The excessive detector background from beam halo" **---95MuMu Symp.**
1.1.3 "They don't live any long", "since the ideas are all new,they might not work"
1.1.4 "Very thick beampipe", "and detectors would lose 20° cone" **---96 HEP Conf.**
1.1.5 "With machines of 4 TeV or more, the intensity of neutrino from muon decay becomes a radiation hazard". **---97 PAC Conf.**

1.2 Linear colliders

1.2.1 Richter's Europe map effect and SLC **---86 LINAC Conf. and 97 PAC Conf.**
"Represent the realistic way forward and a major theme of 97 PAC"
1.2.2 R&D of JLC(S), JLC(C), JLC(X), NLC, TESLA, CLIC, VEPP are fruitful.
1.2.3 However, FLCs have still lagged behind Livingston line, but LHC leaps back.

1.3 Challanges and cooperation

1.3.1 Laser accelerator have made considerable progress.

2 Why consider Quantum?

2.1 If ionization cooling can not reach the expectant emittance at all

2.1.1 then one has to decrease the beta instead to reach the luminosity

$$L=\frac{N^+N^-f}{4\pi\sigma_x\sigma_y}=\frac{N^+N^-f}{4\pi\varepsilon_N\beta^*}\beta\gamma\approx\frac{N^+N^-f}{4\pi\varepsilon_N\beta^*}\gamma$$

2.1.2 **Cline-Bogacz Micro-beta** make luminosity increase more than beam loss

$$\beta^*\equiv\sqrt{\frac{E_\mu}{\phi}}=4\ \text{microm},\quad \phi_{Si}=6\times10^{12}\ \text{GeV/m}^2\ \text{(for Si)},\quad E_\mu=100\ \text{GeV},$$

2.1.3 Furthermore, according to **Palmer-Sessler-Skrinsky-Tollestrup et al.**

$$\frac{d\varepsilon_n}{ds}=-\frac{dE_\mu}{ds}\frac{\varepsilon_n}{E_\mu}+\frac{\beta_\perp(0.014)^2}{2E_\mu m_\mu L_R},\quad \frac{1}{L_R}=4\alpha r_e^2\frac{N_A}{A}\left\{Z^2\left[L_{rad}-f(Z)+ZL'_{rad}\right]\right\}$$

$$\frac{d(\Delta E)^2}{ds}=2\frac{d\left(\frac{dE_\mu}{ds}\right)}{dE_\mu}\left\langle(\Delta E_\mu)^2\right\rangle+\left[\frac{d\left(\Delta E_\mu\right)^2_{strag}}{ds}\right],\ [\ ]=4\pi\left(r_e m_e c^2\right)^2 N_0\frac{Z}{A}\rho\gamma^2\left(1-\frac{\beta^2}{2}\right)$$

2.1.4 Different quantum effects between

$$\frac{dE_\mu}{ds}\ \text{and}\ \frac{d\left(\frac{dE_\mu}{ds}\right)}{dE_\mu},\quad \frac{\beta_\perp}{L_R}\ \text{and}\ \frac{d\left(\Delta E_\mu\right)^2_{straggling}}{ds}$$

2.2 If the backgrounds in detector couldn't be shielded by nose perfectly

2.2.1 Then one has to tolerate the backgrounds in the detector
2.2.2 It must increase the resolutions and create the new idea of read out events
2.2.3 Parallelism, terabit/s data flow, quantum devices

2.3 Bit-rate growth of readout is lagging behind pixel rising of HEP imaging

2.3.1 AGS-SLA matching leapt ahead Livingston line in 1963-1967 opened SM
2.3.2 SSC-FLCs are lagging behind Livingston line in 1993-1997
2.3.3 Bit rate growth in FEE & DAQ are lagging behind the jet event imaging,
~ Track number growth law in imaging
~ Multiplicity
$\langle n\rangle=A+B\ln s=C+Dt,\ \because s=E^2=L\times10^{2w}$
~ Charged multiplicity
$\sum\langle n\rangle=\sum n\sigma_n/\sum\sigma_n$
~ Track number growth rate
J/psi (1974), $D^0+\delta$(1984), Z^0 (1989), Higgs (2007), pp-SUSY(2010)
~ Track cluster of jet
~ Track number from Detector Background of muon decay
150 000 hits (863 cm^2 vertex, 400 μ^2 pixel) × 0.3% / Xing
15 000 hits (34m^2 tracker, 1 mm × cm) × 0.1% / Xing
2.3.4 The additional huge bit rate of background hits

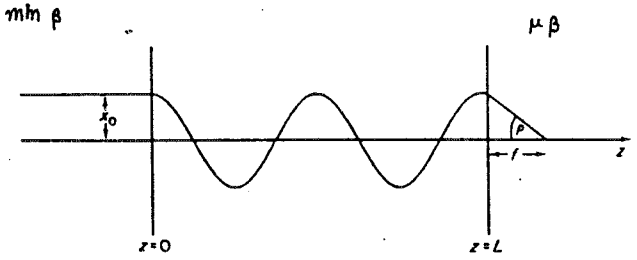

mm β → μ β by Bogacz-Cline potential of channeling

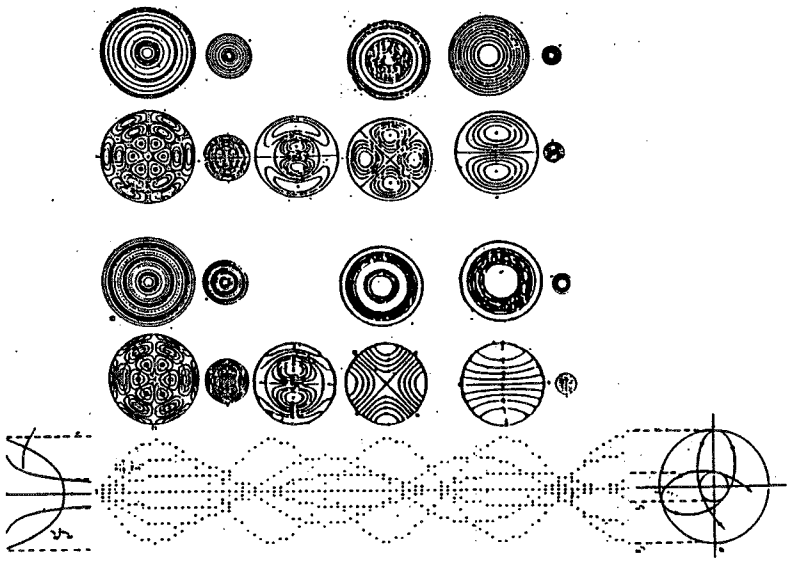

Mini-beta beam.

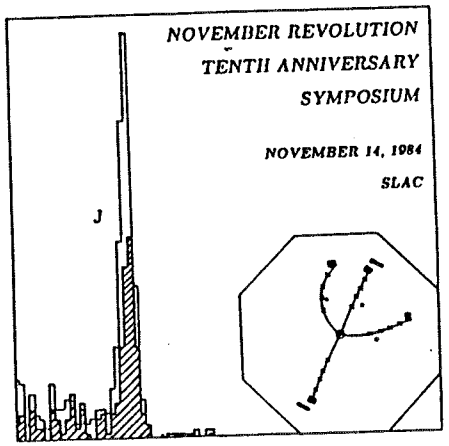

Double Arm Spectrometer
AGS BNL

Mark J
SPEAR SLAC

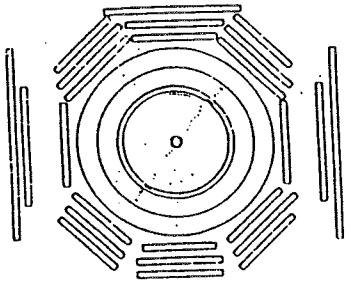

Large angular Bhabha event

BES
BEPC IHEP

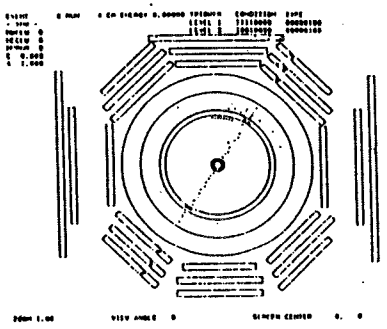

J/ψ → 2μ

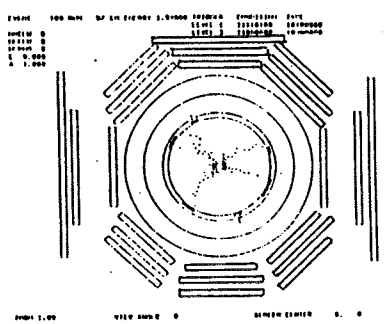

J/ψ → h's

BES BEPC IHEP 1990

11-88 6164A9 $H^0 \rightarrow Z^0 Z^0 \rightarrow e^+e^- \mu^+\mu^-$

SSC Central Design Group R. Donaldson Ed.

SSC-SR-1039 . Apr 1989

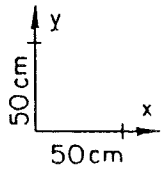

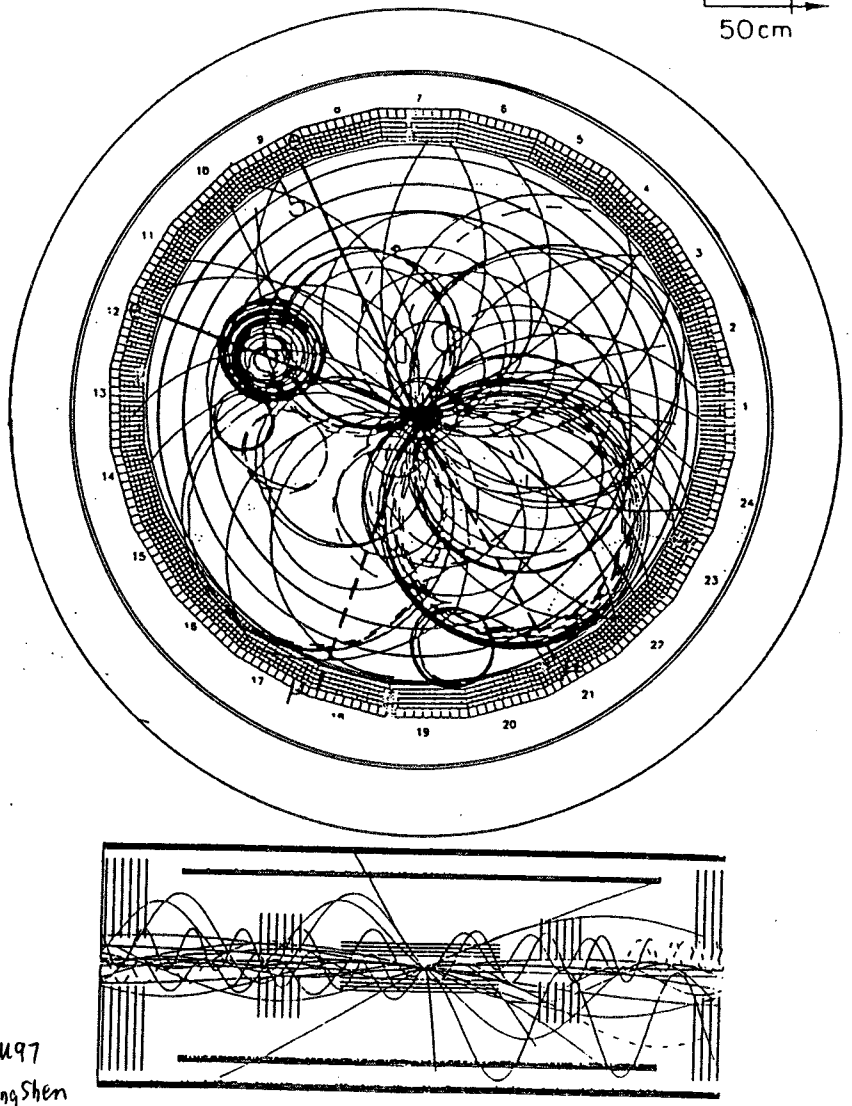

μμ97
JingShen

Fig. 2.1. Event in the CMS detector [1] This picture is based on simulations. The tracker is in the middle of the detector, where the intensity of the particles at energies

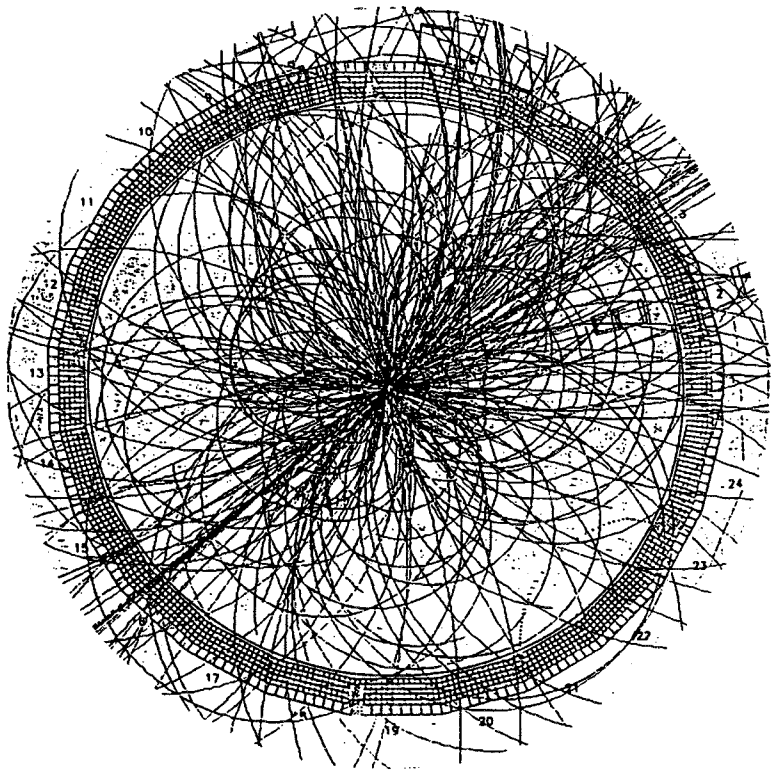

ICFA School of Instrumentation Trieste 1989.

3 What is Quantum Muon Collider?

3.1 Emittance of muon beam and cooling spectrum

3.1.1 Ultra-slow muon sources eV
3.1.2 Frictional cooling below 10 KeV
3.1.3 Cherenkov cooling about 100 MeV
3.1.4 Ionization cooling in 1-5 GeV
3.1.5 Radiation cooling above 4 TeV

3.2 Beta band shifter of guiding muon beam in IR

3.2.1 Bogacz-Cline strong focusing transfer line of crystal channeling
3.2.2 Quantum waveguides of Dirac field of Fermion-Nanom and Sub-nanom
3.2.3 Betatron trajectory of muon in quantum waveguide
3.2.4 Modes of muon betatron and the cutoff effect of beta-wave
3.2.5 Relativistic Lee-Yang angular distribution of polarized muon decay electrons

3.3 Background beam dynamics beyond dosimetry

3.3.1 Emittance and luminosity of muon decay electrons
3.3.2 Emittance and luminosity of muon decay neutrinos
3.3.3 Emittance and luminosity of muon decay electron radiations

3.4 Steering radiation of guiding backgrounds

3.4.1 Breamsstrahlung of muon decay electron
3.4.2 Synchrotron radiation of muon decay electron couldn't be steered
3.4.3 Channeling radiation of guiding muon decay electron could be steered
3.4.4 Bethe-Heitler muon pairs

3.5 Bunch Fields and background field of RF waveband

3.5.1 Real photon modes of bunches in beampipe
3.5.2 Virtual photon modes of bunches in beampipe
3.5.3 Coherent RF beamsstrahlung

3.6 The most of advantages

3.6.1 Higgs factory: Muon beams are 40 000 times stronger then electron's
3.6.2 Base: Existing and constructing proton machine
3.6.3 Compact and lower cost: Muon machines are the best
3.6.4 Quantum Collider: Muon's nuclear cross-sections are smaller then proton's
Muon's breamsstrahlungs are smaller then electron's
3.6.5 Quantum Detectors: Muon decay backgrounds expedite.

3.7 Muliti-factories

3.7.1 Muon factories with electron exposuring facility
3.7.2 Neutrino factories: eV, 100 MeV, 100 GeV, 4 TeV
3.7.3 Higgs factories

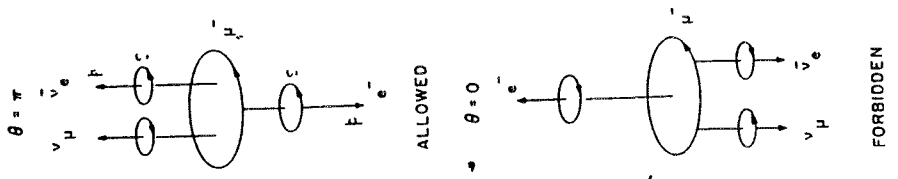

$d^2N_e = (1 \mp \cos\theta)\, dx\, d\cos\theta$, $x \equiv 2$ momentum of e / m_μ

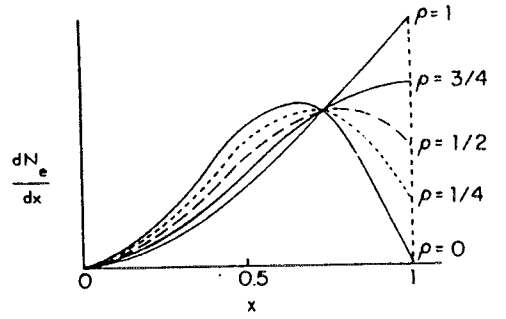

Spectrum (21.9) for different ρ values.

$d^2N_e = x^2 [3 - 2x \pm (\cos\theta)(1 - 2x)]\, dx\, d\cos\theta$

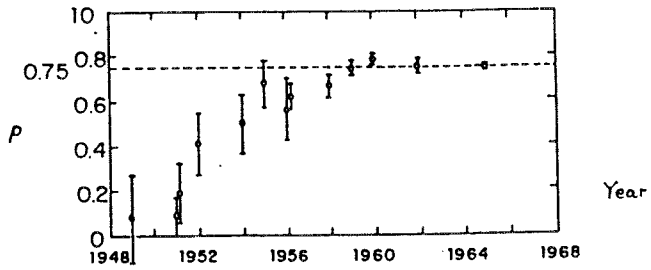

$$\frac{dN_e}{dx} = 6x^2 \left[\left(2 - \frac{4}{3}\rho\right) - \left(2 - \frac{16}{9}\rho\right) x \right]$$

Experimental determination of the Michel parameter ρ versus time.

Lee-Yang anguler distribution of decay electron-neutrino of polarized muon beam

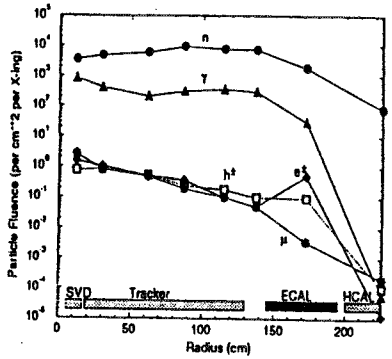

Figure 10. Particle flux radial distributions in a ±1.2 m detector region around the IP per 2 × 2 TeV $\mu^+\mu^-$ bunch crossing.

Table 3
Background fluxes (cm^{-2}) from the IP accumulated over 1 year (1) and *effective* (2) in central tracker, endcap calorimeter and forward muon spectrometer at different radii

Detector	r (cm)	LHC	NLC	$\mu^+\mu^-$
		(1)		
Tracker	30	2×10^{13}	10^{7}	6×10^{6}
ECAL	50	10^{14}	10^{8}	10^{8}
Forward	100	10^{11}	5×10^{3}	8×10^{3}
		(2)		
Tracker	30	0.6	0.01	2×10^{-4}
ECAL	50	0.9	0.8	2×10^{-2}

Table 4
Accumulated over 1 year and *effective* accelerator related fluxes (cm^{-2}) in detector components at r = 50 cm, with all the protective measures on

	LHC	NLC-1000	$\mu^+\mu^-$
Integrated	10^{8}	1.6×10^{6}	4×10^{14}
Effective	3×10^{-6}	10^{-3}	20

Table 2
Mean energies of particles in inner tracker for 2 TeV muon decays in the interaction region.

Particle	γ	$e^{\pm}$	μ	$h^{\pm}$	n
⟨E⟩, MeV	2.5	80	3630	249	0.2

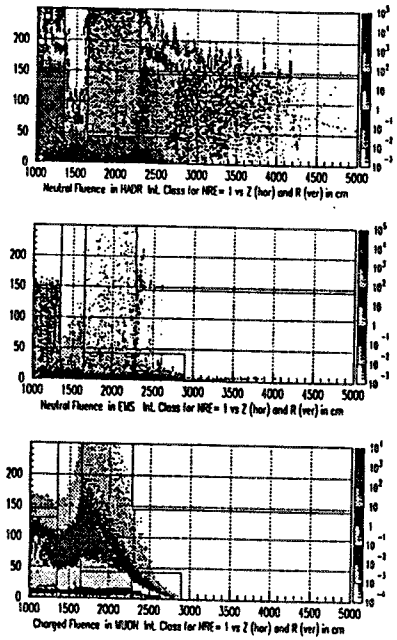

Figure 11. Particle fluxes in the vicinity (2.5 m in radius and 50 m long) of 2 × 2 TeV $\mu^+\mu^-$ IP (at z=10 m in the plots). The units are $10^n cm^{-2}$ per bunch crossing, where the shade indicates the power n. From top to bottom: n, γ and μ.

Detector	vertex	tracker
Radius	5 cm	1 m
Number of photons	50 10^6	15 10^6
Number of hits	150,000	15,000
Detector Area	863 cm^2	34 m^2
Pixel size	20 x 20 μm	1 mm x 1 cm
Sensitivity	0.3 %	0.1 %
Occupancy	.07 %	0.4 %

Table 8
Detector Backgrounds from μ decay/xing (Palmer et al)

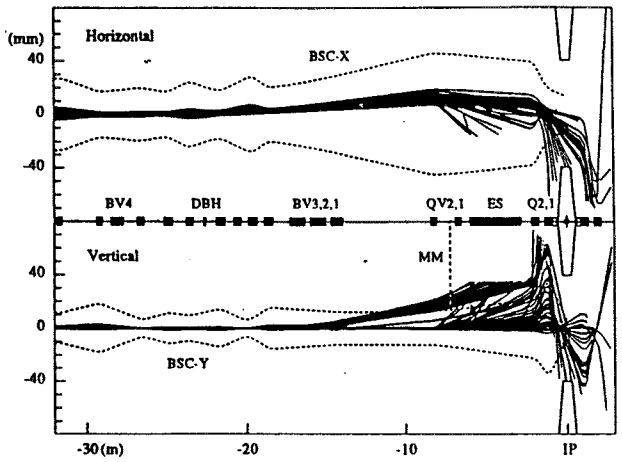

Typical trajectories for bremsstrahlung particles which hit the vacuum chamber wall in the IR. Also shown is the position to place a movable mask (MM).

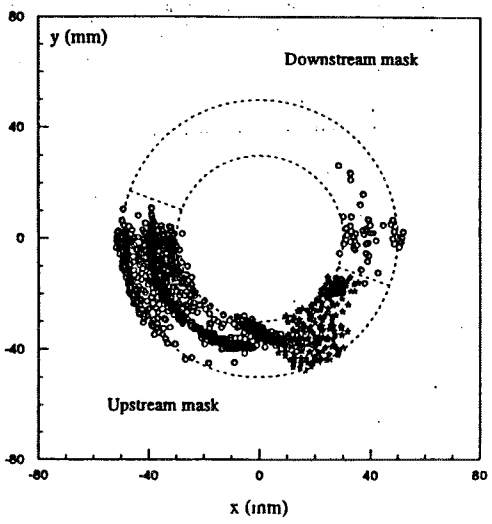

Spatial distribution for bremsstrahlung particles (circles) and photons (stars) when they hit the upstream mask and beam pipe. The half-circle shaped masks are shown with dash lines.

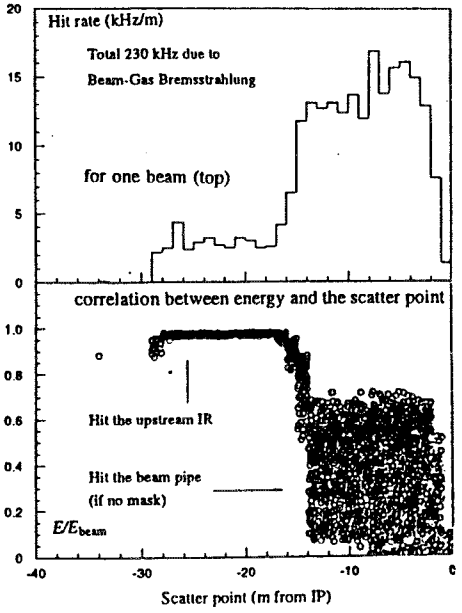

Hit rate as a function of the bremsstrahlung point

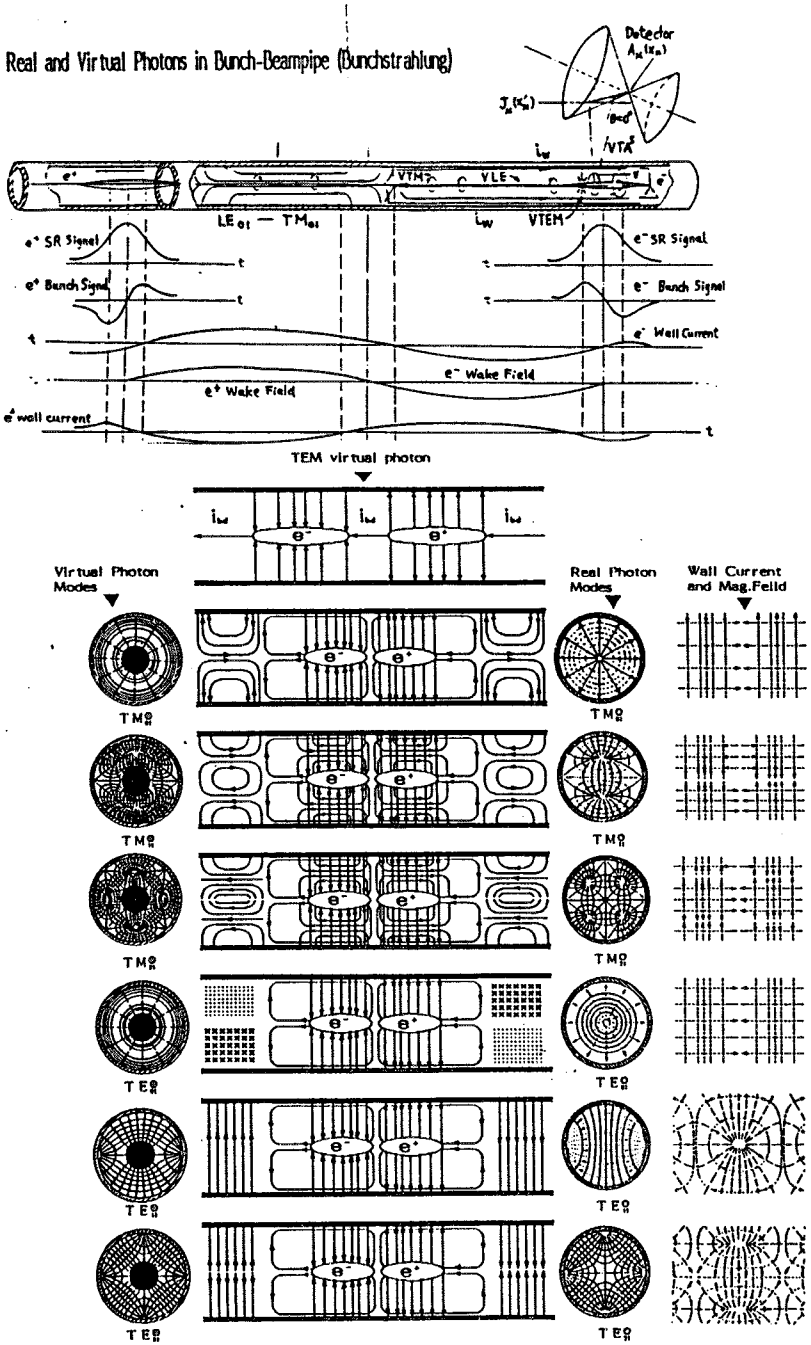

4 What is quantum detector? Could it shares muon collider's heavy duty?

4.1 New materials, new effects, radiation hardness

4.2 Terabit/s microm waveguides
4.2.1 Multi-mode fibers for Cherenkov photons
4.2.2 Non-linear fibers for scintillating photons
4.2.3 Improve resolutions of timming, imaging, and calorimeter

4.3 Waveguide amplifier of terabit fibers
4.3.1 Doped fiber amplifier
4.3.2 Cherenkov fiber amplifier be timing, PID and calorimeter
4.3.3 Scintillating fiber amplifier be timing, PID and calorimeter
4.3.4 Nanom wave shifter

4.4 Quantum electronic-photonic devices
4.4.1 Super lattice devices
4.4.2 Nonom devices
4.4.3 Single photon devices
4.4.4 Single electron devices

4.5 New topology of circuits and system matching quantum devices
4.5.1 Back Propagating Neural Network
4.5.2 Boolean cubic connections
4.5.3 Crossing optic connections

4.6 What should be in detector heart?
4.6.1 20° shielding *Tungsten collimeter* in the heart of detector in IR of collider
4.6.2 looks like a great wall in Wall street
4.6.3 Is it possible an active bit rate devices instead?

4.7 Could be an electronic collimator in detector?
4.7.1 Could make the backgrounds become tolerable in detector?
4.7.2 Inverse PET triggering rejects backgrounds

4.8 Would be possible by a little story of BES-BEPC
4.8.1 BEPC's bunch length was correctly measured at first by TOF of BES person
4.8.2 By quantum effects

4.9 Event imaging under huge backgrounds
4.9.1 Back to bubble chambers
One can see events easily, but 300 000 pictures for discovering
4.9.2 A basic problem of triggering electronic detector
Parallelism data-out from detector but **Serialization** readout electronics

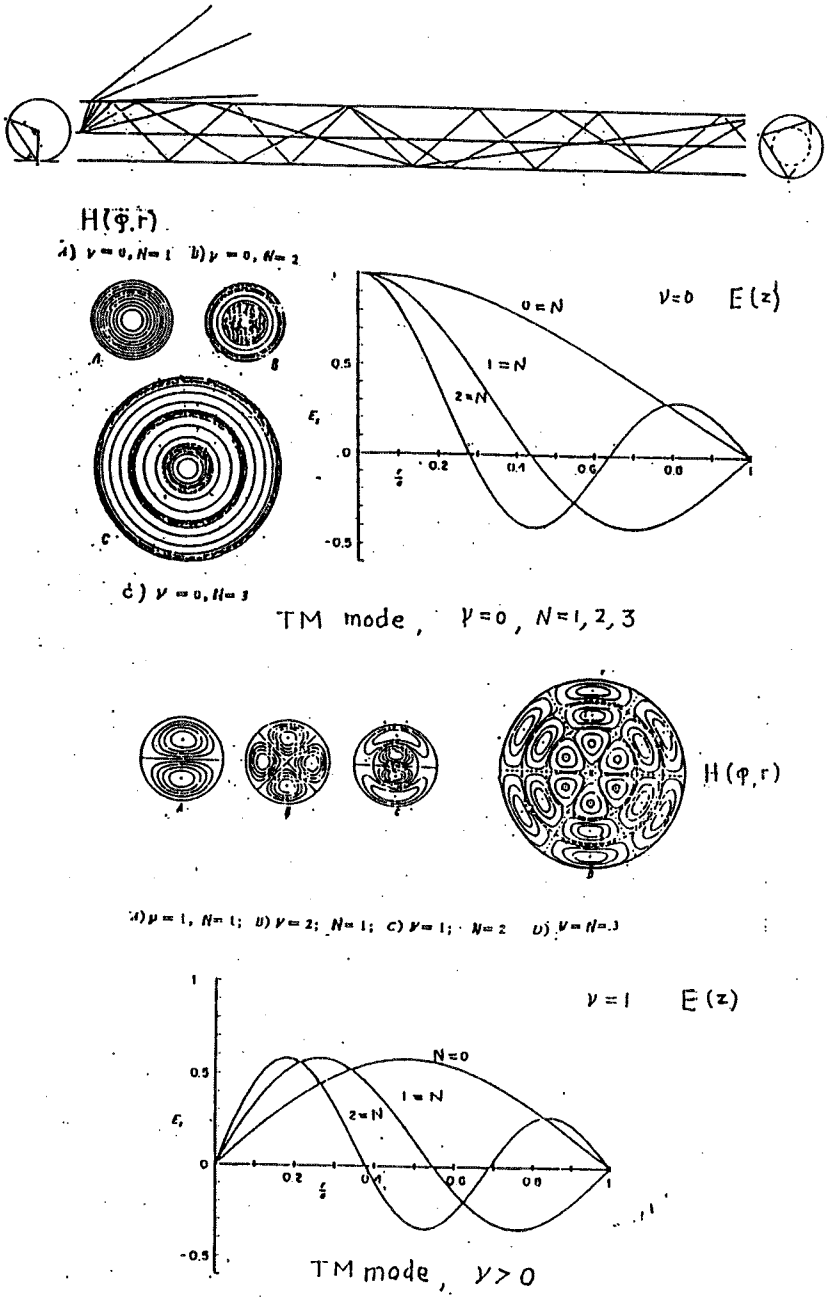

Fig.6.3 TE, TM mode guiding wave of circular polarizing scintillation

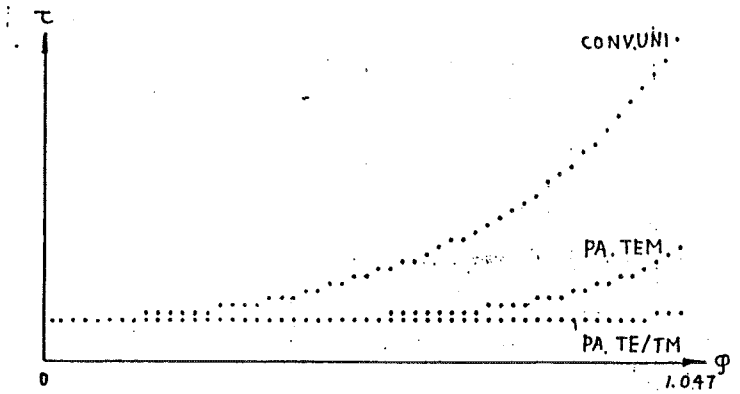

Fig.5.1 The transit time of scinti-photons in different types of scintillator as a function of ray angle ——— conventional mode of uniform types; TEM, TE or TM mode of parabolic profile slab clad.

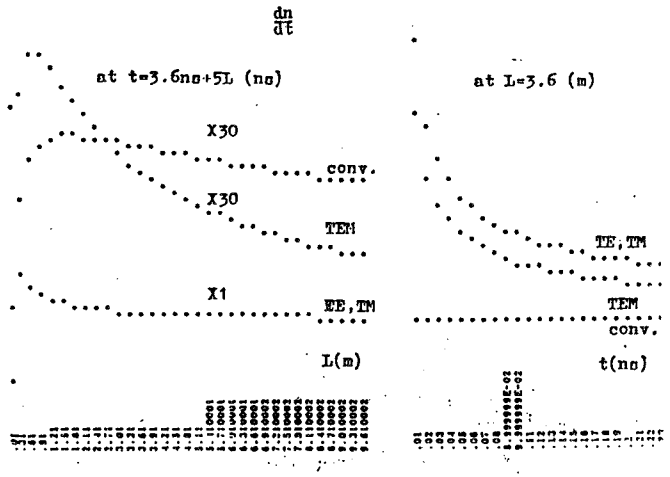

Fig.6.1 The Scinti-photon output rate in different types of scintillator as a function of scintillation position ——— conventional mode of uniform types; TEM, TE or TM mode of parabolic profile slab clad

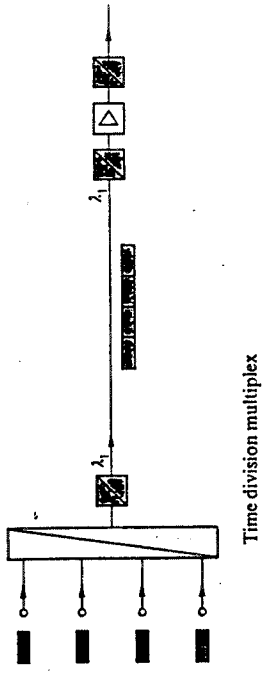

Time division multiplex

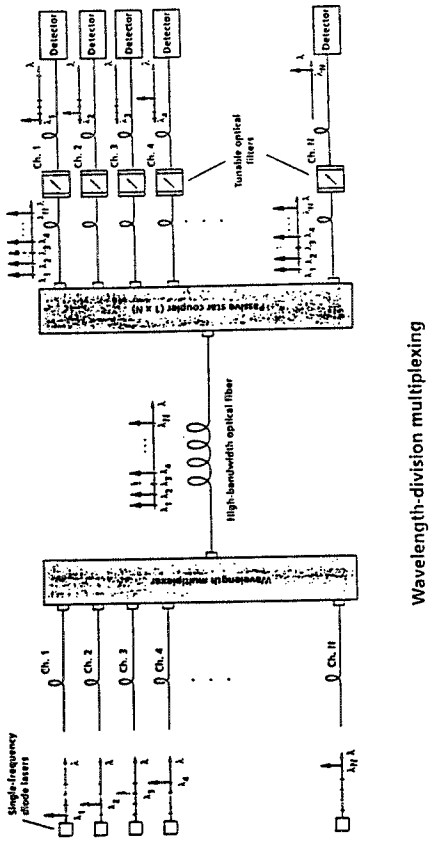

Wavelength-division multiplexing

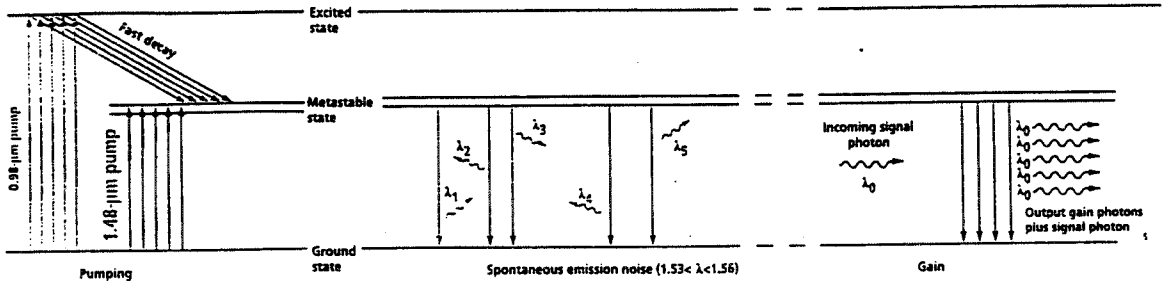

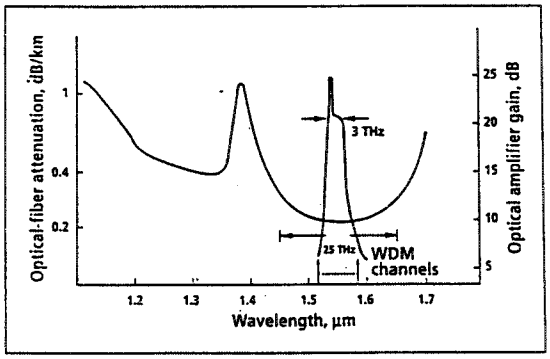

[3] Optical-fiber attenuation [black curve] varies with wavelength and is least at 1.55 μm. This region of the fiber's greatest transparency coincides with the wavelength region (1.53–1.56 μm) of the erbium-doped fiber amplifier's greatest gain [red curve]. The International Telecommunication Union has proposed a wavelength standard for wavelength-division–multiplexed (WDM) systems; WDM wavelengths would be referenced to 1552.5 nm (193:1 THz) with channels [vertical arrows] every 100 GHz—about 0.8 nm apart.

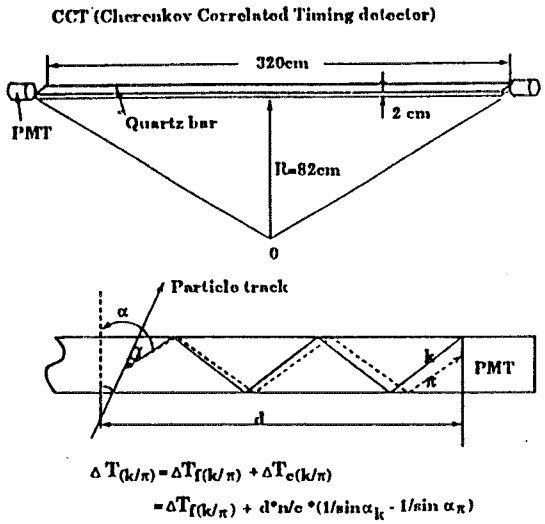

The schematic view of CCT formation and the principle of CCT.

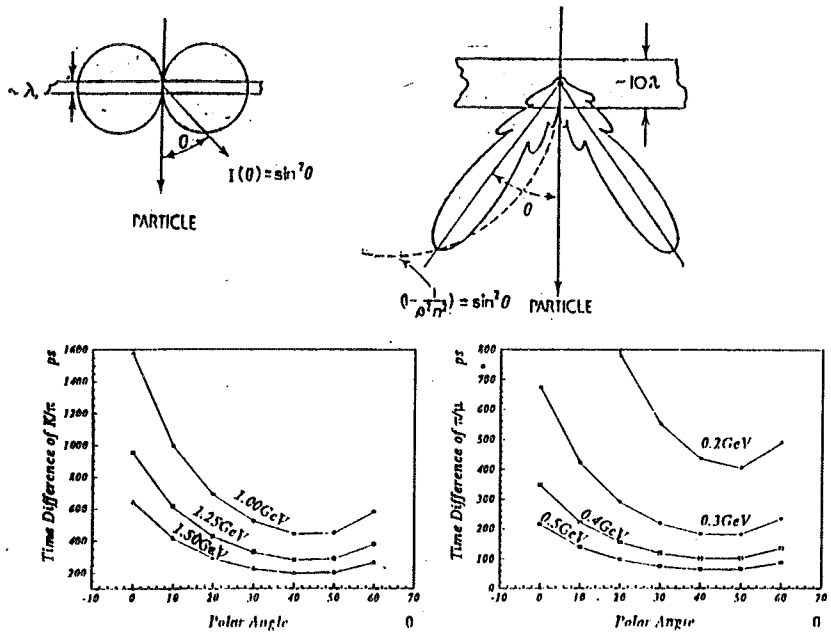

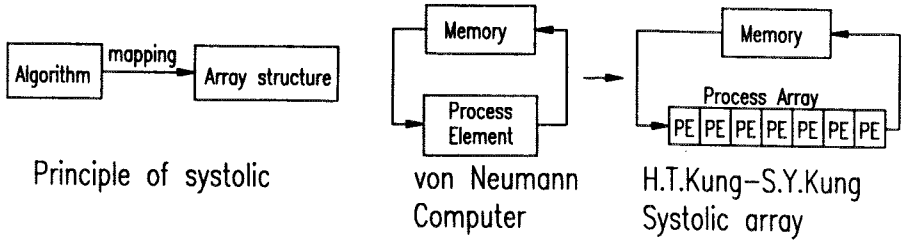

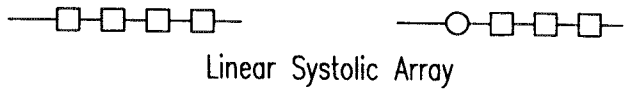

Linear Systolic Array

Degenerate 2D Systolic Array

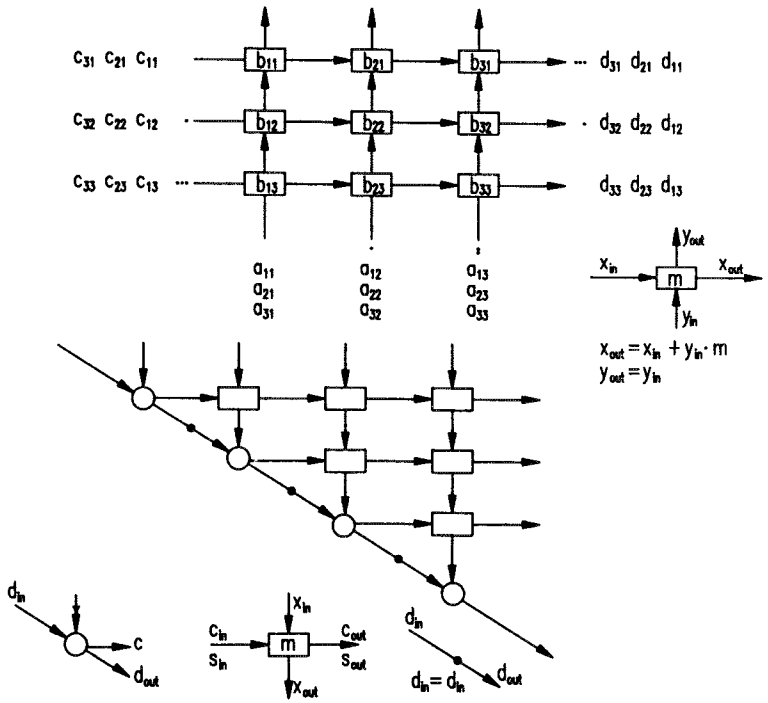

Matrix mutiply and othogonal disintegrate systolic array

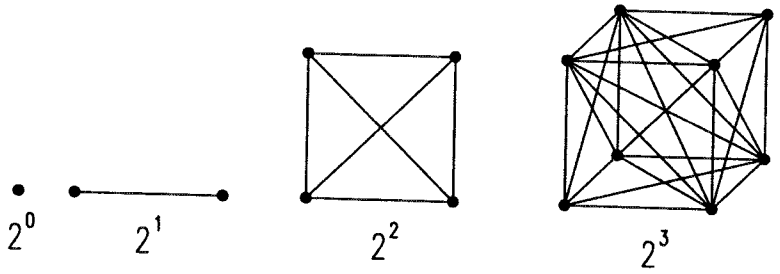

n=17, Nodes=131,072

Connections=2^n X(2^n−1)/2

=8,589,869,056

Non−xing topology of direct connection

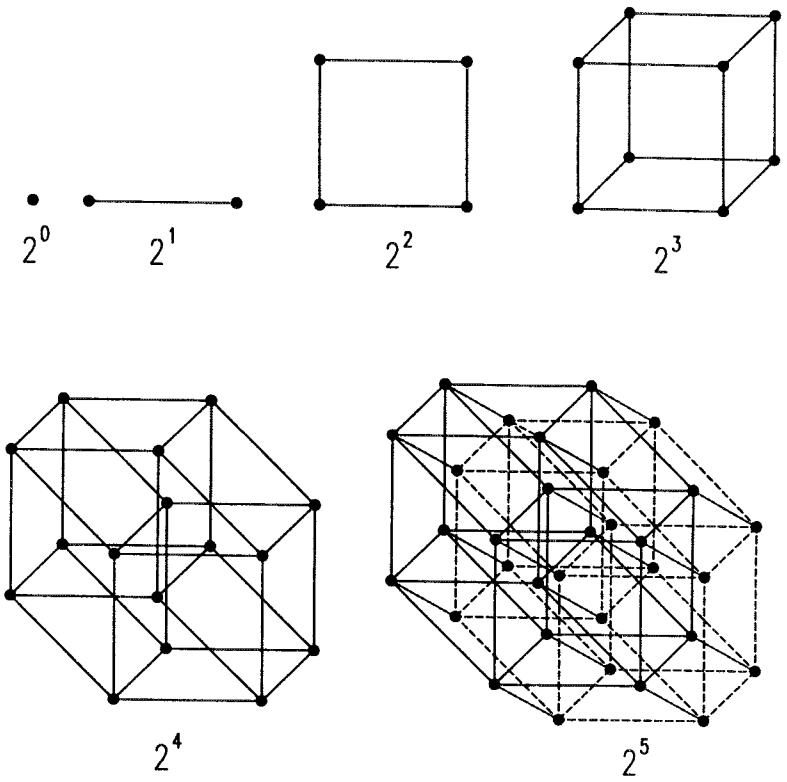

n=17, Nodes=131,072

Connections=n X2^{n-1}

=1,114,112

Non−xing topology of Boolean cubic connection

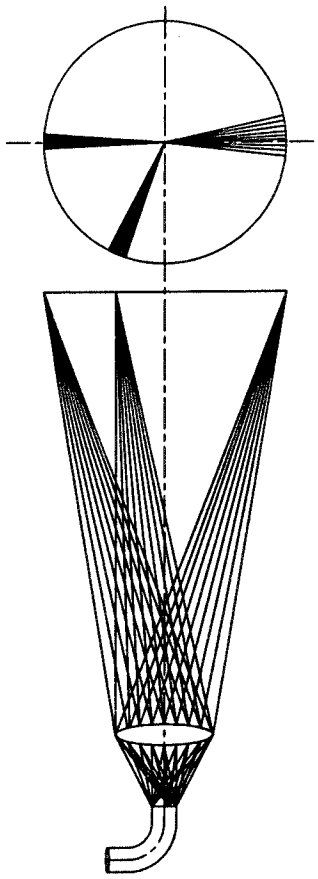

Xing topology of non-crosstalk optic link

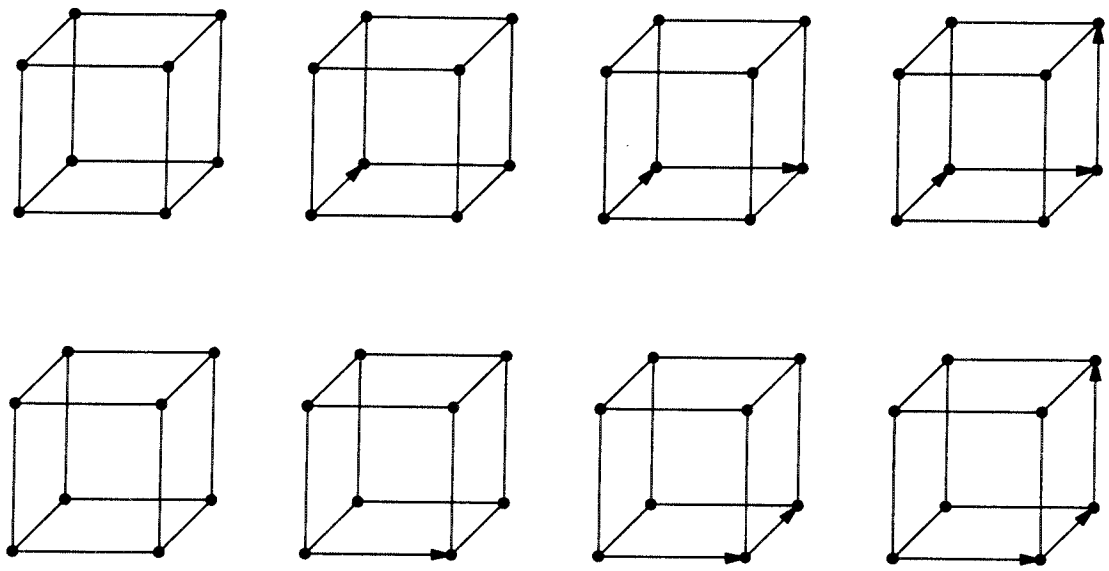

3 steps of communication in 3 dimension Boolean cubic

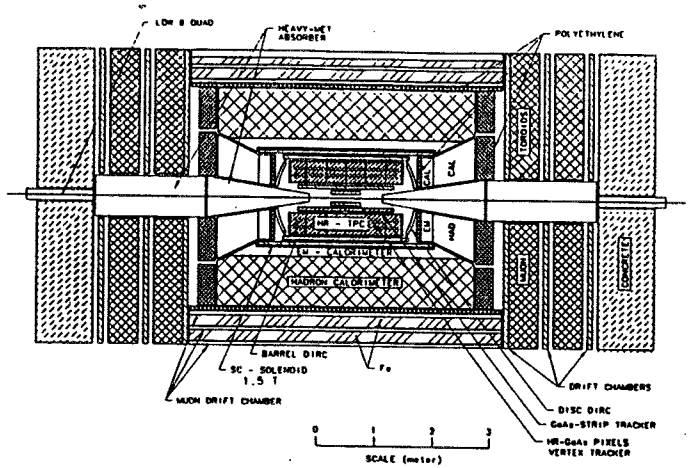

Figure 1. Proposed $\mu\mu$ detector, a modified version of the CDF.

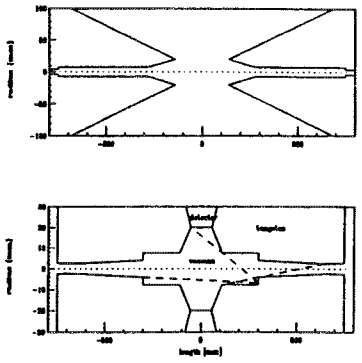

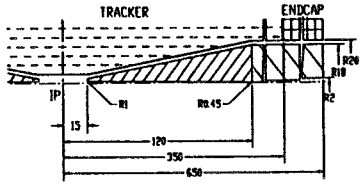

Figure 7. Collimating tungsten nose and copper collimator at a muon collider IP. Dimensions are in centimeters.

Figure 22. Schematic of the detector nose.

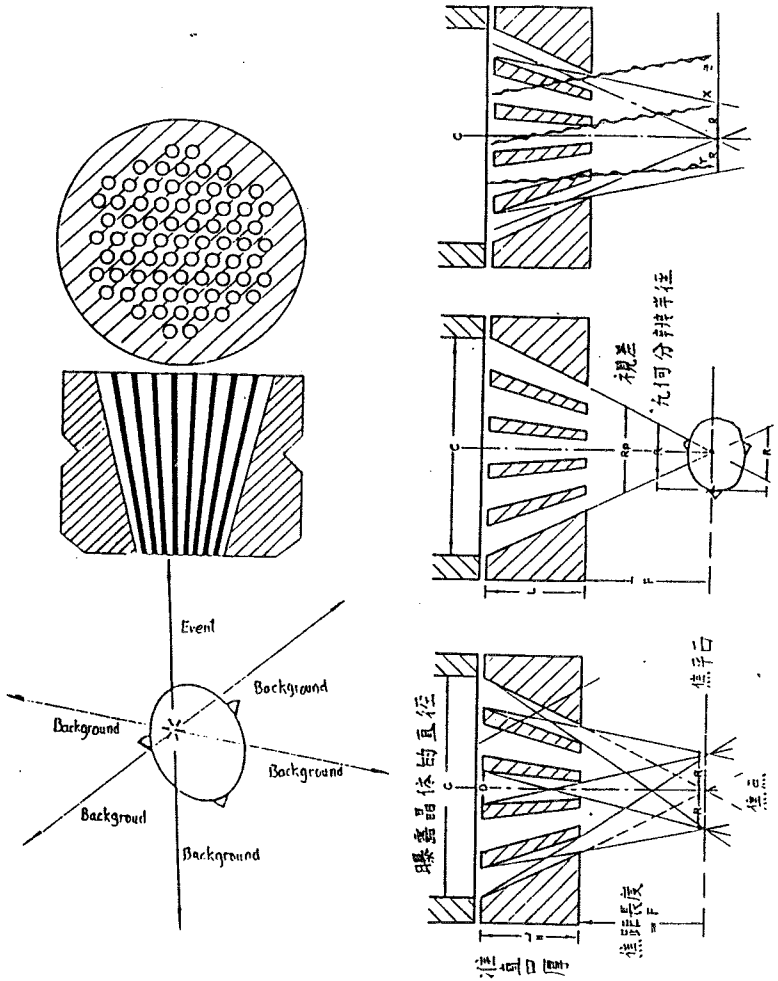

幾何平面源効率 $G=\frac{\pi ND^4}{64L^2(1+L/F)^2}$ 聚焦深度 $\lambda=2R\frac{F+L}{C}$

幾何分辨半徑 $R=D\frac{F}{L}$

Lead (Tungston) Collimator, Most of rays are backgrounds

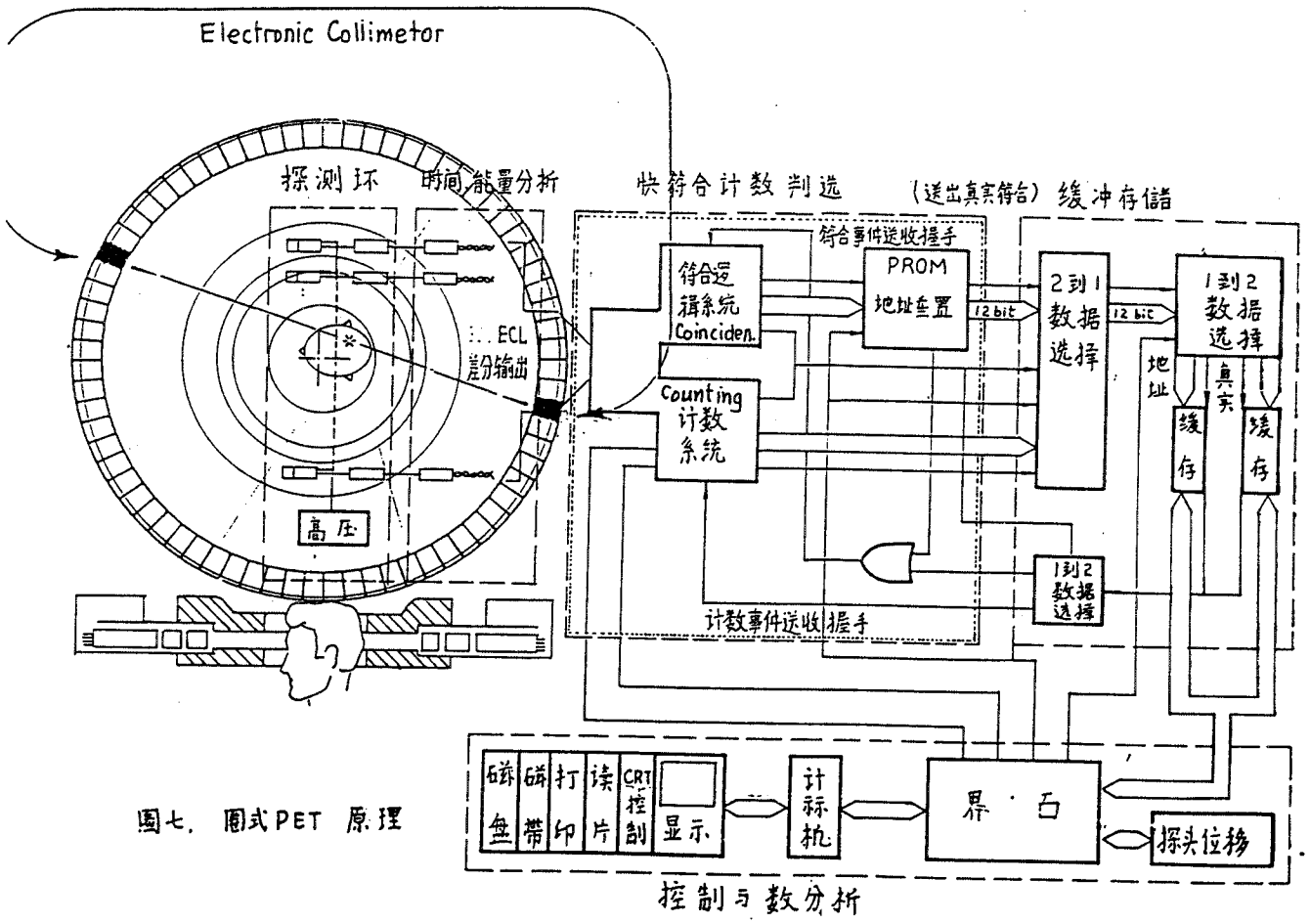

图七. 圈式PET 原理

IEEE Standard DAQ

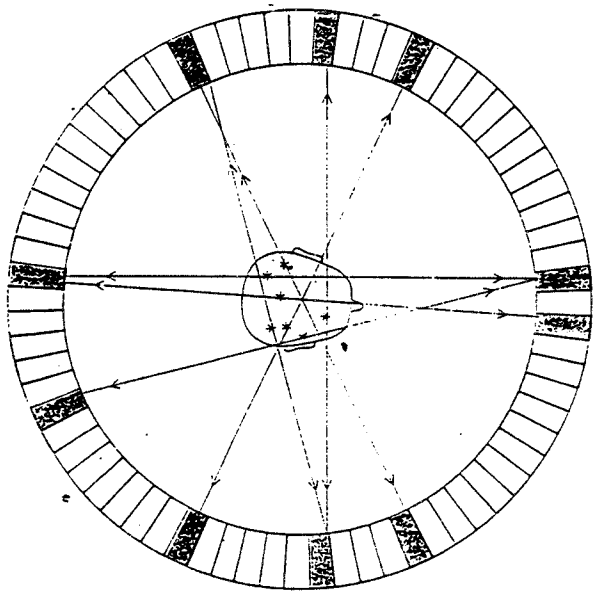

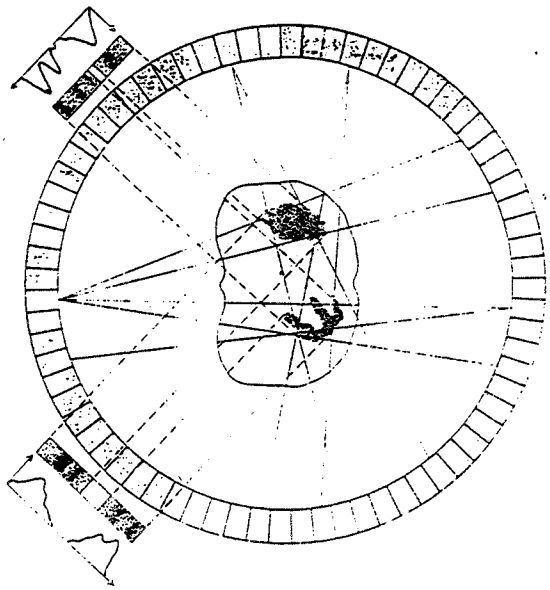

Electronic Collimator, All rays are events

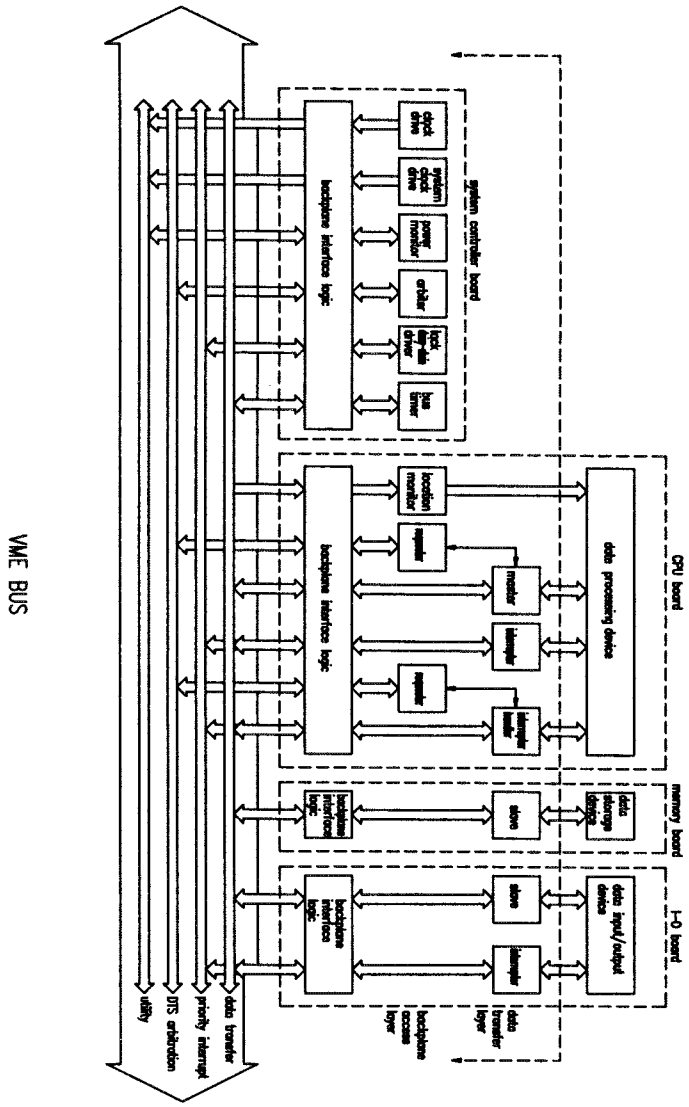

5 Serialization and Parallelism

5.1 **Parallelism data-out in detectors** (An example from M. Atac)
5.1.1 GaAs pixel array vertex
5.1.2 GaAs strip tracker
5.1.3 TPC
5.1.4 Quartz Fiber Cherenkov PI and Calorimeter
5.1.5 Muon Chamber

5.2 **Serialization of FEE**
5.2.1 Front End Electronics in detector
~ Front End Card of Pre-amplifiers, shift register, CCD,
5.2.2 FEE VME on detector
~ Amplifier, Discriminator, Multiplex,
~ TDC, QDC, FADC, WFM, Latency Buffer
~ Encoding, DSP, DPM
5.2.3 VME in counting room
~ Switch network
~ Triggering level 1, 2, 3

5.3 **Serialization of Buses in DAQ**
5.3.1 Gamma-camera to PET
~ IEC-TC45 (Nucl. Instr.), TC62 (Med. Instr), TC65 (Syst.), TC66 (Meas.)
5.3.2 J/psi
~ NIM: Committee of US DOE
~ CAMAC: ESONE/EUR4100e (1969),...; IEC516,...;
US-DOE-TID25875,...; ANSI/IEEE583 (1975),...
5.3.3 Z' 3 generations
~ FASTBUS: ANSI/IEEE std 960-(1986)
5.3.4 ϕ Factory, $\tau - c$ Factory, B Factories
~ VME/VXI: IEC 821 bus, IEEE P1014/D1.0 (1985)

5.4 **Serialization of calibration VME**

5.5 **Serialization of on-line computer**

5.6 **Bottle neck of data flow**
5.6.1 Parallel detector data out, but serial FEE read out, DAQ bus, on-line computer
5.6.2 Huge backgrounds pile up, block the data of events

5.7 **Beyond serialization of Higgs imaging**
5.7.1 Local Parallel VME/VXI, large granule-small array
5.7.2 Back Propagation Neural Network of triggering (1989)

6 How is Quantum in Parallelism

6.1 **Three laws on detector**
6.1.1 ∵ Slopes of: data-rate/yr < tracks/yr < Moore law << Beyond Moore law
6.1.2 ∴ Parallel electronics matching the intrinsic parallelism is possible

6.2 **FEE from serialization to parallelism**
6.2.1 Non-xing topology of parallel electronic connection
- ~ One way bus NIM, CAMAC
- ~ Local two way bus Fast Bus
- ~ Pipe line VME, VXI
- ~ Multi-layer one way feedback BP-NN
- ~ Systolic Algorithm-topology mapping
- ~ Boolean Cubic CM/SIMD
- ~ Two way neural network

6.2.2 Xing topology of Parallel Optic Connection
- ~ Terabit per sec. fibers
- ~ Xing photon path links

6.3 **Triggering from serialization to parallelism**
6.3.1 Programmable Logic
6.3.2 Trainable Back Propagation ANN

6.4 **DAQ from serialization to parallelism**
6.4.1 Bus BEPC
6.4.2 Pipe Line BTCF
6.4.3 Systolic
6.4.4 Boolean Cubic

6.5 **On-line computer from serialization to parallelism**
6.5.1 Large granularity of CPU-Memo small array
6.5.2 Small granularity large array

6.6 **Progress within Moore law**
6.6.1 Paralleling electronics and computer
6.6.2 Terabit/s devices
6.6.3 Sub-microm technologies

6.7 **Potential of beyond Moore law**
6.7.1 Devices of ultra high resolutions of time, space, and energy
6.7.2 Nanom tech
6.7.3 Single Electron tech
6.7.4 Single Photon tech.

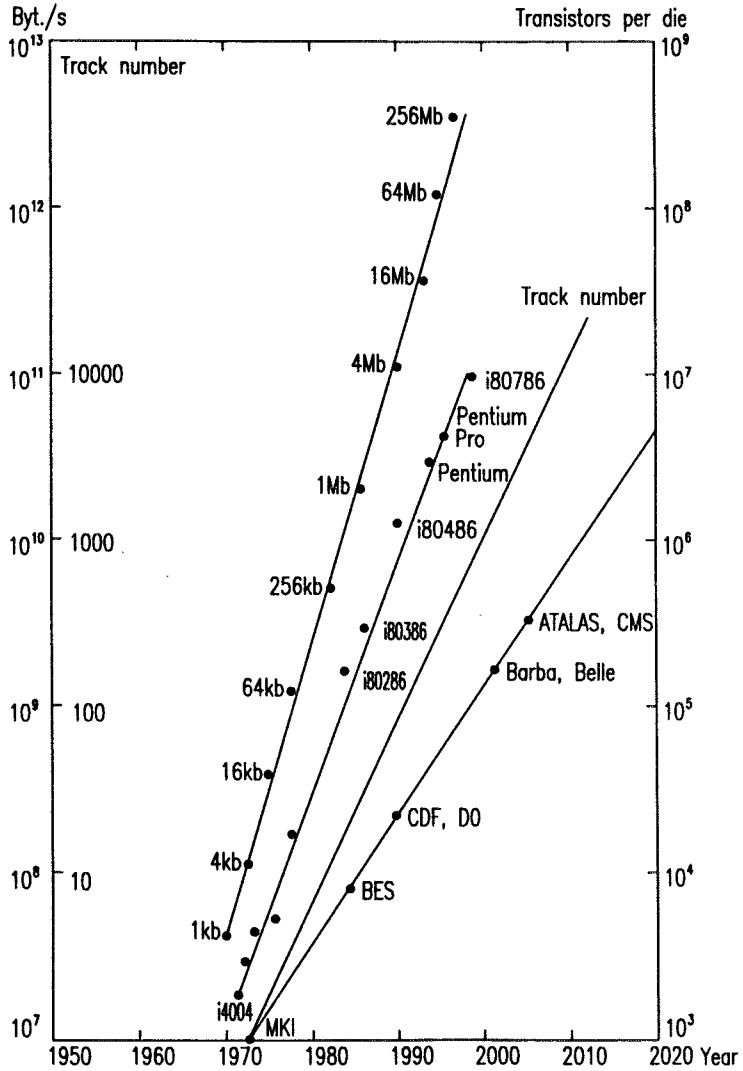

Track number, Data rate and Moore's Law

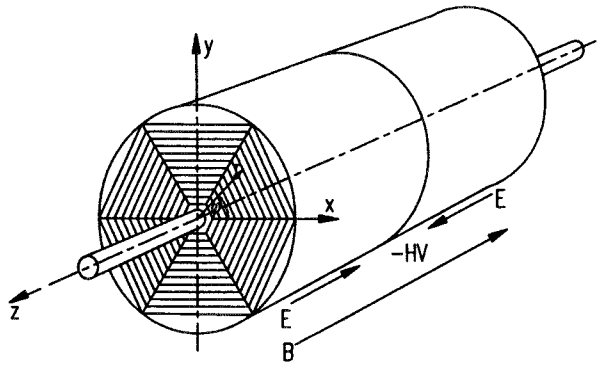

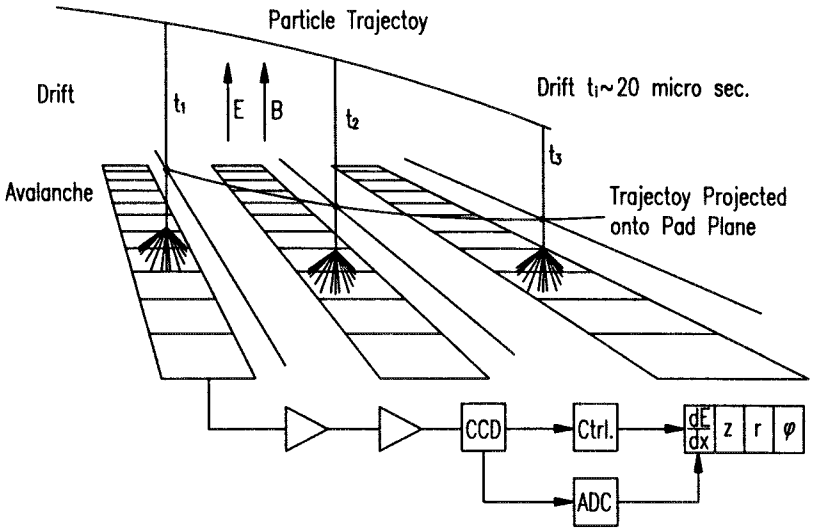

TPC and CCD readout

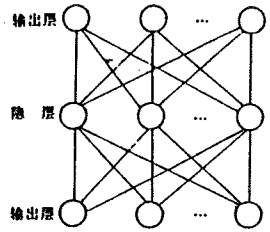

(a)BP 学习网络

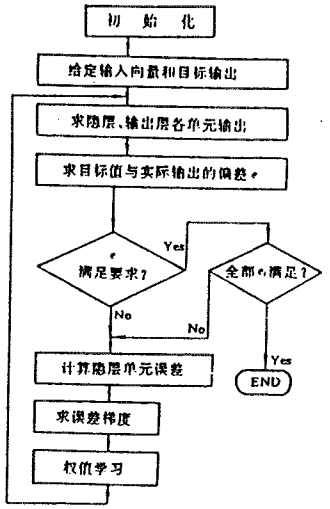

(b)BP 算法框图

图 11.3 BP 学习网络与算法框图

Higgs Gamma Jet Backpropagation Network, BrownHEP D0 Group

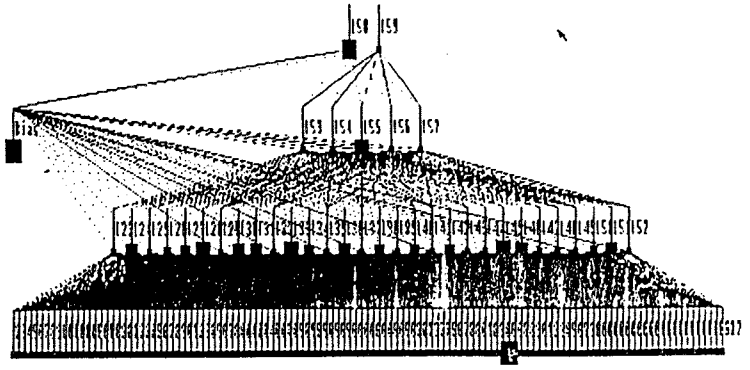

Fig. 9 Response of the trained network to a typical Higgs $\rightarrow \gamma\gamma$ shower.

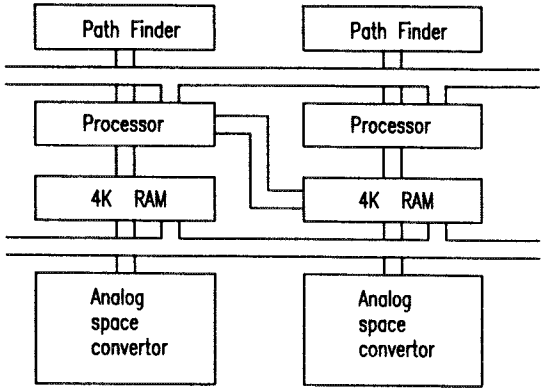

The mono chip computer as a readout follower of Fiber pixel array

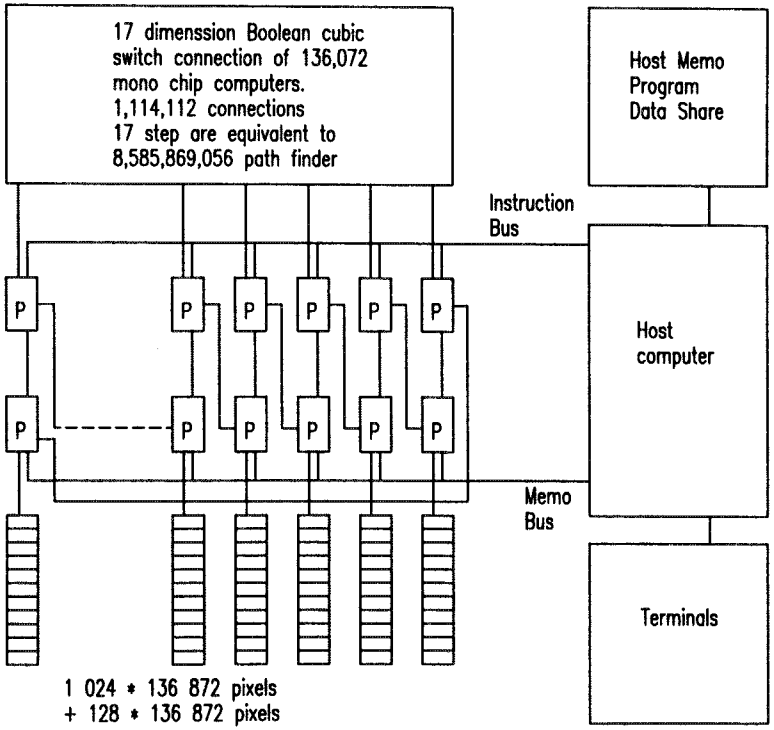

The connection of CONTO ROSY and Host computer

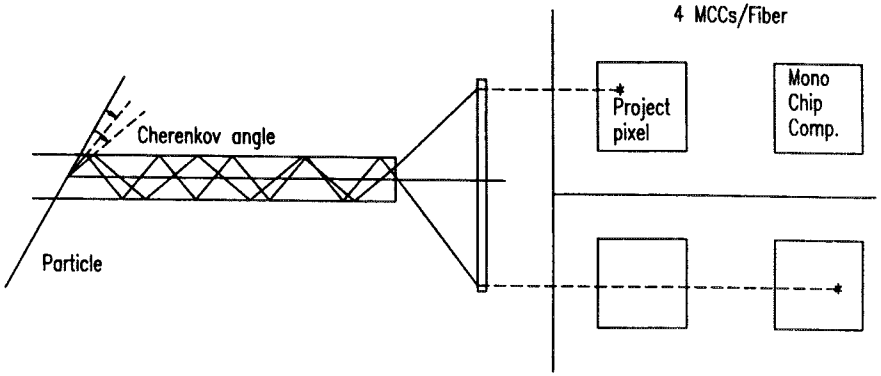

Project dispersion imaging as a spetial amplifier

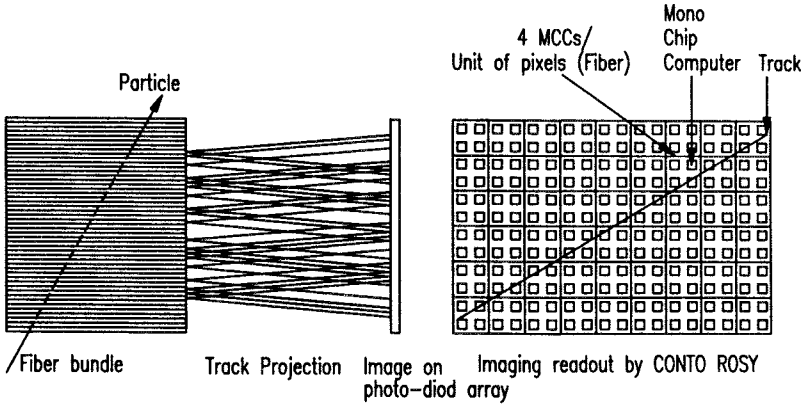

Fiber Cherenkov Imaging and Timing

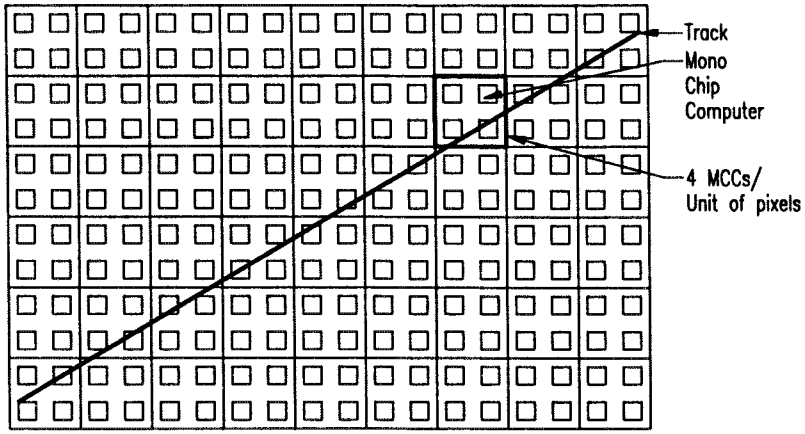

Hardware of CONTO ROSY

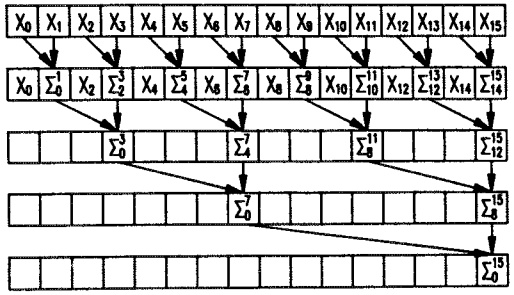

Sum algorithm

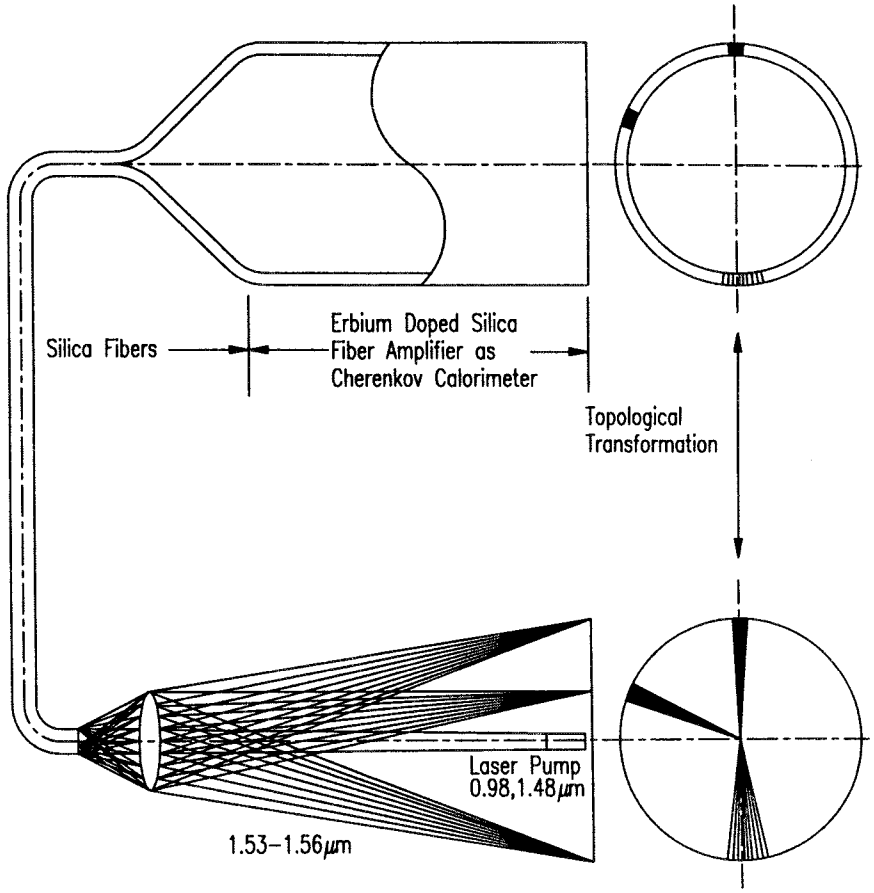

Output gain photons of Cherenkov calorimeter

7 EEEE Megatrends of PPPP

7.1 Laws and rules on HEP

7.1.1 Though PPPP is behind **Livingston law** at the moment,
7.1.2 But now it is coming into blocking *nuclear cold war*
7.1.3 Because social demand MIPS-MLPS rising rapidly ahead HEP *
7.1.4 and it is coming into also beyond **Moore law**

7.2 Possibility

7.2.1 Nash c-game of the prototype of 100 GeV muon colliders
7.2.2 Harsanyi i-game of quantum muon collider and detector

7.3 Causality

7.3.1 EEEE dynamics in Hilbert space of HEP state
7.3.2 Increasing micro electronics-photonics,
7.3.3 Introducing nano electronics-photonics.
7.3.4 Feynman path integral and HEP state transition in Hilbert space of DPPD-TEEET-CDDC and PPPP-CDDC-EEEE

7.4 Social meanings of muon collider ---beyond 20th century's laws

7.4.1 Beyond Nucl. defence law
7.4.2 Beyond Bit-rate law
7.4.3 Beyond Moore law
7.4.4 Beyond Livingston law

8. Conclusion

8.1 **HEP tripod of p,e, μ is right because the nature likes the number three**
8.2 Concentrative proton machine looks like the great wall of Chin dynasty.
8.3 Distributive linear electron machines looks like the way of United States.
8.4 Cooperative muon machines looks like the World Wide Web on internet.
8.5 **Starting Quantum** Colliders and Quantum Detectors
8.6 **Moore law & beyond ensure** that the **EEEE base** of QMC-QMD is a solid foundation for **Higgs factory** and other PPPP like **neutrino** etc.

*

Model	MillionLinkPerSec (MLPS)	Relative Performence
Micro Vax	0.008	0.296
Sun3/75	0.01	0.370
VAX780	0.027	1.0
Sun3/160	0.034	1.259
VAX8000	0.06	2.222
Convex	0.80	29.630
Cray-2	7	259.259
CM(64)	13	481.481
SX-2	72	2666.667

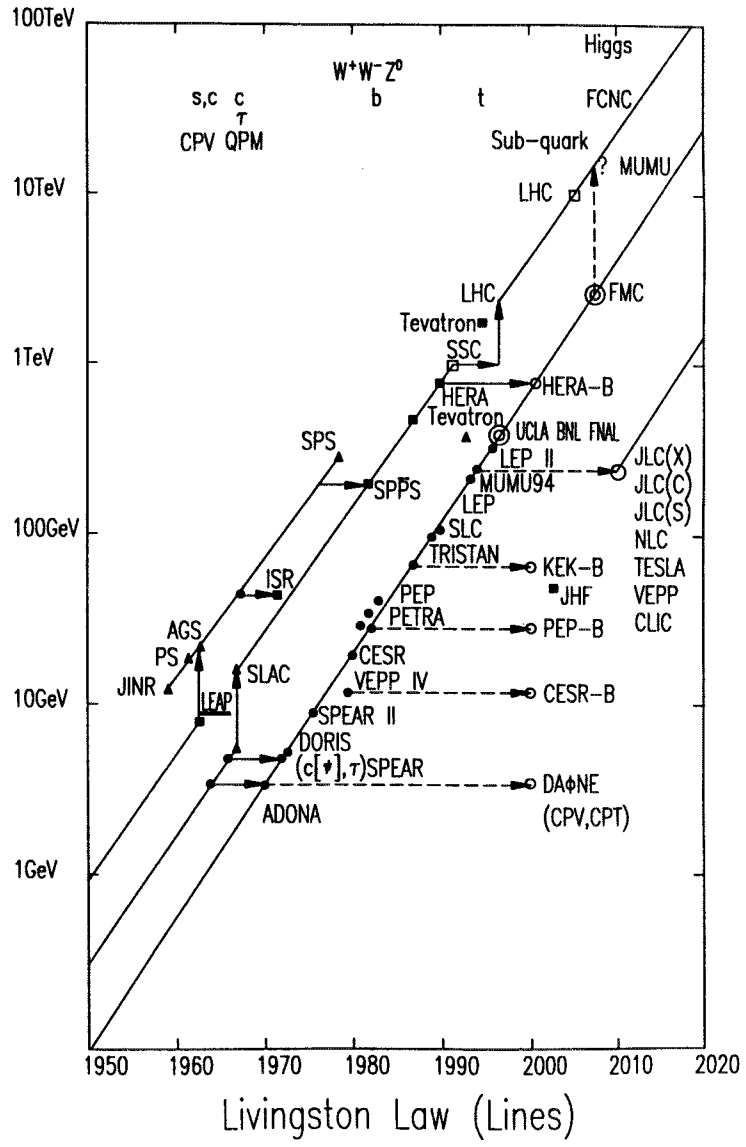

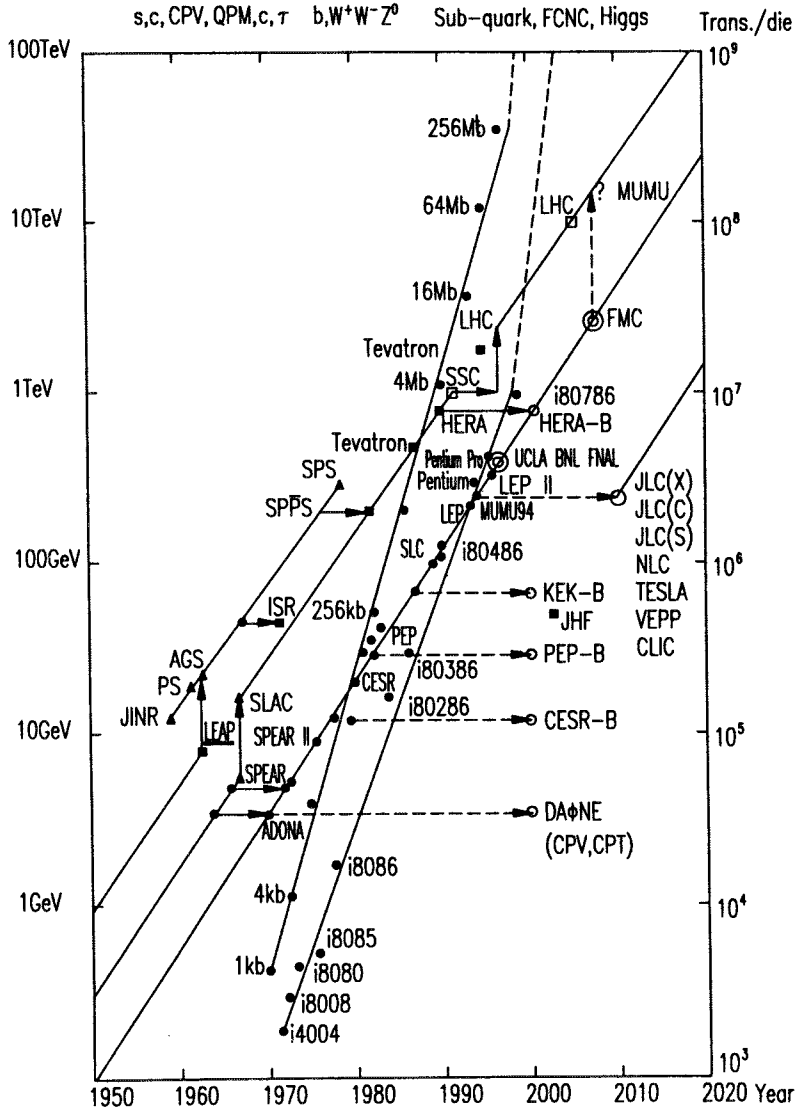

Behind Livingston Law and Beyond Moore Law

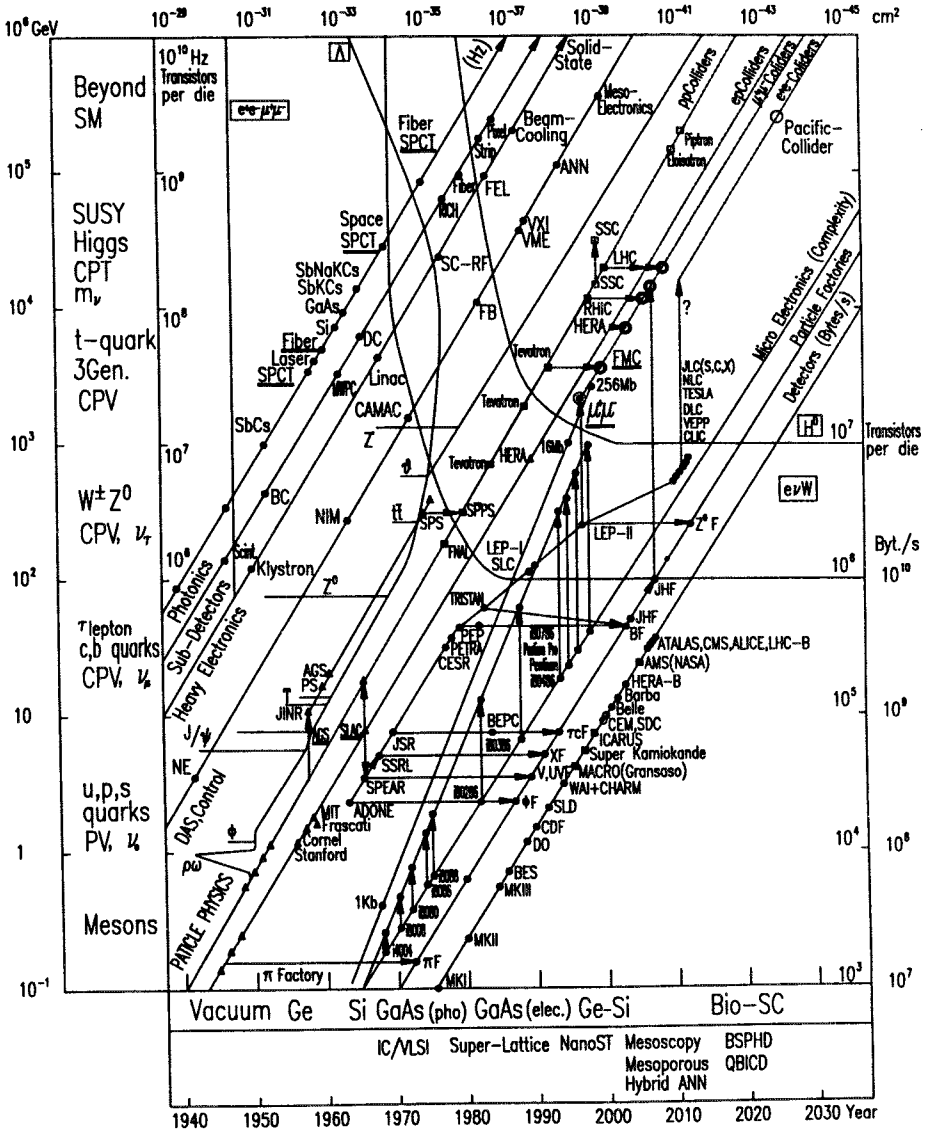

State Space of DPPD-TEEET-CDDC

Bunching Near Transition in the AGS

M. Brennan, L. Lawrence, V. Mane,
T. Roser, D. Trbojevic, W. van Asselt
BNL

C. Ankenbrandt, K-Y. Ng, J. Norem,
M. Popovic, Z. Qian
FNAL

San Francisco, Dec. 1997

Bunching to $\sigma \sim 2$ ns is desirable because:

Polarization states are easier to separate by bunch rotation if the bunch is short.

Less cooling is required if the initial proton / pion / muon bunch is as small as possible.

The 2 ns requirement has been relaxed somewhat since polarization is not so interesting in the early stages of operation.

We have studied a number of methods of bunching:

1) snap coalescence

2) rebunching at a higher frequency

3) bunching near transition

1) and 2) are comparatively well understood, but in this experiment, we have looked primarily at 3) which is interesting because:

- Flexible Momentum Compaction Lattices (which will probably be used to avoid crossing transition) offer a way to easily manipulate the transition energy of a ring.

- Bunches naturally become narrow at transition and optimizing this effect is interesting.

- No additional hardware (harmonic cavities etc.) are required.

Nonlinearities limit the degree of bunching that is possible.

- Synchrotron frequency depends on amplitude.

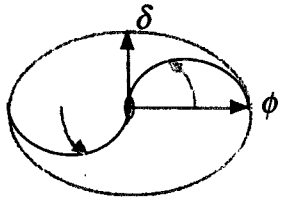

- Phase shear is nonlinear near transition.

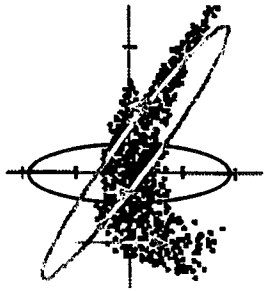

$d\phi/dt \sim \eta\delta \sim \delta^2$

if $\eta \sim \alpha_0 - 1/\gamma^2 + \alpha_0(\alpha_1+1.5)\delta +$

want $\alpha_1 = -1.5$

- Space Charge distorts bunches.

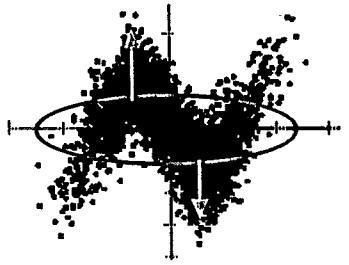

Operating Mode of the AGS

$n_p \sim 4 \times 10^{12}$ /bunch

$-0.05 < \gamma_t - \gamma < 0.05$

$E \sim 7$ GeV

$A \sim 1.5$ eV/s

Machine parameters:

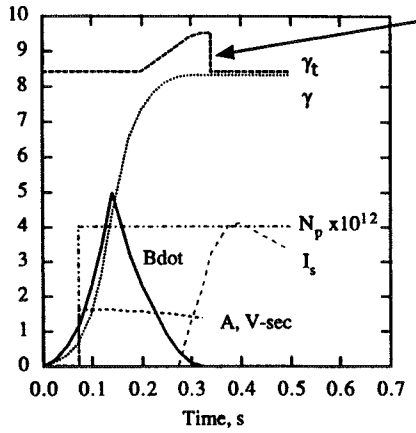

Suddenly makes bunch very tall.

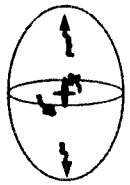

Bunch area measurements:

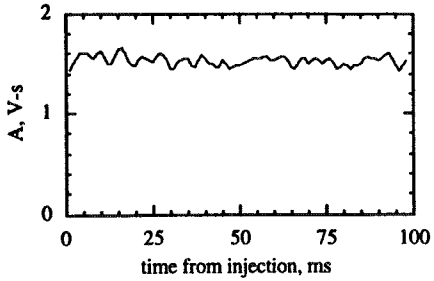

Tune of $\gamma_t(\delta)$

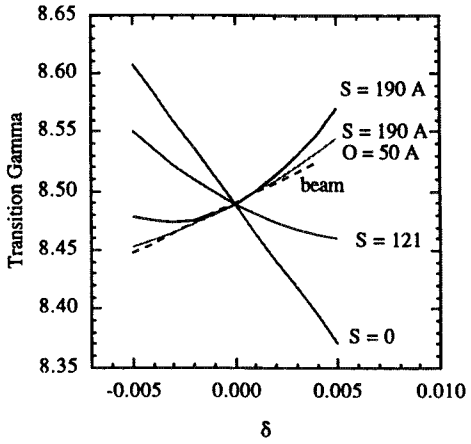

Increasing sextupole currents change the slope of $\gamma_t(\delta)$, but octupole magnets are required to make it linear.

Results: Bunching

Time evolution of the bunch was stable.

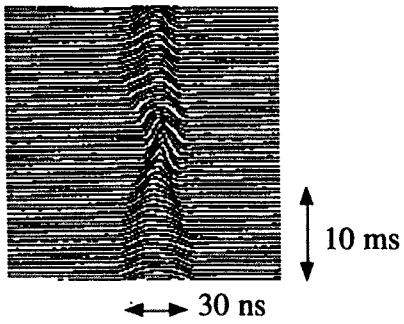

bunch parameters

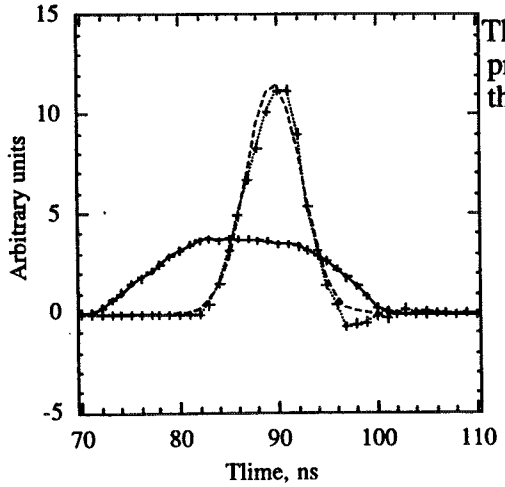

The shortest bunch was produced by modifying the initial state.

$\sigma \sim 2.3$ ns

FW = 11.9 ns

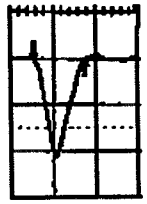

The data can be modeled with ESME

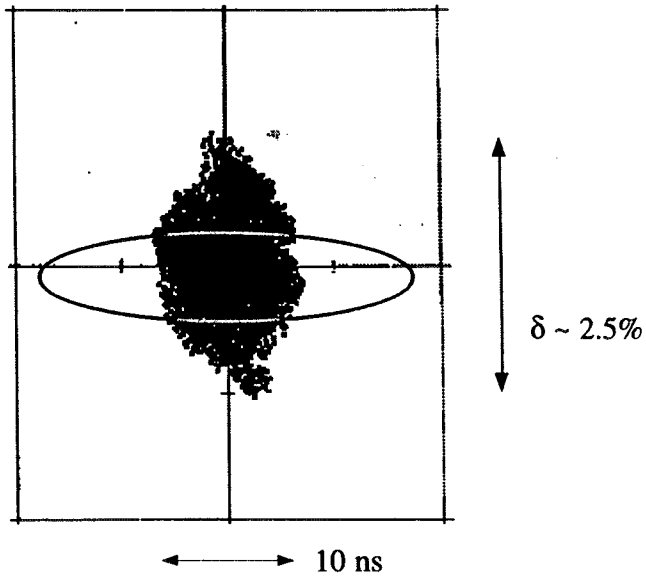

Tracking codes can produce an estimate of momentum width, as well as the value of α_1 from the asymmetry of the final bunch distribution.

Results:

Measurement of γ_t

Phase flip	$\gamma_t = 8.34 \pm 0.05$
synchrotron freq	$\gamma_t = 8.43 \pm 0.05$
previous data	$\gamma_t = 8.45$
Debunching	$\gamma_t = 8.45 \pm 0.04$

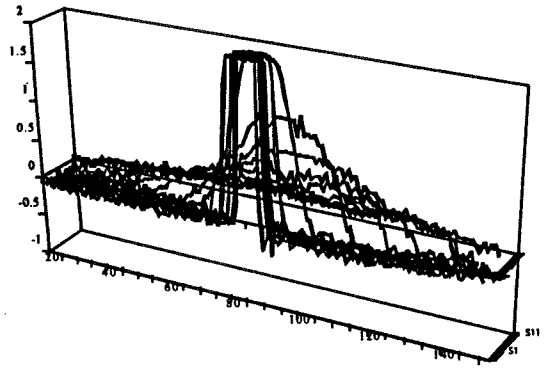

Measurement of α_1

beam loss vs freq	$\alpha_1 = 3.5 \pm 1.5$ @ $I_s = 100A$
bunching simulations	$\alpha_1 = 0. \pm 1.$

Conclusions:

- Bunching at transition works.

  (*almost* good enough for the muon collider now)

  (There seem to be a number of ways we could get even shorter bunches, for example by mismatching the initial bunch to the bucket by using the rf program.)

- Bunches seem unexpectedly stable.

- Measurements of γ_t and α_1 are consistent with other data.

- Useful additional experiments:

  Look at high space charge

  Move γ_t quickly both ways
  (which can compensate space charge)